NOVEL MECHANISMS FOR REGULATING POLYPHOSPHATE METABOLISM IN *Saccharomyces cerevisiae*

A Dissertation

by

DANIEL WILHELM NEEF

Submitted to the Office of Graduate Studies of
Texas A&M University
in partial fulfillment of the requirements for the degree of

DOCTOR OF PHILOSOPHY

August 2004

Major Subject: Biochemistry

NOVEL MECHANISMS FOR REGULATING POLYPHOSPHATE METABOLISM IN *Saccharomyces cerevisiae*

A Dissertation

by

DANIEL WILHELM NEEF

Submitted to the Office of Graduate Studies of
Texas A&M University
in partial fulfillment of the requirements for the degree of

DOCTOR OF PHILOSOPHY

Approved as to style and content by

Michael Kladde (Chair of Committee)	Mary Bryk (Member)
Sumana Datta (Member)	Andy LiWang (Member)
Gregory Reinhart (Head of Department)	

August 2004

Major Subject: Biochemistry

ABSTRACT

Novel Mechanisms for Regulating Polyphosphate Metabolism in

Saccharomyces cerevisiae. (May 2004)

Daniel Wilhelm Neef, B.S., Valparaiso University

Chair of Advisory Committee: Dr. Michael Kladde

To ensure a continuous supply of phosphate, living organisms have devised complex mechanisms to regulate the uptake and subsequent utilization of this essential nutrient. An important aspect of phosphate metabolism is the storage of excess phosphate as the polymer, polyphosphate. Despite the importance of this polymer to all living organisms, much needs to be learned about its synthesis, storage, or utilization. Furthermore, little is known about the regulatory mechanisms that determine when polyphosphate synthesis or degradation is appropriate. Our work has shown that polyphosphate is a dynamic molecule whose levels fluctuate during the cell cycle. Polyphosphate levels are high in G1, and subsequently drop as the cell uses free phosphate during cell division. Mitotic induction of phosphate regulatory genes, including the acid phosphatase gene *PHO5*, replenishes polyphosphate levels late in the mitosis. Furthermore, we have shown that Mcm1 and Fkh1, two cell cycle dependent transcriptional activators, contribute to mitotic activation of *PHO5*. In addition, we have elucidated the importance of regulating polyphosphate synthesis. Strains lacking the cyclin Pho80 have increased expression of the polyphosphate synthase genes, *PHM1-4,* and thus have highly elevated polyphosphate levels. Hyperaccumulation of polyphosphate results in severe growth

defects on medium containing high levels of sorbitol, presumably through the polyphosphate-dependent overacidification of the vacuole.

TABLE OF CONTENTS

LIST OF FIGURES

LIST OF FIGURES

LIST OF TABLES

CHAPTER I

INTRODUCTION

Scope

The primary scope of this dissertation is to discuss novel mechanisms of regulating the poorly understood process of polyphosphate metabolism in the model organism *Saccharomyces cerevisiae.* It will present evidence that polyphosphate levels fluctuate during the cell cycle and how these fluctuations affect the expression of phosphate-responsive genes. Furthermore, evidence will be presented showing that cell cycle-dependent transcription factors are employed to maximize the induction of a subset of these phosphate-responsive genes. Finally the dissertation will show the importance of maintaining proper regulation of polyphosphate metabolism.

Significance

Phosphate metabolism. Inorganic phosphate (P_i) is an integral component of most cellular functions, making it an essential nutrient to all organisms. It plays important roles in the generation of such macromolecules as DNA, RNA and certain lipids. Due to its essential nature, all organisms are equipped with complex systems that ensure adequate supplies of P_i under virtually any condition. If P_i becomes limiting, cells will respond by producing proteins specialized in acquiring more P_i (76). Alternatively, if P_i is in excess, P_i will be stored as a polyphosphate (polyP) polymer, so as to not waste the essential nutrient (66). The appropriate execution of P_i acquisition or P_i storage is essential for survival under P_i-limiting conditions (140). Significant advances in

---

This dissertation follows the style of Molecular and Cellular Biology.

understanding how cells acquire P_i have been made through the use of model organisms, like *Saccharomyces cerevisiae* (14) and *Neurospora crassa* (84, 85, 156). Utilizing the knowledge gained from microorganisms, similar P_i acquisition systems were found in higher eukaryotic species like plants and mammals (20, 75, 114, 121, 130). Unfortunately, little is known about the mechanisms involved in how P_i is stored as polyP in eukaryotic species. Our work will begin to shed light on these mechanisms, utilizing *Saccharomyces cerevisiae* as a model system with hopes that mechanistic insights will extend to higher eukaryotes.

Phosphate and plants. While storage of essential molecules, like P_i, is important for all organisms, it may be especially important for plants. Continuous P_i supplies are essential for maintaining processes like photosynthesis which are highly susceptible to small fluctuations in P_i concentration (152). Since most soils are limiting for P_i (93, 127), cellular polyP may be required to maintain adequate levels of P_i, essential for continued growth. Fertilizers containing high levels of P_i are often applied to supplement P_i-limiting soil. Since these additives often contain excess P_i, run-off can cause high levels of contamination in surrounding lakes and rivers. To avoid the use of high-P_i fertilizers, many researchers are bioengineering crops with novel mechanisms to more efficiently import and retain P_i (12).

Like the *Arabidopsis thaliana* P_i-transporter, Pho1, many of the enzymes involved in plant P_i metabolism are similar to those of yeast. It is therefore likely that plant enzymes involved in polyP metabolism will be similar to the corresponding yeast enzymes (Fig. 1-1). Incorporation of yeast P_i transporters and/or polyP synthases into

plants could potentially lead to higher uptake and more efficient storage of P_i, potentially reducing the need to apply fertilizers.

Phosphate and mammals. Understanding P_i metabolism is similarly important in mammalian species. The loss of P_i homeostasis in humans is known as either hyper- or hypophosphatemia and can result in serious physical ailments such as weakness in smooth muscle tissue, impaired neurological function, and reduced respiratory rate (10, 31). Furthermore, the loss of P_i homeostasis contributes to chronic renal disease that may ultimately require kidney transplantation (31). Maintaining P_i homeostasis in mammals is in large part achieved through a high-affinity Na-P_i co-transporter (*NPT2*) (94). While yeast also has a Na-P_i co-transporter (Pho89), no significant similarities exist between the yeast and mammalian transporter (data not shown). However, the receptors for gibbon ape leukemia (GLVR1) and murine leukemia virus (GLVR2) were shown to be a P_i transporters homologous to those of several fungal species, including the low-affinity P_i transporters of *Saccharomyces cerevisiae* (Pho87 and Pho90) (18, 56). This relationship has been extended to the xenotropic and polytropic retrovirus receptor (Xpr1) of humans (8), which is also predicted to be a P_i transporter (Fig. 1-1). More specifically, significant homology exists in a region termed the SPX (Syg1, Pho81, Xpr1) domain, located in the N terminus of the protein. Though their function is unknown, four highly conserved residues (Phe3, Leu7, Tyr22, and Lys26) form the basis of this domain (Fig. 1-1). A second homologous region of unknown function exists in the middle of the protein (Fig. 1-1). Surprisingly, recent evidence has shown that

proteins required for polyP synthesis in *S. cerevisiae* (Phm1, Phm2, Phm3) also have this domain (Fig. 1-1) (110).

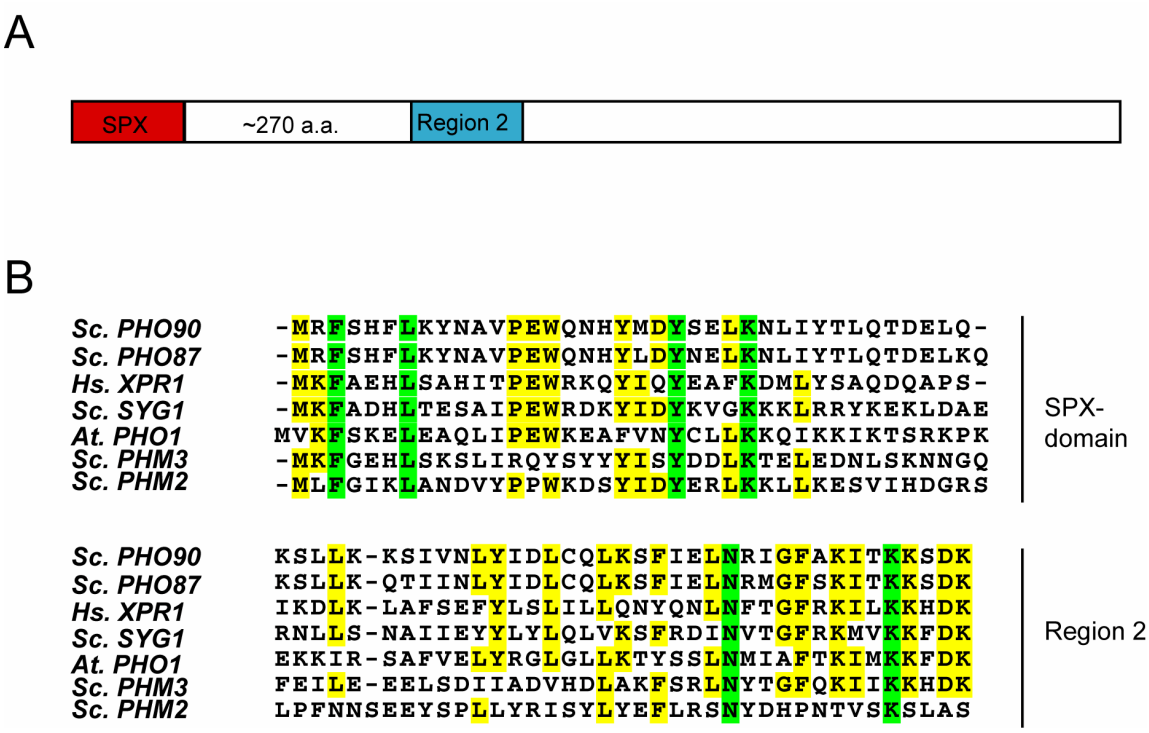

FIG.1-1. Sequence alignment of various SPX-containing proteins. (A) Relative position of the two regions of highest sequence homology within all seven proteins. (B) Sequence alignment of various proteins. Completely conserved residues are in green, while partially conserved residues are in yellow. *Sc., Saccharomyces cerevisiae, Hs., Homo sapiens, At., Arabidopsis thaliana.*

Since evidence from *S. cerevisiae* has shown that strains deficient in polyP synthesis are partly defective in P_i import (110), it is possible that polyP will play a significant role in the import of P_i and possibly leukemia virus infection in mammalian cells. Finally, recent evidence has suggested that in human cells polyP is thought to

activate the target of rapamycin (TOR), a protein that is up-regulated in a variety of tumors (160).

Polyphosphate and prokaryotes. Most of the research on polyP has been done in prokaryotic species. A detailed review of these findings was written by Arthur Kornberg in 1999 and should be referred to for more detailed information (66). In short, polyP has important functions in the stress survival of prokaryotic species. During stationary phase, *E. coli* elevate guanosine nucleotides levels thereby inducing expression of *rpoS*. *rpoS* codes for the σ^{38} subunit of RNA polymerase, which in turn induces expression of over 50 genes required for survival of stationary phase. In strains deleted for *ppk1*, hence lacking polyP, many of these genes are not expressed and consequently only 7% of population survives in comparison to nearly 100% of wild-type cells (66). These cells are also 10- to 100-fold more sensitive to a variety of stresses including heat, H_20_2, high salt, and UV-radiation (66). While it is not yet clear what the basis for this phenomenon are, it has been suggested that Ppk1 can serve as nucleoside diphosphate kinase, utilizing polyP as a substrate for generating guanosine nucleotides (66). It is possible that the loss of Ppk1 results in reduced levels of guanosine nucleotides, and consequently in reduced expression of *rpoS*. Though their function is unclear, large amounts of polyP accumulate in response to some stresses, like osmotic shock and nitrogen starvation. However, this stress-dependent accumulation, is not universal, as it does not occur during temperature, pH, and oxidative stress (66). In response to amino acid starvation, polyP has been shown to stimulate the ATP-dependent Lon protease to degrade the S2,

L9, and L13 ribosomal proteins. It is proposed that the polyP-dependent degradation of these proteins will supply the lacking amino acids to other cellular functions (71).

In *Pseudomonas aeruginosa* loss of *ppk1* renders cells unable to form a biofilm and defective in the production of the virulence factors elastase and rhamnolipid that are synthesized during stationary phase. In mice, the virulence of strains lacking *ppk1* is greatly reduced with severe defects in the colonization of tissues (128, 129).

In *V. cholerae* the loss of *ppk1* results in diminished adaptation to high calcium levels as well as reduced motility (112). In *Shigella flexneri* and *Salmonella enterica,* loss of *ppk1* results in a defective response to stress and starvation and sensitivity to polymyxin, acid, and heat (59). It is unclear if polyP has similar functions in eukaryotic species as it is not required for survival of osmotic stress in yeast, and its loss does not result in significant growth defects (110).

Background

Polyphosphate. A brief overview of polyP metabolism will be given below. It is important to note that our knowledge of the mechanism involved in synthesizing and regulating polyP in eukaryotes is sketchy at best. While significantly more information is known about polyP synthesis and degradation in prokaryotes than eukaryotes, this review will focus on the latter. PolyP consists of individual orthophosphate residues covalently attached to one another by high energy phosphoanhydride bonds. These chains can range from as short as 3 residues to as long as 700 residues. Budding yeast has a much higher concentration of polyP (120 mM) than *E. coli* (0.1-50 mM) or animal

cells (12-89 μM) (66). In yeast, virtually all of the cellular P_i is stored in the vacuole in the form of polyP (39) and may represent as much as 10%-20% of the cells dry weight (66, 150). The major genes for generating polyP in *E. coli* are two polyP kinases (*ppk1* and *ppk2*). These enzymes respectively catalyze the transfer of the terminal phosphate from ATP or GTP to a preexisting polyP chain as well as the reverse reaction (66). No such enzymes have yet been found in a eukaryotic organism, suggesting a potentially different mechanism of polyP synthesis.

Research exploring what genes are induced during P_i starvation has shed light on a possible polyP synthesis mechanism (110). Several genes, named *PHM1-4*, induced in response to P_i starvation, were found to be essential for polyP synthesis (110). Interestingly, these genes had little to no similarity to the polyP kinases found in prokaryotic cells, supporting the idea that eukaryotic polyP synthesis is mechanistically different. Phm1-4 form a biological complex that is localized to the vacuolar membrane (96). Phm3 and Phm4 are essential for both polyP synthesis and PHM complex stability (96, 110). Phm1 and Phm2 are likely to have redundant functions, as loss of either does not affect polyP synthesis nor complex stability, yet the loss of both confers a phenotype that is similar to loss of function of *PHM3* or *PHM4* (110). Phm1 and Phm2 are homologous proteins, sharing 56% identity, and are thought to contain short transmembrane domains which are inserted into the vacuolar membrane (Fig. 1-2). The remaining portion of both proteins form large, hydrophilic domains localized to the cytoplasm (Fig. 1-2) (97). Phm4 is a 129-amino acid protein, consisting entirely of one transmembrane domain, which is surprisingly homologous (32% identity) to the

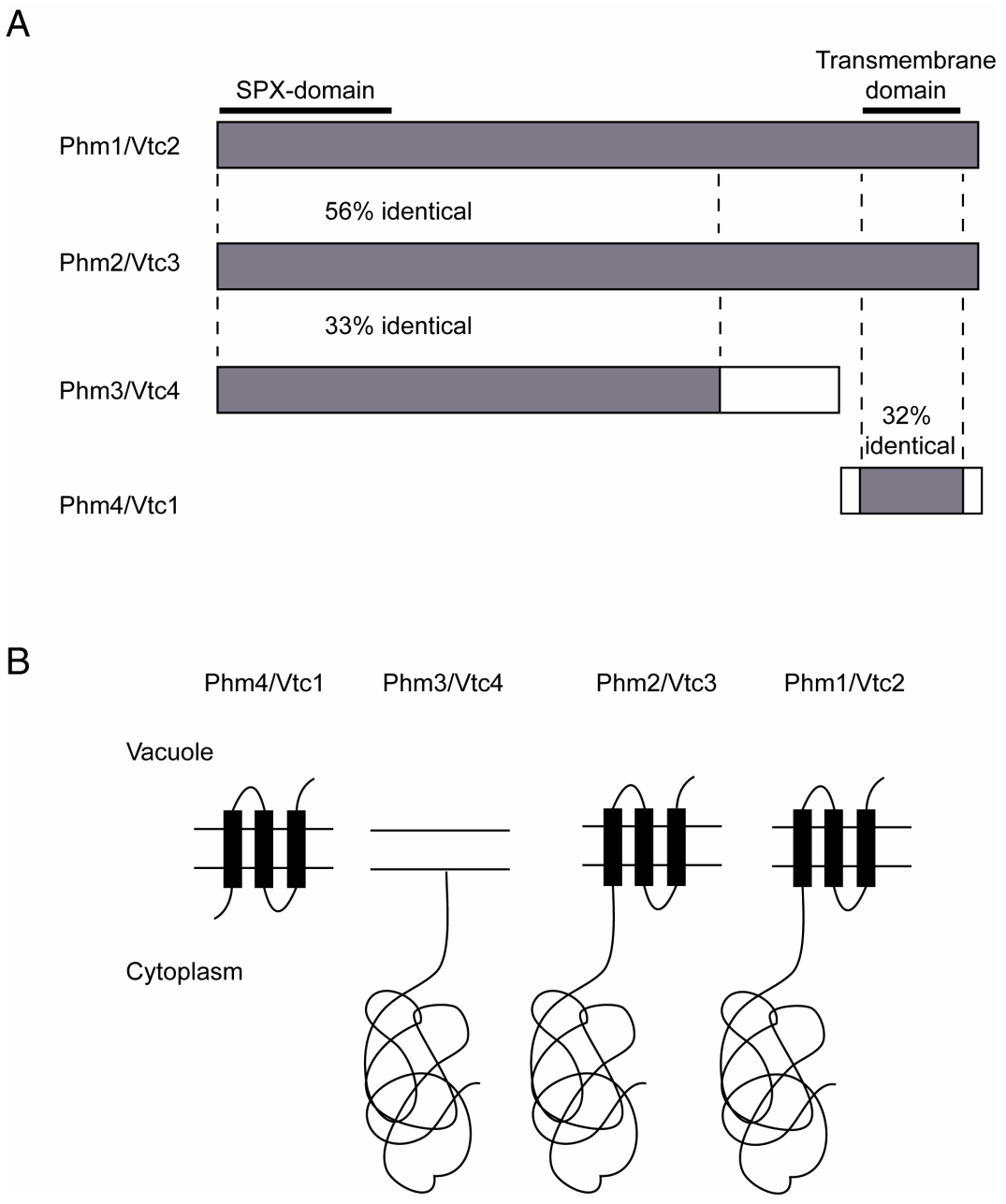

FIG.1-2. The Phm/Vtc proteins of *S. cerevisiae.* (A) The homology between Phm1, Phm2, Phm3, and Phm4. Dashed lines indicate the regions of highest homology. Grey and white boxes represent homologous and non-homologous regions, respectively, and their identities to the Phm1 sequence are indicated by percentage. The SPX- and transmembrane-domains are indicated above the Phm1 box. (B) Predicted structures of Phm1, Phm2, Phm3, and Phm4 (104).

transmembrane domain of Phm1 and Phm2 (Fig. 1-2). Phm3 is a purely cytosolic protein, sharing 33% identity with the cytosolic domain of Phm1 and Phm2 (Fig. 1-2). Despite lacking a transmembrane domain, Phm3 remains constitutively associated with the vacuolar membrane, presumably due to tight interactions with Phm4 (110).

Strong interactions have been shown between Phm3, Phm4, and Vph1, an important subunit of the vacuolar-H^+-ATPase (V-ATPase) (97). It has been hypothesized that the PHM complex is involved in either activating or stabilizing the V-ATPase as loss of either Phm3 or Phm4 results in approximately 80% reduction in vacuolar acidification (23, 104). Phm3 and Phm4 have also been shown to be important for vacuolar fusion, most likely through their tight interaction with the v-SNARE component Nyv1 (96). Since vacuolar acidification and the V-ATPase are also important for vacuolar fusion, it is unclear if their roles are direct or indirect.

While only little is known about how polyP is synthesized in eukaryotic cells, more is known about polyP degradation. Like *E. coli* and other prokaryotes, yeast cells express one or more exopolyphosphatases (*e.g.* Ppx1), which hydrolyze polyP chains at their termini (163). Ppx1, which is expressed constitutively, is localized to the cytoplasm. Deletion of *PPX1* elevates cellular polyP by approximately 3-fold, but causes no defects in growth. Unlike prokaryotes, budding yeast contains an additional enzyme to hydrolyze polyP. Ppn1, an endopolyphosphatase, hydrolyzes polyP chains internally to produce multiple smaller chains (137). Expression of *PPN1* is not constitutive, but is rather controlled through Pho4 and P_i levels. Evidence has shown that Ppn1 hydrolyzes polyP chains preferentially as 3- or 60-mers. While the exact

function of these chain lengths is unknown, the loss of *PPN1* results in extremely long polyP chains, but does not increase the overall mass of polyP. Surprisingly, deletion of *PPN1* results in significant growth defects. Ppn1, like the PHM complex, is localized to the vacuole and has recently become a popular marker for studying vacuolar targeting (131). It is unclear what the direct relationship between Ppx1 and Ppn1 is, though the loss of both proteins has a synergistic effect and results in 8-fold more polyP. An important biological question that remains unanswered is how polyP is transferred from the vacuole to the cytoplasm for exopolyphosphatase-dependent hydrolysis.

Low phosphate induction of *PHO5*. As this dissertation addresses the relationships between polyP and the transcription of P_i-responsive genes (see Chapters 2 and 3) in the context of chromatin and the cell cycle, background on these and other relevant topics will be provided below. In *S. cerevisiae,* regulation of P_i homeostasis is achieved by controlling the transcription of genes important for P_i metabolism. This transcriptional control is conferred by the P_i or "PHO" system. A schematic representation of the PHO regulatory system is shown in Figure 1-3.

The helix-loop-helix transcription factor Pho4 is inactivated through phosphorylation by the cyclin/cyclin-dependent kinase complex Pho80/Pho85 under high P_i conditions. As a result, Pho4 is exported to the cytoplasm (57). P_i starvation initiates a signal transduction cascade in which the cyclin-dependent kinase inhibitor (CKI) Pho81 is activated and inhibits the ability of Pho80/Pho85 to phosphorylate Pho4 (135), thereby resulting in Pho4 activation and nuclear import via the nuclear importer

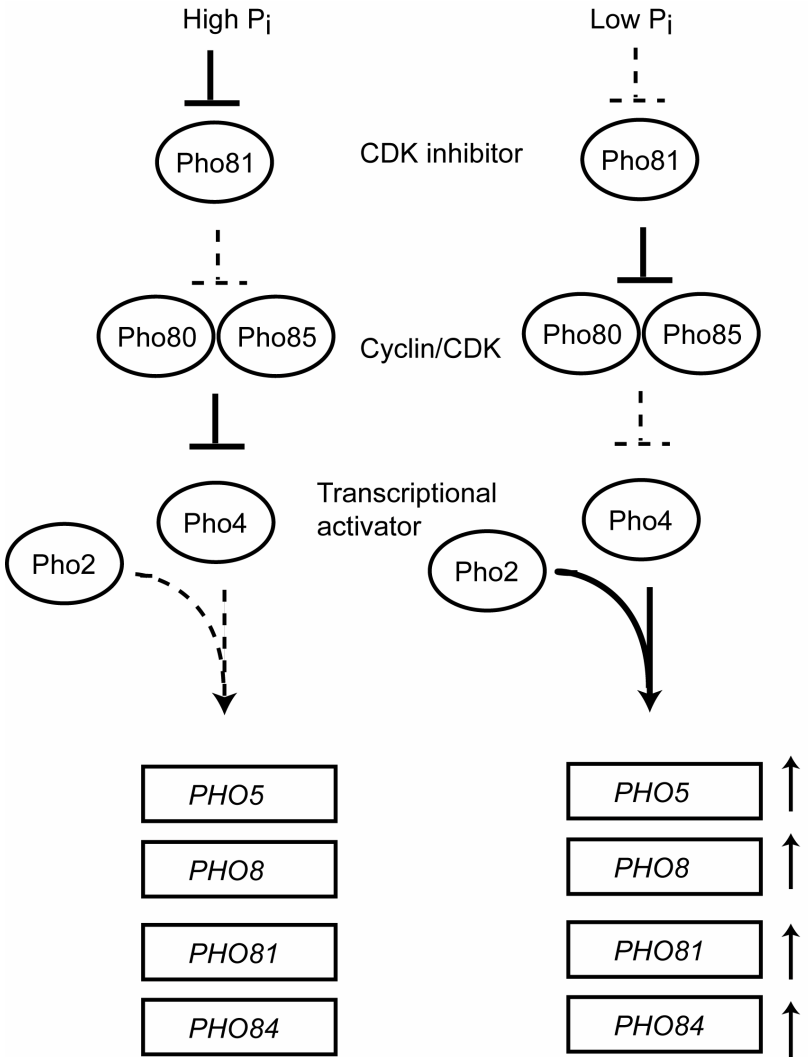

FIG. 1-3. The PHO regulatory system of *Saccharomyces cerevisiae*. Ovals represent proteins while rectangles represent genes. The thick lines represent signals being transduced to a downstream target, while the dashed lines represent the absence of signals.

Pse1 (109). Activation of Pho4 is achieved by the loss of phosphorylation at five different positions, each site controlling different aspects of its regulation (57, 64). Similarly, deletion of *PHO85* and/or *PHO80* enables Pho4 to be active and localize to the nucleus (109). In the nucleus, Pho4 can form a heterodimer with Pho2, a constitutively nuclear homeodomain protein (138) required to activate *PHO5* (139, 159). Heterodimerization allows for binding to the promoters of over 20 genes in the PHO regulatory pathway, thereby leading to their expression (6, 110, 111). Among these genes are those encoding various acid phosphatases (*PHO3, PHO5, PHO11,* and *PHO12)* that are secreted to the periplasm of the cell to scavenge extracellular P_i (141). Also expressed is *PHO8,* which encodes an alkaline phosphatase that mobilizes P_i from the vacuole (61). *PHO84* (coding for a high-affinity P_i transporter), as well as *PHO87* and *PHO89* (coding for low-affinity P_i transporters), are expressed and serve as the main means of transporting inorganic P_i into the cell (14, 15, 86). The gene encoding the cyclin-dependent kinase inhibitor *PHO81* is expressed, thereby providing a positive feedback loop for repression of the Pho85/80 complex (135). This positive feedback is essential for full activation of the PHO system (24).

***PHO5* expression and chromatin remodeling.** *PHO5* is the most widely-studied gene in the PHO pathway. Work studying its P_i-dependent transcription has provided valuable information on how cells respond to starvation stress, and has also explained much about basic transcriptional control. Significant advances have been made on how chromatin regulates transcription. Like many promoters, the yeast *PHO5* promoter is subject to regulation by chromatin. The *PHO5* promoter contains two upstream

activating sequences (UAS), constituting binding sites for Pho4, both of which are flanked by Pho2 binding sites (37, 100). The first UAS element is located in the linker region between two positioned nucleosomes, whereas the second UAS element is located within a nucleosome, rendering it inaccessible to transactivator binding (Fig. 1-4) (146, 155). Prior data have shown that this nucleosome is remodeled in response to shifting the cells to a low-P_i environment, thereby allowing Pho4 full access to the promoter. In total, five positioned nucleosomes are remodeled (Fig. 1-4) in response to gene activation by multi-subunit chromatin remodeling complexes, often divided into two groups. The first group acetylates histones causing a remodeling event, that is most often associated with gene activation (144). The second type of chromatin remodeler is an ATP-dependent remodeler (45, 123). Dependence of gene expression on chromatin remodeling complexes varies greatly. Some genes have been shown to be highly dependent on both types of remodeling complexes, whereas others are dependent on one or the other complex, and some require neither (51). Prior research has shown that *PHO5* activation in high-P_i, rich media, and sub-maximally inducing conditions (*pho80*Δ) is dependent on several chromatin remodeling factors. One such factor, Gcn5, has been show to acetylate lysine residues in the N-terminal domains (often referred to as tails) of histone H3 (42). In addition, expression of *PHO5* in rich media is dependent on the histone H4-specific acetylase complex NuA4 (32), as well as the ATP-dependent chromatin remodeling complex SNF/SWI (145). When cells are shifted to a P_i-limiting environment, *PHO5* activation is dependent on *GCN5* during early times of activation, reaching only 25% of wild-type levels within 3 hr.

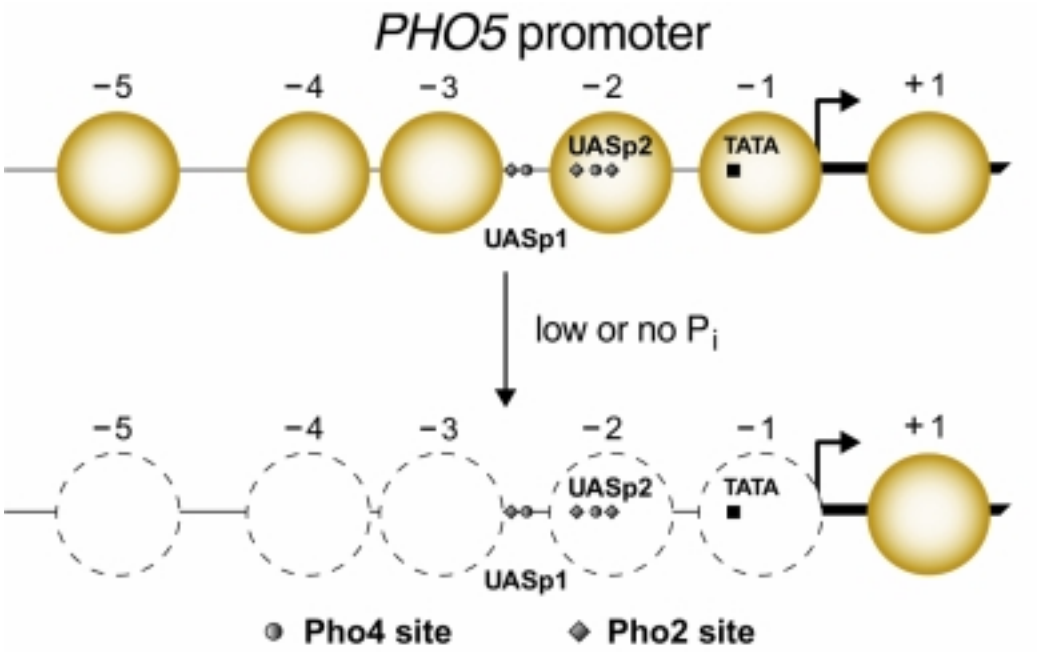

FIG. 1-4. The *PHO5* promoter is remodeled in response to P_i starvation. A schematic of the *PHO5* promoter in the presence or absence of P_i. The dashed lines represent the remodeled nucleosomes. Grey circle and diamonds represent Pho4 and Pho2 binding sites, respectively.

However, as starvation progresses, this requirement for chromatin remodeling is relieved; within 18 hr of starvation, *gcn5*Δ and wild-type strains induce *PHO5* expression similarly (7, 103). Also of interest is that *PHO8* expression is dependent on chromatin remodeling factors even under maximally inducing conditions, despite that it is controlled via the same acidic activator (Pho4) as *PHO5*. Since *PHO8* expression is approximately 5-fold lower than that of *PHO5* (110), these observations show an interesting correlation between requirements for chromatin remodeling enzymes and the amount of gene activation.

The yeast cell cycle and mitotic induction of *PHO5*. The cell cycle of *S. cerevisiae*, like that of other eukaryotic organisms, is divided into four stages (Fig.1-5). Two gap phases (G1 and G2) precede S phase (DNA replication) and M phase (mitosis), respectively. The transition from one phase to another is controlled primarily through a central regulator, a cyclin-dependent kinase, Cdc28 (Fig.1-5). While Cdc28 acts as the main regulator of the yeast cell cycle, no fluctuations in its expression are observed. Instead, fluctuations occur in cyclins, the binding partners of Cdc28. Activation of this kinase through pairing with appropriate cell cycle stage-specific cyclins allows for phosphorylation of various target proteins that promote cell cycle progression. Cyclins can be divided into two subgroups, the G1 cyclins (Cln1-3) and the B-type cyclins (Clb1-6). More specifically Cln1, Cln2 and Cln3 are all required for execution of cell cycle Start, the progression from G1 to S phase. Clb1, Clb2, Clb3 and Clb4 are all required for entry into mitosis. Finally Clb5 and Clb6 are both important for events in S phase (90, 101).

The cell cycle is controlled through a number of biochemical mechanisms. One such mechanism involves the proteolysis of specific targets (22). Two distinct proteolytic pathways exist to control cell cycle progression. First a Cdc34-based mechanism leads to the transition from G1 to S phase. Cdc34, an E2 ubiquitin-conjugating enzyme (40), leads to the ubiquitination and subsequent degradation of Sic1, the primary inhibitor of the G1-S transition (136). A second proteolytic mechanism, regulating mitotic exit, is controlled through a large group of proteins referred to as the

anaphase-promoting complex (APC). The APC leads to degradation of a variety of proteins that include the prophase inhibitor Pds1 as well as the B-type cyclin Clb2 (158).

A second, well-defined mode of cell cycle regulation is the cell cycle stage-specific transcription of genes. Expression of cell cycle-specific genes occurs through a handful of transcriptional activators, each dedicated to a specific phase of the cell cycle (Fig.1-5). For example, Mbp1 and Swi6, together referred to as MBF, activate transcription of genes involved in DNA synthesis (62). Swi4 and Swi6, together called SBF, regulate the expression of G1 cyclins (95). Transcription of mitotically induced genes, like *HO* or *SIC1*, is activated by Swi5 and Ace2. Mcm1 is another mitosis-specific transactivator, whose exact function and regulation will be discussed below.

Induction of *PHO5* during mitosis of the yeast cell cycle was first shown as part of a larger project to identify all genes under cell cycle regulation (143). *PHO5*, *PHO3*, *PHO11*, *PHO12*, *PHO81*, and *PHO84* were all found to be expressed during mitosis. It was unclear why the PHO system was activated during mitosis, as all experiments were conducted in rich media and the cells were presumably not starved for P_i. Also, *PHO5*, *PHO3*, *PHO11*, and *PHO12* were transcribed in response to overexpression of the mitotic cyclin C*LB2*, and repressed in response to the overexpression the G1 cyclin *CLN3*. Since expression of the *PHO5* responded to increased Clb2 levels, these results suggest that mitotic expression was under the control of the cell cycle machinery, a novel mode of regulating *PHO5*. Further exploration of what causes mitotic *PHO5* induction and how P_i- and cell cycle-specific regulators interact will be discussed further in chapters 2 and 3, respectively.

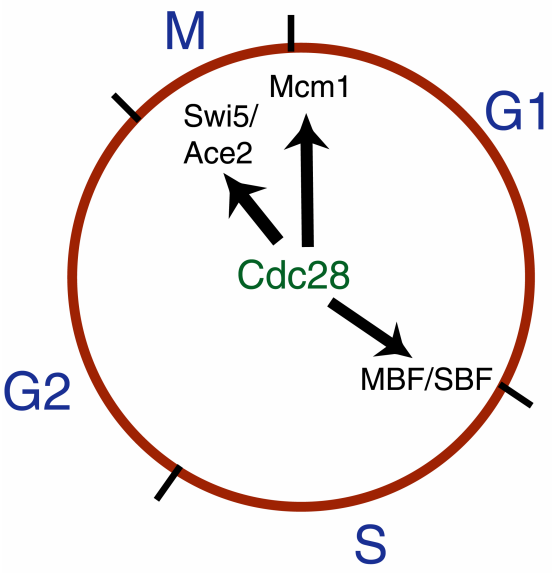

FIG. 1-5. The cell cycle of *Saccharomyces cerevisiae*. Various cell cycle stages are separated by black tick marks. Transcriptional activators are listed next to the transition they are thought to regulate. Black arrows depict activation of various transcription factors by Cdc28.

Mcm1, SFF and the cell cycle. Transcription of mitotically-induced genes is often controlled by Mcm1 (143). Mcm1 is an essential transcriptional activator, and a member of the MADS (Mcm1, Agamous, Deficiens, Serum response factor) family of transcription factors. Besides its role as a cell cycle transcription factor, Mcm1 is also involved in the regulation of mating-type (118), arginine-biosynthetic (91), and pheromone-response genes (55). Mcm1 has also been shown to be important for minichromosome maintenance (83), and possibly DNA replication (16). Depending on the gene, Mcm1 can function as either an activator or repressor of transcription.

Mcm1's function at a given locus is usually dictated by a specific DNA-binding partner. For example, in *MAT*α cells, α-specific genes are induced by Mcm1 and the transcription factor α1, while **a**-specific genes are repressed by Mcm1 and the homeodomain protein α2 (Fig. 1-6) (33). Mcm1, together with the transcriptional activator Arg80, the zinc-finger protein Arg81, and the inositol 1,4,5-trisphosphate 6-kinase Arg82, activate transcription of various genes important for arginine biosynthesis (Fig. 1-6) (4). Together with Ste12, Mcm1 activates expression of pheromone-responsive genes (Fig. 1-6) (53). Finally, in conjunction with switch five factor (SFF), Mcm1 regulates the expression of many M- and M/G1-expressed genes (Fig. 1-6) (80). Recently, SFF has been identified as Fkh1 and Fkh2, deriving their names from their close homology to mammalian forkhead proteins. While both Fkh1 or Fkh2 can bind to the SFF binding site in conjunction with Mcm1 and activate transcription, recent evidence suggests that perhaps Fkh2 is a more common binding partner for Mcm1 (65). While Mcm1 binding sites differ depending on its binding partner, all contain a similar consensus sequence (CCNNNWWRGG) (117). *In vitro* gel shift studies have shown that mutating the conserved cytosines to guanines or the guanines to cytosines reduces Mcm1 binding by over 100-fold (142). However, some recent evidence has suggested that these mutations may be less severe *in vivo,* as partial binding is still detected (38).

Since both Mcm1 and Fkh2 are constitutively bound to the promoters of mitotically-expressed genes (80), appropriating Mcm1-Fkh2 function for mitosis is achieved by cell cycle-dependent phosphorylation by Cdc28-Clb2. Since Mcm1 phosphorylation does not change over the cell cycle, it is likely that either Fkh2 or Ndd1,

an essential co-activator, are modified (132). It is unclear if Mcm1 and/or Fkh2 are repressed during G1 via Cdc28-Cln or if the mere absence of Clb2 is enough to repress Mcm1-Fkh2 dependent transcription.

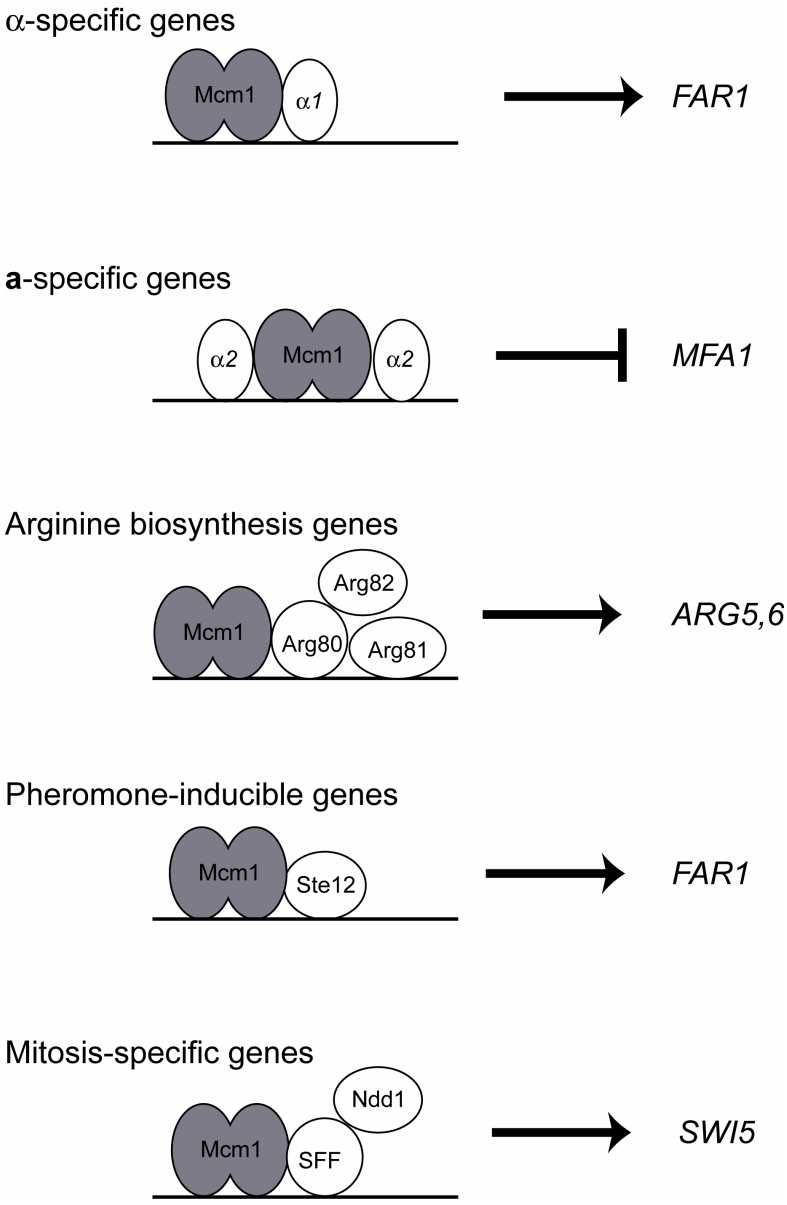

FIG. 1-6. Various roles of Mcm1 in regulating gene expression. In α-cells, Mcm1 induces expression of α-specific genes in conjunction with α1, while repressing **a**-specific genes in conjunction with α2. Mcm1 induces expression of arginine biosynthesis genes in conjunction of Arg80, Arg81, and Arg82. Mcm1 and Ste12 induce expression of several genes in response to pheromone, while Mcm1, SFF, and Ndd1 induce expression of specific genes in mitosis.

CHAPTER II

POLYPHOSPHATE LOSS PROMOTES SNF/SWI- AND GCN5-DEPENDENT MITOTIC INDUCTION OF *PHO5**

Introduction

Coordination of cell growth and division is essential to all living organisms and is innately tied to the cell division cycle. Periodic increases in certain transcripts at distinct cell cycle phases can meet specific, one-time requirements. For instance, histone and nucleotide biosynthetic genes are activated prior to and during S phase, respectively, to ensure adequate substrate concentrations for chromosomal duplication (35, 47). In addition, the sequential activation and proteolytic destruction of cyclins that partner with cyclin-dependent kinase (CDK) activities drive progression through the cell cycle (77). In contrast to this post-translational mode of cell cycle control, it is clear that much cell cycle regulation occurs at the level of initiation of transcription by RNA polymerase II. In *S. cerevisiae*, three major classes of transcriptional activators, MBF and SBF, Swi5/Ace2, and Mcm1-associated factors predominantly regulate various gene clusters at the G1/S transition, M and the M/G1 boundary, and G1, M, or M/G1, respectively (143).

Spellman *et al*. (1998) (143) identified *ca*. 800 genes exhibiting cell cycle oscillation. While the regulation of ~500 of these genes can be ascribed to the three known classes of cell cycle transactivators, the mode of regulation of the rest is not

*Reprinted with permission from "Polyphosphate Loss Promotes SNF/SWI- and Gcn5-Dependent Mitotic Induction of *PHO5*" by Daniel W. Neef and Michael P. Kladde, 2003. Molecular and Cellular Biology, Vol. **23**, p. 3788-3797. 2003 by American Society for Microbiology.

understood. Many of these latter ~300 genes participate in nutrient acquisition and their transcripts show peak expression in M or M/G1. For instance, mitotic expression has been observed for genes involved in P_i (PHO) metabolism (76, 115) encoding low- (*PHO89*) and high- (*PHO84*) affinity transporters of P_i as well as repressible acid phosphatases (rAPases; *PHO5*, *PHO11*, and *PHO12*) and constitutive APase (*PHO3*). Based on the timing of their expression, the mitotically induced rAPase genes are grouped with 34 other genes comprising the MCM cluster (143). However, there is no evidence for a direct or indirect role of Mcm1, or another known DNA binding cell cycle regulator, in their transcriptional activation. Moreover, as all experiments in Spellman *et al*. (1998) (143) were conducted in rich media that contains P_i, it is unclear why these *PHO* genes, which ordinarily are induced upon P_i deprivation, are activated at specific cell cycle phases. Thus, *PHO5*, *PHO11*, and *PHO12*, as well as other cell cycle-regulated *PHO* genes, fall into a large group of genes involved in maintaining nutritional homeostasis for which it is not understood how cell cycle periodicity is accomplished or why it is needed.

To date, studies of the mechanisms of yeast *PHO* gene activation have focused on regulatory events that occur in asynchronous cultures as a function of limiting P_i. By an as yet unknown mechanism, P_i limitation initiates a signal transduction cascade that activates Pho81, a CDK inhibitor (CKI). Pho81 inhibits the phosphorylation activity of the cyclin-CDK Pho80-Pho85 (135), leading to nuclear retention of the otherwise cytoplasmic helix-loop-helix factor Pho4, the primary PHO transactivator (64, 109). In the nucleus, Pho4, either by itself or as a heterodimer with Pho2, a nuclear

homeodomain protein, activates over 20 different genes in the PHO system (52, 110). These include several P_i metabolism (*PHM*) genes, *PHM1* (*VTC2*), *PHM2* (*VTC3*), *PHM3* (*VTC4*), *PHM4* (*VTC1*), and *PHM5* (*PPN1*). Phm1-4 form a biochemical complex *in vivo*, the integrity of which is disrupted by *phm3* or *phm4* null mutations (23, 96). As polyP, a linear polymer of up to hundreds of P_i residues linked by high-energy phosphoanhydride bonds, is not detectable in such strains, the Phm/Vtc complex is proposed to be a polyP synthetase (110). However, this complex is also needed for the proper morphology of vacuoles (96), where 99% of the total cellular polyP is stored (150).

PolyP is present in all organisms examined to date and, in *S. cerevisiae*, can reach concentrations as high as 120 mM in the vacuole, as much as 60% of the total P_i content (66). It has been suggested that polyP functions as a P_i reservoir since its levels drop when cells need P_i, *e.g.*, during log-phase growth or in P_i-limiting growth media (39, 140). It has also been suggested that polyP serves a cellular protective function in that it chelates cations, such as Ca^{2+}, in the vacuole (66). However, yeast strains deficient in polyP accumulation are not sensitive to high concentrations of calcium (110). Finally, polyP levels increase as yeast cultures approach stationary phase for reasons and by mechanisms that are not clear (137, 163). Thus, while conditions and enzymes involved in polyP synthesis and hydrolysis in eukaryotes have been identified, its metabolic, regulatory, and physiologic function(s) remain obscure.

Relative to our understanding of the connection between nutrient sensing and the decision to execute Start (126), little is known about how nutrient levels influence

regulation in other stages of the cell cycle. To gain insight into this problem, we have focused on elucidating both the molecular mechanisms and physiological basis for M phase activation of *PHO5*. We report that the unexpected mitotic induction of *PHO5* in rich medium is under control of Pho4, Pho2, and Pho81. Increasing metabolic pools of polyP represses mitotic expression of *PHO5*. Conversely, elimination of polyP by deletion of *PHM3*, leads to *PHO5* activation. Moreover, we demonstrate that polyP levels are influenced by progression of the cell cycle, declining prior to and being replenished after M phase. Our results suggest that polyP is a dynamic P_i reserve and define a regulatory influence of polyP on *PHO* mitotic gene expression. Further, our studies demonstrate that Pho4/Pho2 mediates a novel, cell cycle stage-specific mode of regulation that is fine-tuned in response to nutrient availability and operates mostly independent of activities that drive cell cycle progression. More generally, our findings suggest that nutrient deficiencies may underlie the transcriptional periodicity of a large class of nutrient transporters that are cell cycle regulated.

Materials and methods

Yeast strains and methods. All *S. cerevisiae* strains were constructed by standard genetic methods (133) from CCY694, *MAT***a**/*MAT*α *leu2*Δ0/*leu2*Δ0 *lys2*Δ0/*lys2*Δ0 *ura3*Δ0/*ura3*Δ0 *pho3*Δ::R/*pho3*Δ::R (S288C background) (11), where R is a *Zygosaccharomyces rouxii* recombinase site that remains after intramolecular recombination (60). The strains and their relevant (all are *MAT***a** *leu2*Δ0 *lys2*Δ0 *ura3*Δ0 *pho3*Δ::R) genotypes are DNY742 (wild-type; *MAT***a** *bar1*Δ::R-*URA3*-R), THY868

(*MAT***a** *bar1*Δ::R-*URA3*-R *pho4*Δ::*kanMX4*), DNY989 (*MAT***a** *bar1*Δ::R-*URA3*-R *pho2*Δ::*kanMX4*), DNY925 (*MAT***a** *bar1*Δ::R-*URA3*-R *pho81*Δ::*kanMX4*), DNY986 (*MAT***a** *bar1*Δ::R-*URA3*-R *gcn5*Δ::*kanMX4*), DNY1309 (*MAT***a** *snf2*/*swi2*Δ::*kanMX4*), DNY1673 (*MAT***a** *bar1*Δ::R-*URA3*-R *phm3*Δ::*kanMX4*), DNY2464 (*MAT***a** *his3*Δ1 *phm1*Δ::*kanMX4*), DNY2465 (*MAT***a** *bar1*Δ::R-*URA3*-R *met15*Δ0 *phm2*Δ::*kanMX4*), and DNY2467 (*MAT***a** *bar1*Δ::R-*URA3*-R *his3*Δ1 *phm4*Δ::*kanMX4*).

Media and growth conditions. Cells were grown at 30°C on plates or in liquid cultures of complete synthetic medium/2% glucose (CSM; Bio101), yeast extract (Difco)/peptone (Difco)/2% glucose (YPD), or YPD supplemented with 13.4 mM KH_2PO_4 (YPD + P_i) as indicated. The defined, P_i-free medium used in one step of the phosphate overplus as well as for P_i starvation contained 0.7 g yeast nitrogen base (YNB) without $(NH_4)_2SO_4$, phosphate, or amino acids (Bio101), 2 g glutamine, 20 g glucose, and 3.9 g MES (2-N-morpholino ethanesulfonic acid), pH 5.5 per liter.

All cultures, including overnight cultures, were maintained in early to mid-logarithmic phase growth. When P_i starvation was employed, cells grew only 2-3 additional generations after washing and resuspension in P_i-free medium. Phosphate overplus experiments were performed as previously described (110); pregrowth in YPD or YPD-low P_i, YPD in which P_i was removed by precipitation (46), followed by 2 hr-P_i starvation in defined, P_i-free medium, and finally made 13.4 mM with KH_2PO_4 for 2 hr. Note that, while YPD is limiting for P_i, the designation YPD-low P_i indicates that the medium is decreased further in P_i concentration but is not P_i-free. For measuring rAPase activities in asynchronous cultures, overnight cultures (10 ml) were grown as indicated

and diluted the next day to OD_{600} = 0.03 in the indicated fresh medium, and incubated for 6 h more. For the P_i starvations experiments, strains were plated on defined, P_i-free medium with 13.4 mM KH_2PO_4 added back for 3 d. After overnight growth of starter cultures (10 ml) in the same medium, the cells were diluted into defined, P_i-free medium at an OD_{600} of 0.2 and assayed at the indicated times for rAPase activity and/or *PHO5* mRNA.

Cell cycle synchronizations, FACS analysis, and RNA/polyP isolation. Yeast cultures in early logarithmic growth in YPD were arrested at late G1 and G2/M by the addition of α factor and nocodazole to final concentrations of 12 ng/ml and 17 μg/ml, respectively. After 2 h, cells were released from cell cycle arrest by filter-washing three times and subsequent resuspension with YPD containing 0.1 mg/ml pronase E (α factor arrest) or YPD (nocodazole arrest).

For flow cytometric analysis (FACSCalibur, Becton Dickinson), cells (1 ml) were removed every 15 min after release from cell cycle arrest and fixed overnight in 70% ethanol at 4°C. RNA was degraded by overnight incubation at 37°C in 50 mM sodium citrate, pH 7.1 containing 0.25 mg/ml RNase A. The cells were then washed and the DNA was stained by overnight incubation at 4°C in 50 mM sodium citrate, pH 7.1 containing 1 μM Sytox Green (Molecular Probes).

Total RNA isolation, which also recovers polyP, was performed as described in Cross *et al*. (25) except that cells were resuspended in 350 μl 1× LETS buffer (0.1 M LiCl, 10 mM EDTA, 10 mM Tris, pH 8.0, 0.5% w/v SDS) and 350 μl acid phenol:chloroform (1:1), and lysed with glass beads by vortexing at 4°C for 15 min.

Following centrifugation at 14,000 × g for 15 min, RNA and polyP were recovered from the aqueous phase by ethanol precipitation. The pellet consisting of RNA and polyP was resuspended in 0.1% SDS, quantified by absorbance at 260 nm, and stored at –80^{o}C.

Northern hybridization and polyP analysis. For analysis of *PHO5* transcript levels, 10 μg RNA was electrophoresed at 100 V for 3 h in 1% agarose gels buffered with 1× MOPS [20 mM MOPS (3-N-morpholino propanesulfonic acid), pH 7, 5 mM sodium acetate, 0.5 mM EDTA) containing 1.85% formaldehyde. RNA was blotted by 10× SSC (1.5 M NaCl, 0.15 M sodium citrate) to a positively-charged nylon membrane. Membrane prehybridization and hybridization were performed in Church-Gilbert buffer (0.25 M Na_2HPO_4, pH 7.4, 7% w/v SDS, 10 mg/ml fraction V bovine serum albumin, 1 mM EDTA, and 0.5 mM sodium pyrophosphate). Hybridization probes, generated by PCR amplification using oligonucleotide primers DNO425 (5'-TCTTTCCCTGGCGA-3') and DNO426 (5'-GTCATCCAAGTAGGTTGTGT-3') or DNO429 (5'-GCCAAGAAAGAGAGCTGC-3') and DNO430 (5'-GAACTTAGAACCTGGTCTGTCC-3') for *PHO5* and *TCM1*, respectively, were radiolabeled with [α-^{32}P]dCTP by random priming. Messenger RNA levels were quantified by Storm 860 phosphorimager analysis (Molecular Dynamics).

Gel analysis of polyP was performed by electrophoresis of 10 μg RNA on native 6% polyacrylamide gels followed by staining with toluidine blue O as described in Ogawa *et al*. (2000) (110). To quantify total levels of polyP, 10 μg of isolated RNA/polyP was treated with RNase A (after removal of SDS by chloroform extraction, if necessary), polyP was ethanol precipitated, and resuspended in 50 μl dH_20. Ten

microliters of the purified polyP was mixed with 1 ml of toluidine blue solution (6 mg/l toluidine blue O dye, 40 mM acetic acid) and the metachromatic shift in the ratio of absorbance at 530 nm to 630 nm was measured (21). The A_{530}/A_{630} of toluidine blue solution alone is a constant of 0.175, which was used as a blank. All samples were diluted to assure assay linearity and polyP levels are expressed as $[(A_{530}/A_{630}) - 0.175]/\mu g$ RNA. As expected, samples from a *phm3*Δ strain yield a value of 0.

Acid phosphatase activity assays. After the specified growth conditions, cells were chilled to 4°C and washed twice and resuspended in 0.1 M sodium acetate, pH 3.6 at 4°C. After preincubation (10 min) of 500 µl of cell suspension at 30°C, the rAPase activity was assayed by addition of 500 µl 20 mM *p*-nitrophenylphosphate (Roche) and incubation at 30°C for 10 min. Enzymatic activity was terminated by the addition of 250 µl 1 M Na_2CO_3 and quantified by measuring the absorbance at 420 nm. Activities are reported in Miller units $[(A_{420\ nm} \times 1000)/(OD_{600\ nm} \times$ volume (ml) cells assayed $\times$ 10 min)].

Results

Mitotic induction of *PHO5* requires the PHO activators Pho2, Pho4, and Pho81. Earlier genome-wide determinations of cell cycle-regulated transcripts suggested that expression of *PHO5* and other *PHO* genes is induced during mitosis (143). However, significant cross hybridization of mRNA species can occur above 75% DNA sequence identity (48). Since *PHO5* and *PHO3* constitute a duplicated gene pair (87% identity over 1404 bp), we re-analyzed the cell cycle expression profile of *PHO5* in a strain

deleted for the entire *PHO3* coding sequence. Cultures in rich (YPD) medium were arrested at late G1 with the mating pheromone α factor and released synchronously by washing with YPD. Northern analysis of RNA samples isolated at 15 min intervals demonstrates that *PHO5* mRNA levels oscillate during the cell cycle, with maximal expression occurring at 45-60 and 120 min after α factor removal (Fig. 2-1A,B). Transcript from the ribosomal protein L3 locus, *TCM1*, remains constant throughout the cell cycle (19, 143) and serves as a loading control. Flow cytometric analysis confirmed that the cells synchronously traversed two cell cycles, and that the points of maximal *PHO5* transcript accumulation coincide with M phase (Fig 2-1C).

To examine whether the canonical PHO signal transduction pathway is involved in *PHO5* mitotic activation in YPD, we deleted three different positive regulators of the low P_i induction pathway and assayed *PHO5* expression during synchronous growth in YPD. Deletions of *PHO4* and *PHO2*, encoding DNA site-specific transactivators of *PHO5*, abrogate mitotic induction of *PHO5* (Fig. 2-1A,B). A null allele of the CDK inhibitor *PHO81* eliminates approximately 95% of the mitotic expression. Since *PHO5* activation is completely dependent on Pho81 for inhibition of the Pho80-Pho85 cyclin-CDK (135), the residual level of expression in the *pho81*Δ strain is unexpected and suggests that a weaker, Pho81-independent activation mechanism also functions at *PHO5* during mitosis. We also determined the effects of the *pho2*, *pho4*, and *pho81* null mutations on rAPase activity in asynchronous cultures, which can often be used to observe cell cycle-dependent events (54). Approximately 60-110 U of rAPase activity are detected in asynchronous YPD cultures of wild-type strains (Figs. 2-1). Enzyme

activity is reduced by more than 99% in *pho4*Δ and *pho2*Δ strains.

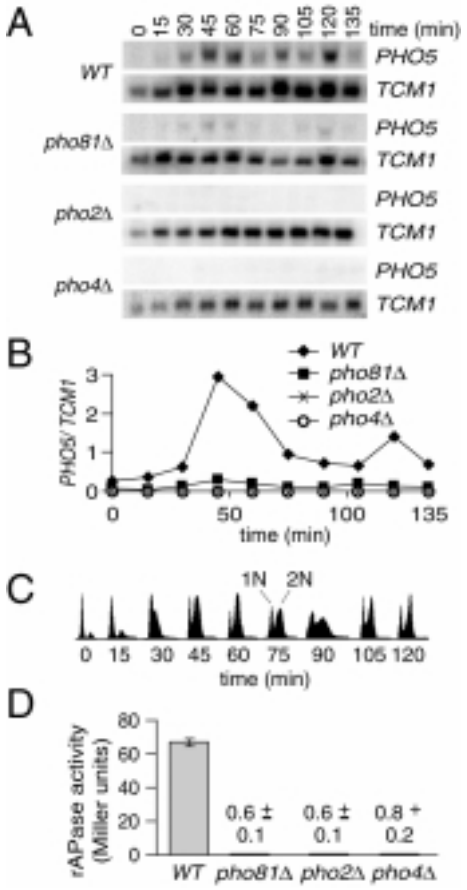

FIG. 2-1. Mitotic induction of *PHO5* requires *PHO2*, *PHO4*, and *PHO81*. (A) Northern analysis of wild-type (*WT*), *pho81*Δ, *pho2*Δ, and *pho4*Δ cultures at various times following release from synchronization with α factor. The wild-type strain was analyzed in parallel to each null strain as a positive control. (B) Transcript levels of *PHO5* (normalized to *TCM1*) from *A*. Data shown are representative of two independent experiments. (C) Flow cytometric analysis of Sytox Green-stained cells. The x- and y-axis indicate the fluorescence intensity and numbers of cells analyzed (which was identical in each panel), respectively. 1N and 2N refer to haploid and diploid DNA content, respectively. (D) Total rAPase activity of asynchronous YPD cultures. The mean ± 1SD from three independent experiments is shown.

Despite the residual level of mitotic *PHO5* mRNA, rAPase activity is also eliminated in the *pho81*Δ strain. We conclude that most of the measurable rAPase activity in asynchronous YPD cultures of strain DNY742 (*pho3*Δ) can be attributed to expression of *PHO5*, and presumably that of the minor rAPases *PHO11* and *PHO12*, in M phase (19, 143). Further, mitotic induction of *PHO5* is strongly dependent on the positive *PHO* effectors *PHO4*, *PHO2*, and *PHO81*.

Mitotic activation of *PHO5* requires the chromatin remodelers Gcn5 and SNF/SWI. Next, we investigated the requirements, in mitotic activation of *PHO5*, for chromatin remodeling enzymes, including Gcn5, the catalytic subunit of several histone H3 acetyltransferase complexes (13, 42) and the Snf2/Swi2 ATPase subunit of the SNF/SWI chromatin remodeling complex (74). Since *gcn5*Δ cells could not be arrested with α factor, presumably because Gcn5 is required for expression of the CDK inhibitor *FAR1* (51), we synchronized cells in G2/M with nocodazole, an inhibitor of microtubule polymerization. After release from G2/M, wild-type cultures progressed through three cell cycles and showed maximal *PHO5* induction at 15, 105, and 150 min (Fig. 2-2A,B), each peak corresponding to M phase (Fig. 2-2C). In contrast, no induction was observed in the *snf2*/*swi2*Δ and *gcn5*Δ strains, indicating that mitotic induction of *PHO5* is highly dependent on these transcriptional coactivators. Greater than 90% of the rAPase activity of asynchronous cultures is eliminated in each null strain, demonstrating that synchrony is not required to observe the requirement for SNF/SWI and Gcn5 (Fig. 2-2D). We conclude that the previously reported Gcn5- (51) and Snf2/Swi2-dependent (145) transcription of *PHO5* in asynchronous YPD cultures is explained by the pronounced

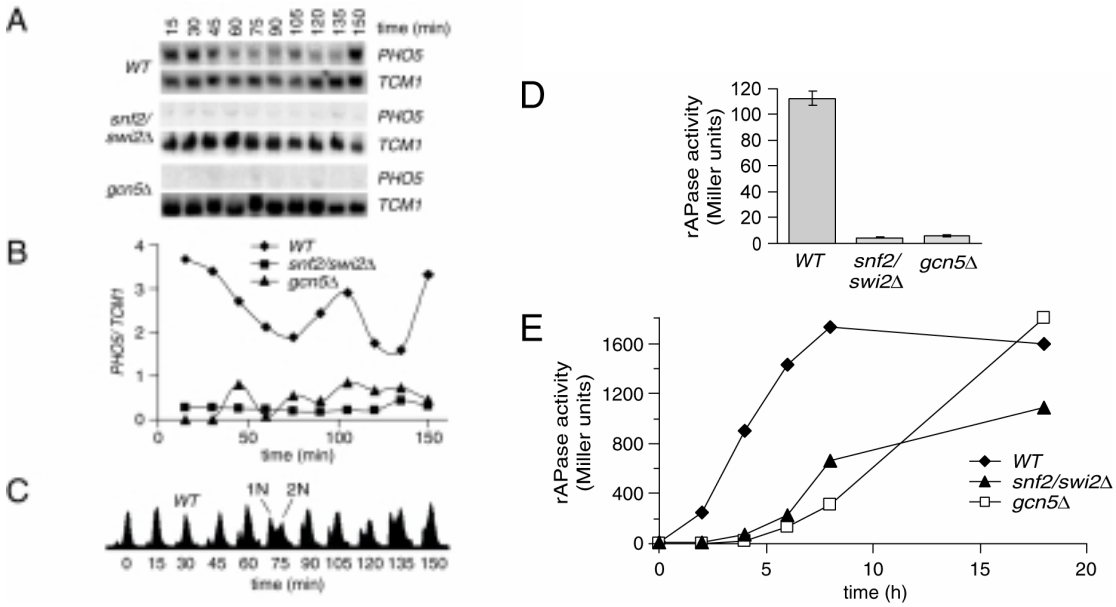

FIG. 2-2. *PHO5* activation is SNF/SWI- and Gcn5-dependent. (A) Northern analysis of synchronous cultures of wild-type (*WT*), *snf2*/*swi2*Δ, and *gcn5*Δ strains released from nocodazole arrest in YPD medium. (B) Normalized *PHO5* transcript levels from *A*. Data shown are representative of two independent experiments. (C) Flow cytometric analysis of wild-type cells in *A*. (D) Total rAPase activity of asynchronous YPD cultures (N = 3, mean ± 1SD). (E) Time course of *PHO5* activation. Asynchronous cultures grown on defined, P_i-free medium with 13.4 mM P_i added back were starved for P_i and assayed for total rAPase activity at the indicated times. Data shown are representative of two independent experiments.

need for these enzymes in *PHO5* mitotic expression.

Previous studies using asynchronous cell populations demonstrated that SNF/SWI and Gcn5 are not required for activation of *PHO5* following overnight starvation for P_i (37, 44). More recently, it has been shown that deletion of *GCN5* decreases *PHO5* activation at early times after P_i starvation, but not at 8 h post-activation (7). Figure 2-2E demonstrates that asynchronous cultures of *gcn5*Δ and *snf2*/*swi2*Δ strains both exhibit a decreased initial rate of *PHO5* transactivation following

transfer to P_i-free medium. Thus, we have defined novel requirements for transcriptional coactivators at *PHO5* thereby including *PHO5* among other genes for which activation in M phase is strongly Gcn5- and SNF/SWI- dependent (67). Our data also confirm a role for Gcn5 in the rate of *PHO5* activation, and extend this observation to the SNF/SWI complex.

Mitotic activation of *PHO5* occurs under conditions of limiting P_i. Activation of *PHO5* by Pho4 in asynchronous cultures is dependent on P_i deprivation and, ordinarily, is rapidly repressed by the addition of exogenous P_i (134). Since increased *PHO5* transcription during mitosis is Pho4-dependent (Fig. 2-1), we tested if this cell cycle-specific activation in YPD is responsive to P_i levels. Surprisingly, despite 12 h of growth in YPD + P_i prior to α factor arrest and release, mitotic activation of *PHO5* is still apparent (Fig. 2-3A, B). However, when the incubation in YPD + P_i is extended to 55 h before α factor synchronization, *PHO5* transcript is not detectable. This result indicates that exogenous P_i attenuates mitotic induction of *PHO5* in a time-dependent manner. Next, we investigated the time dependence of repression of mitotic *PHO5* induction further. Relative to cells growing continuously on YPD, rAPase activity decreased by 50% when cultures were shifted from YPD to YPD + P_i (Fig. 2-4A, compare bar 1 to 2). Full repression of *PHO5* required longer incubation in YPD + P_i (compare bar 1 to 3). In the opposite experiment, pregrowth on YPD + P_i and shift to YPD, full derepression is restored (compare bar 1 to 4). This result suggests that repression of mitotic expression takes longer than its induction. The time required to achieve full repression of *PHO5* was assessed by pregrowth of cells in YPD followed by transfer to YPD + P_i. As in

Figure 2-4A, rAPase activity was reduced to ~60% of the control YPD culture at 6 h (Fig. 2-4B). Maximal *PHO5* repression is achieved after ~29 h and remained at this level for the rest of the time course. The time required to reach full repression is not likely to be due to rAPase stability, since the half-life of rAPase activity is 2-2.5 h as determined by the phosphate overplus procedure (P_i starvation followed by P_i addition; Materials

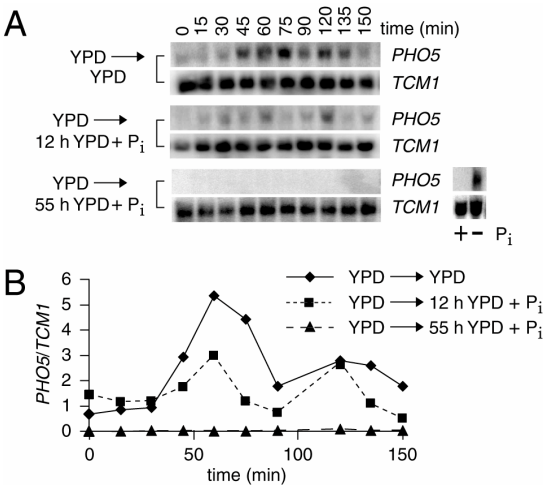

FIG. 2-3. *PHO5* mitotic activation is repressed by addition of orthophosphate (P_i). (A) Northern analysis of α factor-synchronized cultures. Single colonies from a YPD plate were inoculated into YPD overnight cultures and then diluted into YPD or YPD + P_i (13.4 mM) for 12 or 55 h (indicated at left) prior to the α factor arrest. Cells grown for 6 h in defined, P_i-free medium with (+) or without (–) P_i were included as a positive control in the Northern analysis of the samples grown for 55 h in YPD + P_i. (B) Normalized *PHO5* transcript levels from *A*. Data shown are representative of three independent experiments.

and methods; data not shown). The remaining activity may be due to basal levels of *PHO5* expression and that of the more minor rAPases, *PHO11* and *PHO12*, which vary somewhat between experiments. These findings demonstrate that YPD can be limiting

for P_i. The lag in full repression may be due to active growth in YPD that leads to rapid metabolism of a PHO repressive signal.

PolyP reserves increase, but are not essential for, repression of *PHO5*. PolyP is the most prevalent form of phosphate in yeast and it is believed to serve as a P_i reservoir (39, 140, 150). Such a P_i reservoir might sustain intracellular P_i levels more effectively

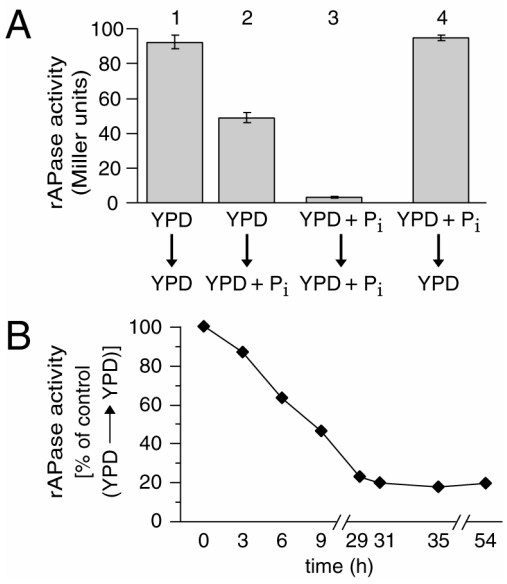

FIG. 2-4. Repression of *PHO5* mitotic expression by added P_i is time dependent. (A) Total rAPase activity of asynchronous cultures. Cultures were grown overnight in either YPD (bars 1 and 2) or YPD + P_i (bars 3 and 4) and then washed and resuspended in YPD (bars 1 and 4) or YPD + P_i (bars 2 and 3) for an additional 6 h as indicated (N = 3, mean ± 1SD). (B) Time course of decrease in total rAPase activity following addition of P_i. Cells were plated and pregrown on YPD and transferred to YPD (control) or YPD + P_i. The percentage of activity of the control (growth in parallel in YPD) as a function of time is plotted. Data shown are representative of two independent experiments.

during P_i deprivation and hence repress M-phase expression of *PHO5*. To test this hypothesis, we asked if strains singly null for four *PHM* genes had increased levels of

total rAPase activity. Strains deleted for *PHM3* and *PHM4* are severely deficient for the Phm/Vtc complex and thus lack detectable polyP, but do not exhibit growth defects. The phenotypic defects of *phm1*Δ and *phm2*Δ strains are much less pronounced (96, 110). In Figure 2-5A, each strain was grown in YPD and then diluted into YPD or YPD + P_i for 6 h. Relative to wild-type cells, rAPase activity during continuous growth in YPD increases 2 to 2.5-fold in *phm3*Δ or *phm4*Δ strains, and only modestly in *phm1*Δ or *phm2*Δ cells (Fig. 2-5A). Thus, the magnitude of *PHO5* derepression in P_i-limiting conditions (YPD) correlates well with the severity of the polyP accumulation defect and extent of disruption of Phm/Vtc complex integrity; *phm1*Δ > *phm2*Δ > *phm3*Δ ≈ *phm4*Δ (96, 110). Interestingly, incubation in YPD + P_i for 6 h reversed the *PHO5* derepression and lower levels of expression were established in the absence of Phm3 and Phm4.

To explore the relationship between *PHO5* mitotic activation and polyP levels further, we tested whether conditions of high P_i increase cellular polyP, and if so, what its effects are on total rAPase activity. Consistent with our finding that YPD is limiting for P_i (Figs. 2-3, 2-5A), a wild-type (*PHM3*) strain grown in YPD has low but significant levels of polyP (Fig. 2-5B, lane 1). The isogenic *phm3*Δ strain has no detectable polyP (110) (Fig. 2-5B, compare lane 1 to 3). In this experiment, rAPase activity is increased 4-fold in the *phm3*Δ strain relative to the wild-type strain, again demonstrating that loss of polyP leads to increased *PHO5* activation in YPD. When wild-type (*PHM3*) cells are

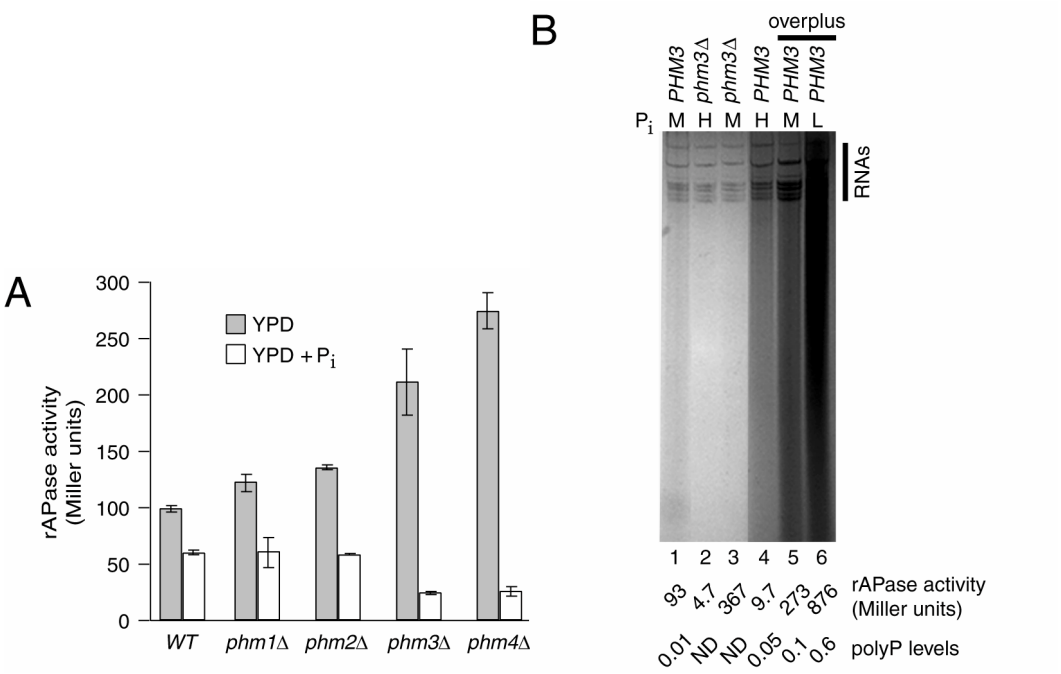

FIG. 2-5. Loss of polyP leads to derepression of *PHO5*. (A) Total rAPase activity of wild-type (*WT*), *phm1*Δ, *phm2*Δ, *phm3*Δ, and *phm4*Δ strains. Cells were grown in YPD and diluted to YPD (shaded bars) or YPD + P_i (unshaded bars) medium for 6 h prior to assaying rAPase activity (N = 3, mean ± 1SD). The severity of loss of polyP accumulation increases from left to right and parallels the extent of disruption of the Phm/Vtc complex, with *phm3*Δ and *phm4*Δ strains having no detectable polyP or Phm/Vtc complex (96, 110). (B) Analysis of polyP levels. Wild-type (*PHM3*) or *phm3*Δ strains were grown 2 d on plates and then 24 h in liquid YPD-low P_i, YPD, or YPD + P_i containing a low (L, lane 6), moderate (M, lanes 1, 3, and 5), or high (H, lanes 2 and 4) concentration of P_i, respectively. For lanes 1-4, after the 24 h incubation period, internal aliquots of each culture were assayed for rAPase activity and polyP levels by the metachromatic absorbance shift method (indicated at bottom; ND, non-detectable). The overplus samples (lanes 5-6) received additional treatments of P_i starvation followed by P_i addition (Materials and methods) before determining rAPase and polyP levels. PolyP was also visualized in the gel after electrophoresis of equal amounts of total RNA (10 μg) and staining with toluidine blue O dye, a basic dye that binds polyanions. RNA species at the top of the gel are labeled 'RNAs'. Data shown are representative of two independent experiments.

grown in high-P_i media (YPD + P_i), polyP amounts increase 5-fold (Fig 2-5B, compare lane 1 to 4), which is accompanied by a 10-fold reduction in rAPase activity and non-detectable *PHO5* transcript levels in M phase (Fig. 2-3). During growth in complete synthetic medium (7.3 mM P_i), wild-type strains accumulate similar levels of polyP [0.07 (A_{530}/A_{630})/μg RNA] and rAPase activity (13 U) as in YPD + P_i (13.4 mM). As expected, the *phm3*Δ strain had no detectable polyP in YPD + P_i (110), but as in Figure 2-5A, had repressed levels of rAPase activity (Fig. 2-5B, lane 2). This indicates that polyP is not required to repress *PHO5* when P_i is plentiful. We conclude that, under conditions of limiting P_i, accumulated polyP acts as a cellular P_i reserve that can contribute to the repression of *PHO5* expression. However, as *PHO5* is completely repressed by excess P_i in strains that are unable to accumulate polyP, the polymer is not necessary for *PHO5* promoter inactivation.

When *S. cerevisiae* encounters a period of P_i starvation followed by a high P_i environment, a phenomenon called "overplus" or "overcompensation" occurs in which large amounts of polyP accumulate (66). This method was previously used to evaluate the role of *PHM* genes in polyP synthesis (110). In parallel with the samples of Figure 2-5B, lanes 1-4, wild-type cells subjected to the overplus procedure (see Materials and methods) accumulate 60-fold more polyP than during continuous growth in YPD (Fig. 2-5B, compare lane 5 to 1). Interestingly, overplus polyP levels surpass that of cultures grown continuously in YPD + P_i (compare lane 4 to 5). The highest level of polyP is observed upon growth in YPD-low P_i before addition of P_i (compare lane 6 to lanes 1-5).

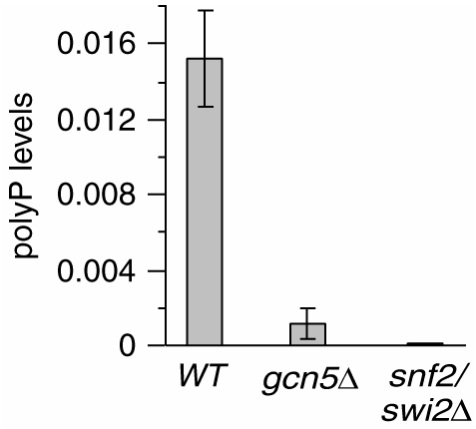

FIG. 2-6. SNF/SWI and Gcn5 are required for polyP accumulation. Steady-state levels of polyP from wild-type (*WT*), *gcn5*Δ, and *snf2*/*swi2*Δ strains were measured (N = 3, mean ± 1SD) by the metachromatic shift method after asynchronous growth in YPD (the same conditions used for rAPase activity measurements in Figure 2-2D).

Therefore, the amount of polyP that accumulates during the overplus procedure is proportional to the severity of prior P_i starvation, consistent with increased transcription of *PHM* and/or other genes that may play direct or indirect roles in polyP biosynthesis (52, 110). In contrast, as relatively high levels of polyP are synthesized in wild-type cells when excess P_i is present, polyP synthesis does not require a preceding period of P_i starvation.

Accumulation of polyP under limiting P_i conditions requires SNF/SWI and Gcn5. Levels of polyP and *PHO5* expression are inversely correlated (Fig. 2-5B, lanes 1 and 4 or 3 and 4). Thus, the loss of mitotic *PHO5* activation in *snf*/*swi* and *gcn5* mutants (Fig. 2-2) might be due to a pleiotropic hyperaccumulation of polyP. We determined, however, that polyP levels were decreased more than 10-fold and near the detection limit in *gcn5*Δ and *snf2*/*swi2*Δ strains, respectively, during continuous growth in YPD (Fig. 2-

6). This result suggests that SNF/SWI and Gcn5 are needed for M phase activation of *PHM* genes as well as *PHO5* when P_i is limited.

Polyphosphate levels fluctuate during the cell cycle. Because *PHO5* expression is inversely related to polyP reserves (Fig. 2-5), we investigated if mitotic activation of *PHO5* is correlated with a decrease in polyP levels before M phase in α factor-synchronized cultures (Fig. 2-7). Maximal levels of polyP are observed at G1 (0-15 min) and reach a minimum when cells are well into S phase, 45-60 min after α factor removal. The 6 to 10-fold increase in polyP levels as compared to Figures 2-5B and 6 is reproducibly observed following synchronization. Nevertheless, a 4 to 5-fold drop in polyP levels precedes peak accumulation of *PHO5* mRNA in mitosis, which occurs at 75 min. PolyP amounts remain at the minimum through 105 min and then increase 5-fold at 120 min. Presumably, this is because enhanced mitotic expression of *PHO5* (Fig. 2-7B), other rAPase genes, and *PHO84*, the high-affinity P_i transporter, lead to increased scavenging of P_i and hence polyP synthesis. These data indicate that, in P_i-limiting medium (*e.g.*, YPD), polyP levels fluctuate with the cell cycle. Importantly, this result also suggests that the physiological basis for mitotic cycling of *PHO5* is due to significant, but not complete, depletion of polyP reserves prior to M phase.

Loss of polyP increases the rate, magnitude, and duration of *PHO5* activation. We also assessed the effects of the absence of polyP deficiency on *PHO5* activation during synchronous cell cycle progression. Following α factor synchronization and release in YPD medium, in comparison to wild-type cells, induction of *PHO5* in the *phm3*Δ strain,

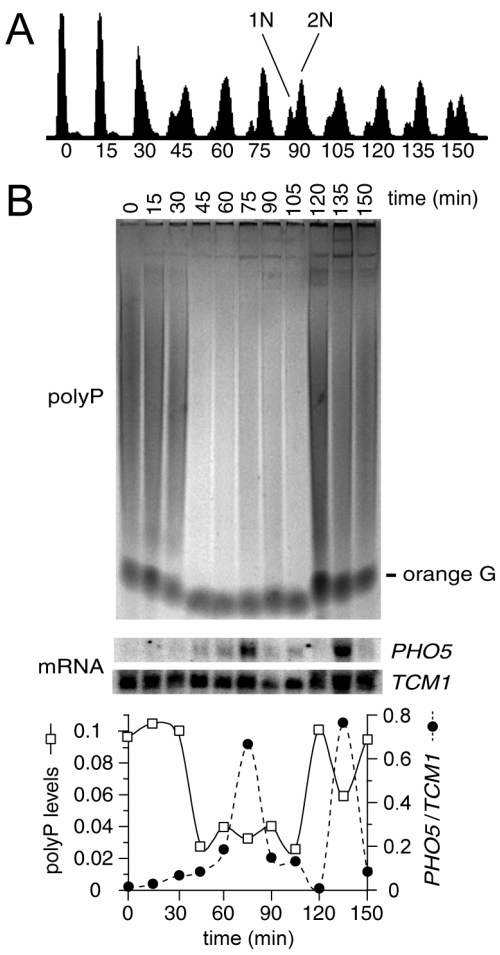

FIG. 2-7. PolyP levels fluctuate during the cell cycle. (A) Flow cytometric analysis of α factor-synchronized cultures. (B) Analysis of polyP and mRNA levels. Total RNA/polyP were isolated at 15 min intervals following release from α factor arrest. PolyP was analyzed as in Figure 2-5B, except that samples were treated with RNase A prior to electrophoresis (polyP gel) and metachromatic shift quantification of polyP levels of an internal fraction (graph at bottom). Northern analysis of *PHO5* and *TCM1* mRNA levels of internal aliquots of RNA/polyP not treated with RNase A (middle) are plotted *versus* time and compared to polyP levels at bottom. Data shown are representative of three independent experiments.

which lacks detectable polyP (110), increases dramatically (Fig. 2-8). Furthermore, *PHO5* mRNA was evident earlier in the *phm3*Δ strain, indicating that the null cells lose the repressive signal inactivating *PHO5* transcription before their wild-type counterparts. Flow cytometric analysis demonstrated that the length and timing of each cell cycle phase in the *phm3* strain was indistinguishable from wild-type (data not shown), consistent with its wild-type growth phenotype (23). Therefore, the absence of Phm3 causes increased levels of *PHO5* transcription that are not due to a higher proportion of cells in M phase.

Strains lacking the Phm/Vtc complex are defective in sustaining transport of P_i that is added during the overplus procedure (110), making it possible that *PHO5* would be derepressed (73). However, a low level of *PHO5* transcript that precedes and follows the mitotic peak (Fig. 2-8A, B) strongly suggests that *PHO5* transcription is not

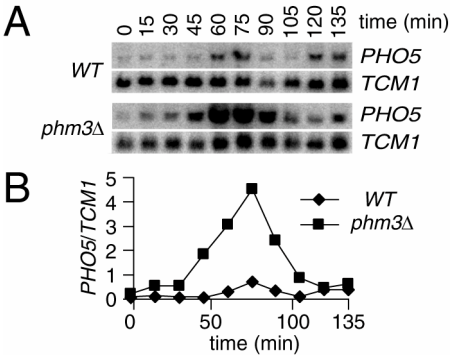

FIG. 2-8. Mitotic activation of *PHO5* is increased in *phm3*Δ strains. (A) Northern analysis of α factor-synchronized cultures of wild-type (*WT*) and *phm3*Δ cells. (B) Normalized *PHO5* transcript levels from *A*. Data shown are representative of four independent experiments.

constitutively derepressed in *phm* strains. Alternatively, it was hypothesized (110) that compromised P_i transport could indirectly result from the inability to synthesize polyP; the failure to divert added P_i to vacuoles leading to increased cytosolic P_i concentrations that signal degradation of Pho84, the high-affinity P_i transporter (164). Nevertheless, employing the overplus treatment with asynchronous wild-type and *phm3*Δ cultures, an identical, precipitous drop in *PHO5* transcript levels occurs between 20-30 min after P_i addition (data not shown). We conclude that the initial 5 min period of P_i transport observed in *phm3*Δ cells during the phosphate overplus (110) is sufficient to signal *PHO5* repression.

The rapid onset of accumulation of *PHO5* transcript in the *phm3*Δ strain (Fig. 2-8), even prior to G2/M where all cells have achieved a 2N DNA content, suggests an increased rate of *PHO5* activation in the absence of polyP reserves. To evaluate this possibility, we tested how polyP stores influence the initial rate of *PHO5* mRNA accumulation in asynchronous cultures in response to P_i starvation (Fig. 2-9). Wild-type and *phm3*Δ strains were first grown in defined, P_i-free medium with 13.4 mM P_i added back so that substantial cellular polyP would accumulate. Subsequently, P_i was removed by washing, both cultures were shifted to P_i-free medium, and levels of *PHO5* mRNA as well as rAPase activity were monitored over time. *PHO5* transcript accumulates linearly in both the wild-type ($R^2 = 0.96$) and *phm3*Δ ($R^2 = 0.99$) strains for 150 and 90 min, respectively. Strikingly, the initial, rapid response to P_i starvation occurs 60 min earlier and at a 3-fold higher rate in the *phm3*Δ strain. Moreover, *PHO5* transcript levels in the

*phm3*Δ strain are significantly higher (120-fold more at 60 min) at every time point up to

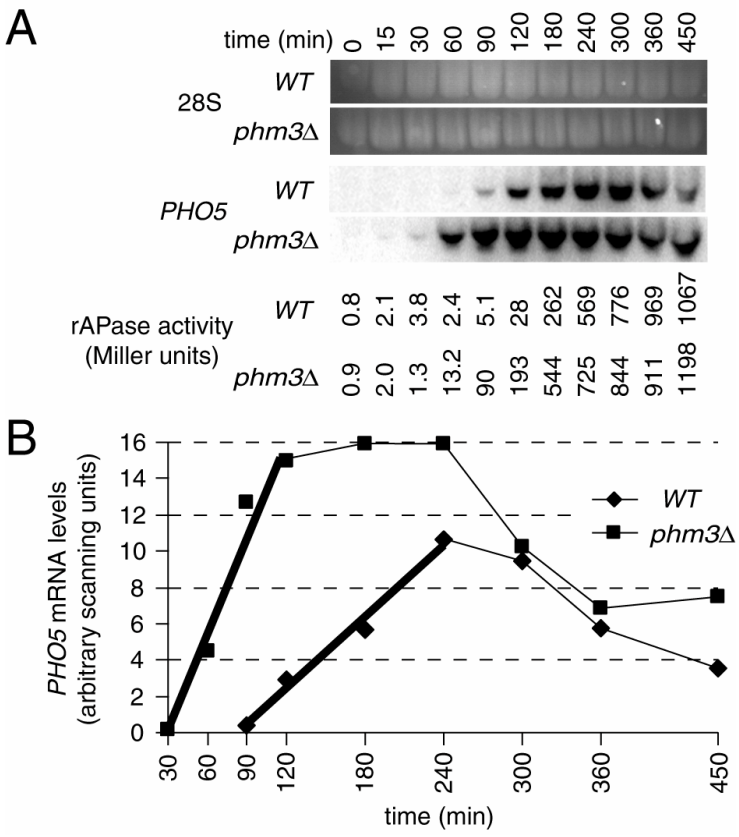

FIG. 2-9. Deletion of *PHM3* increases the rate of *PHO5* activation. (A) Northern analysis of RNA isolated during a time course of *PHO5* activation. Wild-type (*WT*) and *phm3*Δ strains grown on defined, P_i-free medium with 13.4 mM P_i added back (to build up stores of polyP in the wild-type strain) were then starved for P_i by washing and resuspension in P_i-free medium and RNA was isolated at the indicated times. Total rAPase activities obtained from an internal aliquot of each culture are indicated below each lane. (B) Absolute *PHO5* transcript levels from *A*. The thick trendline indicates the initial, linear period of transcript accumulation. Data shown are representative of two independent experiments.

and including 4 h, achieve maximum 2 h earlier, and are maintained at this higher level longer than in wild-type cells. Subsequently, *PHO5* mRNA levels plateau, and then, interestingly, decline to a similar level in both cultures around 6 h after P_i starvation. As

expected, the levels of internally assayed rAPase activity lag behind and qualitatively support these observations (Fig. 2-9A). The absence of a decrease in rAPase activity at the later time points likely reflects the increased stability of the protein relative to *PHO5*, *PHO11*, and *PHO12* transcripts (161). We conclude that the initial rates of accumulation of *PHO5* transcript and rAPase activity, and presumably the rates of transcriptional initiation, are enhanced in cells lacking polyP. Further, the repressive influence of polyP reserves on *PHO5* transcription was observed in a defined medium, which complements our results obtained using YPD medium.

Discussion

We have investigated the molecular mechanisms and physiological basis for activation of *PHO* promoters, which are in a prominent class of mitotically-induced genes with nutritional roles (143). In contrast to previous findings using P_i-starved, asynchronous cultures, we find that *PHO5* activation in M phase in synchronized cultures grown in rich medium is strongly dependent on the SNF/SWI complex, an ATP-dependent chromatin remodeler, and the histone acetyltransferase, Gcn5 (Fig. 2-2). Additionally, our work shows that M phase-induction of *PHO5* requires the transactivators Pho2 and Pho4 as well as the CDK inhibitor Pho81, suggesting that *PHO5* mitotic induction occurs through the PHO signal transduction pathway (Fig. 2-1). In accord with this, addition of exogenous P_i suppresses mitotic activation of *PHO5* (Fig. 2-3) and increases polyP levels, which are inversely correlated with *PHO5* expression in wild-type cells (Fig. 2-5B). Further, in synchronized cultures, polyP amounts decrease between G1 and

M phase, demonstrating that metabolic pools of polyP fluctuate during the cell cycle (Fig. 2-7). Beyond these correlations, we show that strains with non-detectable levels of polyP (*phm3*Δ) exhibit a dramatically enhanced PHO response in both synchronous and asynchronous cultures (Figs. 2-8 and 2-9). These results establish that polyP causally represses *PHO5* expression. Moreover, the physiological stimulus for activation of *PHO5* in M phase is P_i depletion that ensues after reduction of vacuolar polyP reserves. Thus, our results expand the role of the *PHO* signaling system to include coordination of the mitotic activation with P_i availability during cell cycle progression. Our data also highlight a novel function for polyP, as a negative regulator of *PHO* activation in mitosis.

Our findings support the model that a central, physiological role of polyP is that of a P_i reservoir (39, 140). Under conditions of limiting P_i, inasmuch as degradation of polyP increases intracellular P_i pools, the polymer antagonizes *PHO5* activation. It is likely that our findings apply generally to other *PHO* (and *PHM*) genes, since the rate of *PHO84* transcript accumulation is also enhanced upon P_i starvation in a *phm3*Δ strain (D.W.N. and M.P.K., unpublished data). It must be emphasized that Phm/Vtc complex activity, and hence polyP, is not required to maintain (Fig. 2-9, zero point) or establish (Fig. 2-5) repression of *PHO5* when P_i is abundant. Further, a lack of detectable polyP does not impair the ability to repress *PHO5* transcription before and after the mitotic peak in synchronized populations (Fig. 2-8). Thus, polyP is a modulator rather than an essential cell cycle regulator of *PHO* expression, replenishing intracellular levels of P_i when metabolic demand for it is high.

The inability to make polyP in the absence of the Phm/Vtc complex allowed us to address the interplay between polyP and *PHO5* regulation during M phase. Extensive P_i starvation leads to G1 arrest (78), primarily due to controls that operate at Start (126). Although the mechanisms are unclear, it is widely accepted that these controls involve attaining sufficient cell size and nutrient acquisition for cell division. In view of this, while cells have already gauged sufficient phosphate resources to execute Start, why do they rapidly mobilize their polyP reserves with synchronous progression through S phase (Fig. 2-7)? It is possible that polyP reserves are directly sensed as a P_i source prior to Start. However, if this was the case, constitutive activation of *PHO5* outside of M phase would be expected in the absence of polyP (*phm3*Δ cells), which is not observed (Fig. 2-8). Instead, since *phm3*Δ cells lack reserve P_i afforded by polyP, they exaggerate mitotic induction of *PHO* genes (Fig. 2-8). Thus, while the cell division commitment decision is made at G1, our data suggest that the sensing of and response to nutrient imbalances is not restricted to G1 (153). This view is supported further in that *PHO5* is strongly activated by P_i starvation during sustained mitotic arrest (D.W.N. and M.P.K., unpublished data). Since the cells could not anticipate the post-Start starvation, we conclude that they are able to sense P_i at cell cycle stages other than G1.

We propose the following model for *PHO5* mitotic activation under conditions of limiting P_i (*e.g*, YPD). A yeast cell maintains cytosolic P_i at levels sufficient to satisfy metabolic needs and stores any excess as polyP. Upon reaching critical size and nutrient status, the cell will initiate Start and probably decrease cytosolic P_i rapidly while synthesizing nucleotides for DNA replication and transcription, as well as phospholipids

for the enlarging bud. PolyP reduction also correlates with marked increases in sugar phosphates during synchronous entry into S phase (39, 105). As the intracellular P_i concentration declines and is unable to be replenished by preferred extracellular P_i (39), it may first be more expedient to degrade polyP to P_i, presumably by endo- (Ppn1) and exopolyPases (69, 137). Subsequently, when polyP reserves and hence cytosolic P_i fall critically low, transcription of the *PHO* and *PHM* genes is activated. During M phase, and possibly into G1, rAPase synthesis leads to hydrolysis of phosphoesters in the medium, which supplies P_i for import via the high affinity transporter Pho84, which is also expressed in mitosis (143). Increased cytosolic P_i (or some anabolite of P_i) leads to attenuation of the *PHO* mitotic induction. After metabolic growth requirements are met, excess P_i is assimilated into polyP, thus reconciling the seeming paradox that cells synthesize polyP in response to P_i deprivation.

The primary reason for *PHO* mitotic expression may be to sequester as much P_i as is feasible as vacuolar polyP. This view is supported in that *pho4*Δ cells exhibit a wild-type growth rate in YPD, despite the absence of detectable polyP (110) (Fig. 2-5B) and inability to activate PHO genes in mitosis (Fig. 2-1). Hence, the amount of P_i (or phosphate esters) and basal levels of PHO gene expression are adequate for *pho4*Δ cells to meet their P_i growth requirements. Therefore, mitotic PHO activation may simply confer an adaptive advantage through hoarding P_i as polyP or significant conservation of transcriptional resources, antagonizing excessive activation of *PHO5* (Figs. 2-8, 2-9) and ~20 additional *PHO*, *PHM*/*VTC*, and other genes (52, 110).

We find that activation of *PHO5* during mitosis in YPD and the initial period of

P_i starvation are strongly dependent on SNF/SWI and Gcn5 (Fig. 2-2). In contrast, activation of *PHO5* in asynchronous cultures extensively starved for P_i is refractory to the loss of both chromatin-remodeling activities (37, 43). This apparent discrepancy is potentially explained by a global requirement for Gcn5 and SNF/SWI in mitotic gene expression (67). The relatively short time (~15-30 min) of mitotic activation may also contribute to the pronounced Gcn5 and SNF/SWI dependence, since these coactivators are needed for wild-type rates of *PHO5* activation (7) (Fig. 2-2E). Because *snf*/*swi* and *gcn5* mutants have very low levels of polyP (Fig. 2-6), it is unlikely that they exhibit lower rates of *PHO5* activation due to impaired growth and hence slower depletion of cellular P_i. Moreover, the rates of transactivation of double *snf*/*swi phm3* and *gcn5 phm3* mutants with undetectable polyP are also lower than *phm3* cells (data not shown).

PHO5 transcription is also Gcn5- and SNF/SWI-dependent in asynchronous cultures grown in YPD (51, 145), but does not require SNF/SWI in synthetic minimal medium (145). We propose that this media-specific difference for SNF/SWI can now be explained in terms of polyP. Mitotic expression of *PHO5* in cells grown in YPD is higher due to its low levels of P_i and hence vacuolar polyP. In contrast, the high P_i concentration (7.3 mM) of minimal medium leads to substantial increases in polyP that repress M-phase expression (Fig. 2-5).

The antagonism between polyP/P_i levels and the magnitude of PHO activation suggests that nutrient sensing may underlie the transcriptional periodicity of other cell cycle-regulated genes. In particular, transcripts for genes involved in the transport of a variety of nutrients in addition to P_i, including carbohydrates, heavy metals, ions, and

amino acids, fluctuate during the cell cycle (143). Genes involved in glycogen (*GSY1*) and fatty acid synthesis (*FAA1*, *FAS1*) are also cell cycle-regulated in rich medium. Depending on the particular sensing system, the presence or absence of nutrients may lead to periodic increases or decreases in transcription of genes during the cell cycle. Alternatively, the low levels of P_i in YPD may contribute indirectly to the periodic expression of some genes. For example, mitotic induction of the plasma membrane ATPase, *PMA1*, may generate the proton gradient that is requisite for Pho84-mediated symport of P_i (and many other nutrients). Finally, since polyP chelates cations (30), it is plausible that their uptake is coordinated with polyP synthesis. It remains to be seen if the loss of polyP affects transcription of any of these additional cell cycle-regulated genes.

CHAPTER III

NOVEL ROLES FOR MCM1 AND SFF AS TRANSCRIPTIONAL ACTIVATORS OF MITOTIC *PHO5* INDUCTION

Introduction

Propagation of all species requires proliferation at the cellular level. Controlled by the cell division cycle, cellular duplication occurs by the time-dependent execution of predetermined events. Regulation of these cell cycle events occurs through a variety of mechanisms most commonly orchestrated by a master regulator, like Cdc28 in the budding yeast *Saccharomyces cerevisiae*. A significant portion of this regulation occurs at the post-transcriptional level such as targeted protein degradation (122). Recently, however, several groups have confirmed that an important aspect of cell cycle regulation occurs at the transcriptional level, with approximately 13% of *S. cerevisiae* genes being expressed in a cell cycle-dependent fashion (19, 143). Regulation of cell cycle-dependent transcription seems to occur predominantly, yet not exclusively, via three classes of transcriptional activators, including SBF/MBF, Ace2/Swi5, and Mcm1 that regulate G1/S, M, and M/G1-dependent transcription, respectively (143). It is important to note that the roles outlined for these transcription factors are oversimplified as some overlap does occur, most notably for Mcm1, which has been shown to have important functions in virtually all phases of the cell cycle (34, 88).

Control of cell cycle-dependent transcription occurs most likely through cell cycle stage-dependent phosphorylation of transcription factors by Cdc28. It has, for example, been well established that Cdc28-Cln3 and Cdc28-Clb2, respectively, activate

and repress SBF/MBF and thereby control G1-specific transcription (63, 162). It is similarly thought that Cdc28-Clb2 controls mitotic gene activation, as overexpression of Clb2 induces transcription of many M- and M/G1-regulated genes. Clb2-responsive genes almost always contain binding sites for Mcm1 as well as Fkh1/2, commonly referred to as switch five factor (SFF) (143). Fkh1 and Fkh2 are transcriptional activators named for the similarity in their DNA binding domains to the forkhead proteins of higher eukaryotes. While Fkh1 and Fkh2 have redundant roles in controlling pseudohyphal growth (50), Fkh1 is required for silencing of *HMR***a** (50), and Fkh2 cooperates with Mcm1 to activate transcription of genes expressed during mitosis (65, 166). Both Mcm1 and Fkh2 have been shown to be phosphorylated, but only Fkh2 is phosphorylated in a cell cycle-dependent manner (70, 124). Evidence, however, has suggested that transcriptional control by Clb2 may be acting through phosphorylation of Ndd1, an essential coactivator for Mcm1-Fkh2-dependent gene activation (132).

Among the genes induced by Clb2 overexpression are the M/G1-specific acid phosphatases *PHO5*, *PHO3*, *PHO11*, and *PHO12*, which are induced by P_i starvation (110, 143). Cell cycle expression of these, and possibly other nutrient-responsive genes, seems to occur independently of traditional cell cycle regulators, as we showed that their mitotic expression is controlled almost exclusively by the P_i-dependent transcriptional activators Pho4 and Pho2 (103). More importantly, full repression of mitotic *PHO5* induction is achieved by the addition of exogenous P_i to the medium, indicating that induction occurrs not due to predetermined cell cycle events, but rather was responding

to cell cycle-dependent P_i starvation. It is unclear then why mitotic expression of *PHO5* is controlled through both P_i fluctuations, as well as the master regulator Cdc28.

This work elucidates the interplay between the cell cycle-dependent transcription machinery and P_i-responsive transactivators in controlling mitotic expression of *PHO5*. We show that Mcm1 and SFF contribute to mitotic expression of *PHO5*. Binding of Mcm1 to the *PHO5* promoter is not detectable in rich medium, which is partially limiting for P_i, but increases upon P_i starvation and is dependent on both Pho4 and Pho2. We therefore define Mcm1 and SFF as important transcriptional regulators of *PHO5* that ensure maximal mitotic activation during each cell division cycle.

Materials and methods

Yeast strains and media. *S. cerevisiae* strains used in this study are listed in Table 3-1. Strains used for overexpression of *MCM1* contain pSTAR, consisting of a doxycycline-responsive activator (TetA) and repressor (TetR) that are to be described elsewhere (A. Dhasarathy and M. Kladde, personal communication). In the absence of doxycycline, the repressor, TetR, is bound to a promoter containing seven *tet* operator (*tetO*) sites and thereby represses transcription. Upon the addition of doxycycline, TetR is displaced and transcription is activated on TetA binding. Strains used to analyze the effects of FKH gene deletions are derived from the W303 strain background. All other strains are in the S288C background. Strains were grown in standard rich medium (YPD) containing yeast extract (Difco), peptone (Difco), and glucose as indicated. Synthetic, P_i-free medium contained 0.7 g yeast nitrogen base (YNB) without $(NH_4)_2SO_4$, phosphate, or amino acids (Bio101), 2 g glutamine, 20 g glucose, 3.9 g MES

(2-*N*-morpholino ethanesulfonic acid, pH 5.5), and 0.74 g complete synthetic medium lacking histidine, per liter. Growth media were supplemented with KH_2PO_4 to obtain the desired P_i concentration.

TABLE 3-1. *S. cerevisiae* strains used in this study

Strain	Genotype
DNY2772[a,f]	*MAT***a** *mcm1*Δ::*kanMX4* pJM231-[*CEN-HIS3-MCM1*]
DNY2773[a,f]	*MAT***a** *mcm1*Δ::*kanMX4* pJM231-[*CEN-HIS3-mcm1*^{R19A}]
DNY2774[b,f]	*MAT***a**/*MAT*α *ho*::pSTAR/*HO*
DRY2642[b,f]	*MAT***a**/*MAT*α *ho*::pSTAR/*HO K.l. URA3-tetO*$_7$*-MCM1*/*MCM1*
DNY2929[c,g]	*MAT*α
DNY2979[c,g]	*MAT*α *fkh2*Δ::*HIS3*
DNY2980[c,g]	*MAT***a** *fkh1*Δ::*TRP1 fkh2*Δ::*HIS3*
DNY2981[c,g]	*MAT***a** *fkh1*Δ::*TRP1*
DNY1061[d,f]	*MAT***a** *bar1*Δ::R
DNY2768[d,f]	*MAT***a** *PHO5*^{mcm1}
DNY2757[d,f]	*MAT***a** *PHO5*^{sff}
DNY2850[d,f]	*MAT***a** *PHO5* ^{mcm1sff}
MBY1259[d,f]	*MAT*α *MCM1-3HA*
DNY2824[e,f]	*MAT*α *MCM1-3HA pho80*Δ::*kanMX4*
DNY2907[e,f]	*MAT*α *MCM1-3HA pho4*Δ::*URA3*
DNY2927[e,f]	*MAT*α *MCM1-3HA pho2*Δ::*kanMX4*

[a]Strains are also *leu2Δ0 lys2Δ0 ura3Δ0 his3Δ1 pho3*Δ::R-*URA3*-R, where R is a *Zygosaccharomyces rouxii* recombinase site that remains after intramolecular recombination (60).
[b]Strains are homozygous diploids and are also *leu2Δ0*/*leu2Δ0 lys2Δ0*/*lys2Δ0 ura3Δ0*/*ura3Δ0 pho3*Δ::R/*pho3*Δ::R.
[c]Strains are also *ade2-1 his3-11,15 leu2-3,112 trp1-1 ura3-1 can1-100 pho3*Δ::R-*URA3*-R.
[d]Strains are also *leu2Δ0 lys2Δ0 ura3Δ0 pho3*Δ::R.
[e]Strains are also *leu2Δ0 ura3Δ0*.
[f]Strains are in the S288C background.
[g]Strains are in the W303 background.

Phosphatase activity assays. Strains were grown overnight in YPD to mid-logarithmic phase at 30°C and were diluted to an OD_{600} = 0.03 with fresh YPD and grown for an

additional 6 hr. Phosphatase assays were performed as previously described (103). For the *MCM1* overexpression analysis, strains were diluted into YPD or YPD + 2 μg/ml doxycycline. For P_i starvation experiments, cells were grown overnight in synthetic medium containing 13.4 mM P_i at 30°C. Then, cells were washed and resuspended in synthetic P_i-free medium, grown at 30°C for 7 hr and assayed for rAPase activity at the indicated times.

Chromatin immunoprecipitation analysis. Yeast cells were grown overnight in synthetic medium containing 13.4 mM P_i at 30°C. Cells were washed in P_i-free medium, then grown in either P_i-free or 13.4 mM P_i medium for 24 hr, and then 50 ml of culture (at OD_{600} = 0.4-1.0) were treated with 1% formaldehyde for 15 min at room temperature. The cross-linking reaction was quenched by the addition of glycine to 125 mM and incubation for 5 min at room temperature. The formaldehyde-treated cells were pelleted and washed twice with Tris-buffered saline (20 mM Tris, pH 7.5, 150 mM NaCl). Cells were then lysed through the addition of lysis buffer [50 mM HEPES, pH 7.5, 140 mM NaCl, 1% Triton-X 100, 0.1% deoxycholate, protease inhibitors (complete protease inhibitor tablet, Roche) and 1 mM PMSF], and glass beads followed by vigorous agitation in a bead beater (twice for 60 sec). Chromatin extracts were sonicated three times for 25 sec on level 4 (VirSonic100). Immunoprecipitation reactions contained 500 μl sheared chromatin, 120 μl 3.6 M NaCl, and 5 μl monoclonal anti-HA antibody (HA.11, Covance) and were incubated overnight at 4°C. Protein A sepharose beads were added to the immunoprecipitations and incubated for 1 hr at 4°C. Pelleted beads were washed twice with lysis buffer lacking protease inhibitors and PMSF, once with

lysis buffer lacking protease inhibitors and PMSF + 500 mM NaCl, once with wash buffer (10 mM Tris, pH 8.0, 0.75 M LiCl, 0.5% NP40, 0.5% deoxycholate, 1 mM EDTA) and twice with 1X TE (10 mM Tris pH 8.0, 1 mM EDTA). DNA from the immunoselected chromatin was eluted by two additions of 75 µl TES (50 mM Tris, pH 8.0, 10 mM EDTA, 1% SDS) at 65^{o}C for 10 min. Protein-DNA cross-links were reversed by further incubation at 65^{o}C overnight. DNA was purified by the addition of 125 µl H_20 and 0.125 mg proteinase K, incubation at 37^{o}C for 90 min, and isolation by the Wizard Prep PCR purification kit (Promega). DNA was eluted in 30 µl 0.1X TE buffer. For input samples, 30 µl cell extract were incubated with 95 µl TES, cross-links were reversed, and DNA was purified as described for other samples. ChIP samples were quantified by measuring their band intensities using a phosphorimager. Data is presented as a ratio of the immunoprecipitated promoter (*PHO5*, *PHO3*, *PHO11/12*, or *PHO84*) to the control promoter (*WHI4*) normalized to the ratio of the input samples.

Results

***PHO3, PHO5, PHO11,* and *PHO12* share Mcm1 and SFF binding sites.** To explore if cell cycle-dependent transcriptional activators are required for mitotic expression of P_i-responsive genes, we aligned the promoter regions of the acid phosphatase genes *PHO5*, *PHO3*, and *PHO11/12,* and compared them to the promoters of the mitotically-induced genes *SWI5*, *KIN3,* and *SPO12* (143). The promoter regions of *PHO11* and *PHO12* are identical and are therefore shown as one sequence. Consensus Mcm1 and SFF binding sites (82) were found approximately 170, 140, and 170 base pairs upstream

of the start codons of *PHO5*, *PHO3*, and *PHO11/12*, respectively (Fig. 3-1). Interestingly, the Mcm1 binding sites of all four acid phosphatases are 60% identical to those of *KIN3*, *SPO12* (143), and *SWI5* (80), suggesting an important role for Mcm1 in the activation of the acid phosphatase genes. The SFF binding sites are 71% identical, further suggesting a role for Mcm1/SFF in the activation of Pho5, Pho3, Pho11, and Pho12. When we examined the promoters of *PHO84* and *PHM4*, also P_i-dependent genes expressed in mitosis (143), neither binding site was found (data not shown). This suggests that Mcm1 and SFF binding sites, unlike Pho4 and Pho2 sites, are not common to all genes that respond to limiting P_i. Furthermore, when analyzing data of Spellman *et al.* (143), it is evident that mitotic expression of both *PHO84* and *PHM4* is approximately 3-fold lower than that of *PHO5*, *PHO3*, *PHO11*, and *PHO12*. Since *PHO84* and *PHM4* expression are still cyclic, we hypothesized that Mcm1 and SFF are not defining the oscillation of mitotic *PHO5* induction, but rather are assisting in the transcriptional amplitude of each oscillation.

Mcm1 and SFF are activators of *PHO5*. Mcm1 can function as both a transcriptional activator and repressor (33). We determined the role, if any, of Mcm1 in *PHO5* transcription. As Mcm1 is an essential gene, we utilized a partial loss of function allele, $mcm1^{R19A}$, previously shown to be partly defective in both DNA binding and transcriptional activation (1), to assay the effects of reduced Mcm1 activity on *PHO5* expression. Plasmids carrying either the wild-type or $mcm1^{R19A}$ allele were transformed

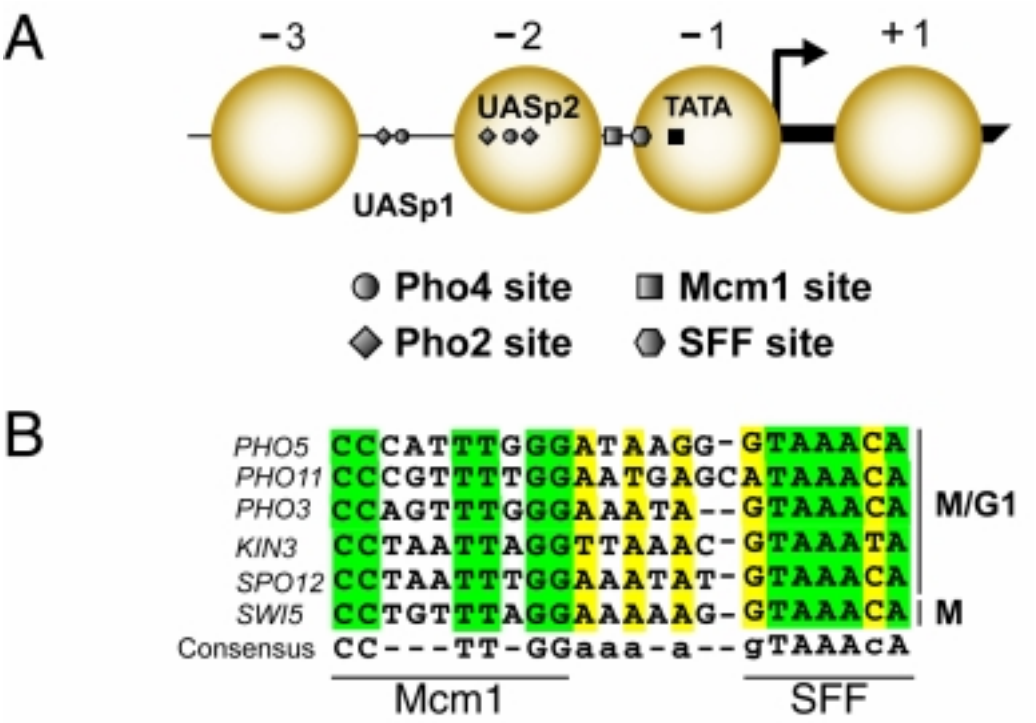

FIG. 3-1. Mcm1 binding sites in the promoters of *PHO5*, *PHO3*, and *PHO11/12* are homologous to those of *KIN3*, *SPO12*, and *SWI5*. (A) Schematic representation of the *PHO5* promoter. Mcm1 and SFF binding sites are positioned close to nucleosome –1 as indicated. UASp1 is positioned between nucleosomes –2 and –3, while UASp2 is blocked by nucleosome –2. (B) Mcm1 and SFF binding sites of selected gene promoters were aligned using the CLUSTALW algorithm. Positions highlighted in green are fully conserved, while those highlighted in yellow vary by one base.

into heterozygous diploid strains lacking one genomic copy of *MCM1*. Strains were sporulated, dissected, and subsequently screened for those carrying only the plasmid-borne copy of *MCM1*. Wild-type and *mcm1*^{R19A} strains were grown overnight in YPD, shifted to fresh YPD, and grown for an additional 6 hr prior to measuring *PHO5* activation by an acid phosphatase activity assay. Our previous work has shown that the repressible acid phosphatase (rAPase) activity of asynchronous YPD cultures is due to mitotic *PHO5* induction (103). Wild-type strains exhibited approximately 170 Miller

units activity, while *mcm1*^{R19A} strains achieved only about 60% of wild-type activity (Fig. 3-2A), suggesting that Mcm1 is required for full mitotic *PHO5* induction.

Overexpression of *MCM1* has served as an efficient way to define its role in either transcriptional activation or repression (3). To confirm further the role of Mcm1 as an activator of *PHO5* transcription, we overexpressed one genomic copy of *MCM1* in a homozygous diploid strain by replacing the wild-type promoter with a doxycycline-responsive promoter in cells expressing a doxycycline-responsive activator. Strains were grown overnight in YPD, and then diluted into either fresh YPD or YPD containing 2 μg/ml doxycycline to induce expression of *MCM1*, and rAPase activity was assayed after 6 hr. While the addition of doxycycline to the wild-type strain had no effect on *PHO5* expression (Fig. 3-2B), it did result in a 5-fold induction of *PHO5* in strains carrying the inducible *MCM1* allele (Fig. 3-2B), further supporting the role of Mcm1 as an activator of mitotic *PHO5* induction.

Like Mcm1, components of SFF have been shown to be important for both transcriptional activation and silencing (50). Recent microarray data have shown that deletions in both *FKH1* and *FKH2* have no detectable effect on the mitotic induction of *PHO5* (166). Nevertheless, the presence of a highly conserved, consensus SFF binding site in all four acid phosphatase promoters does suggest a role for either Fkh1 or Fkh2 in the induction of *PHO5* transcription. To test the hypothesis that SFF is acting with Mcm1 to activate *PHO5* transcription, we assayed the ability of strains lacking *FKH1* and/or *FKH2* to activate *PHO5* in asynchronous YPD cultures. Wild-type, *fkh1*Δ, *fkh2*Δ,

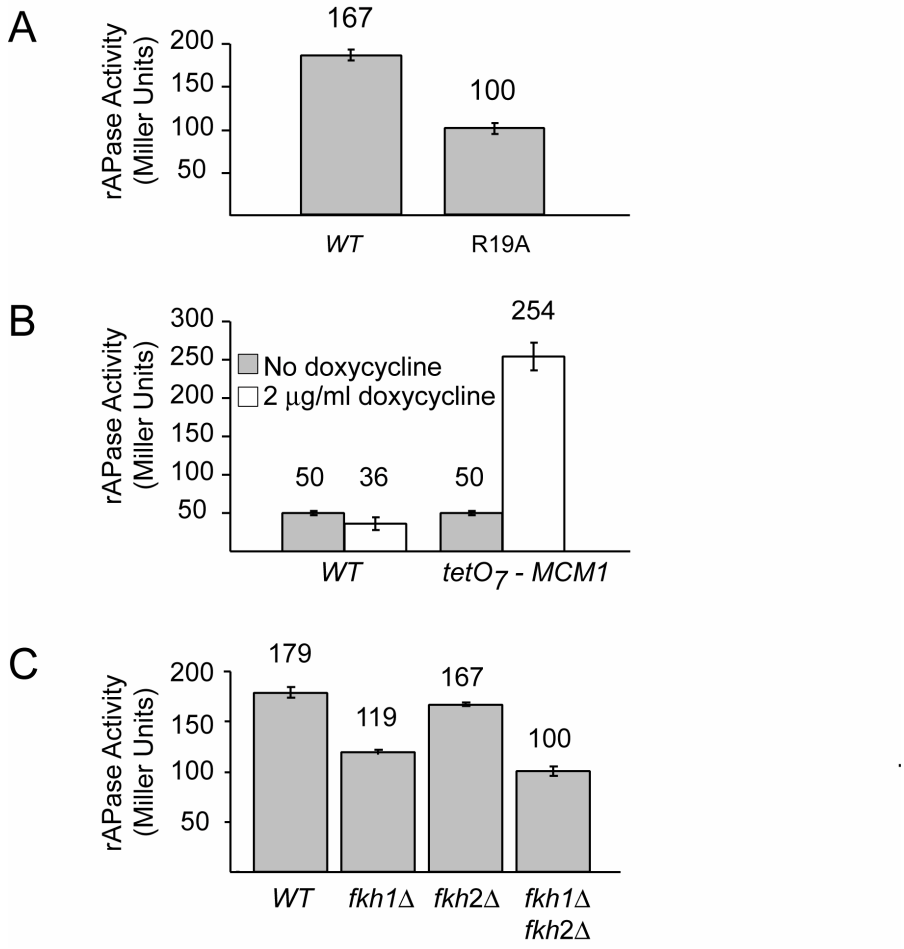

FIG. 3-2. Expression of *PHO5* is dependent on Mcm1 and SFF. Total rAPase activities of asynchronous YPD cultures of (A) Wild-type (*WT*) and *mcm1*^{R19A} strains, (B) Wild-type (*WT*) and *tetO*$_7$*-MCM1* strains in either YPD or YPD + 2 μM doxycycline, and (C) wild-type (*WT*), *fkh1*Δ, *fkh2*Δ, and *fkh1*Δ *fkh2*Δ strains (N = 3, mean ± 1SD).

and *fkh1*Δ *fkh2*Δ strains were grown overnight in YPD diluted into fresh YPD, and grown for 6 hr before measuring rAPase activity. Induction of *PHO5* is unaffected in a *fkh2*Δ strain but is reduced by approximately 30% in a *fkh1*Δ strain (Fig. 3-2C), suggesting that Fkh1 is more important for expression of *PHO5*. This result was surprising as Fkh2 was shown to be more important for Mcm1-dependent activation of

mitotically-induced genes (65). Deletion of both *FKH1* and *FKH2* reduced *PHO5* activation by approximately 40% (Fig. 3-2C).

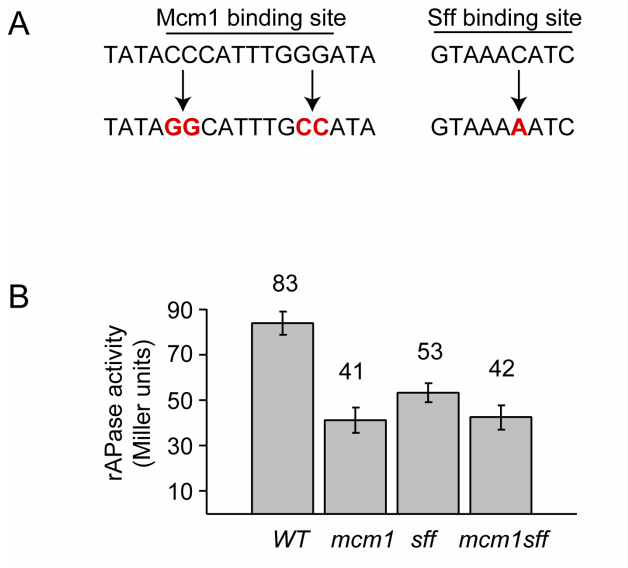

FIG. 3-3. Mcm1 and SFF are direct activators of *PHO5* transcription. (A) Putative Mcm1 and SFF binding sites of the *PHO5* promoter. Mutations in Mcm1 and SFF recognition sequences are shown in red. (B) Total rAPase activities of asynchronous YPD cultures of wild-type (*WT*), $PHO5^{mcm1}$, $PHO5^{sff}$, and $PHO5^{mcm1sff}$ strains in YPD (N = 3, mean ± 1SD).

Direct activation of *PHO5* by Mcm1 and SFF. To test if Mcm1 is a direct activator of *PHO5* expression, we introduced well-characterized point mutations (Fig. 3-3A) to inactivate the Mcm1 (38, 81) and SFF (65) binding sites both singly and together, and assayed their effects on mitotic *PHO5* activation. Wild-type, $PHO5^{mcm1}$, $PHO5^{sff}$, and $PHO5^{mcm1sff}$ strains were grown overnight in YPD, then shifted to fresh YPD medium and grown for 6 hr. rAPase activity was reduced by 50% (Fig. 3-3B) in the

PHO5^{mcm1}strain, similar to the loss seen for the *mcm1*^{R19A} allele (Fig 3-2A). Slightly lower (40%) reduction in *PHO5* expression is observed in the *PHO5*^{sff} strain (Fig. 3-3B), which is similar to that of the *fkh1*Δ *fkh2*Δ strain (Fig. 3-2C). *PHO5*^{mcm1sff} strains showed a 50% decrease in *PHO5* activation, similar to the *PHO5*^{mcm1} strain (Fig. 3-3B). Since no additional loss of *PHO5* activation is seen in the *PHO5*^{mcm1sff} strain, these results suggest that Mcm1 and SFF may be components of the same pathway leading to *PHO5* expression.

We were interested in determining if the role of Mcm1 as a *PHO5* activator is restricted to mitotic induction in YPD or if it has similar functions under fully activating conditions in synthetic P_i-free medium. Wild-type, *PHO5*^{mcm1}, *PHO5*^{sff}, and *PHO5*^{mcm1sff} strains were grown overnight in synthetic medium containing 13.4 mM P_i, then were washed and resuspended in P_i-free medium, and rAPase activity was assayed at the indicated times. *PHO5* activation in *PHO5*^{mcm1} and *PHO5*^{mcm1sff} strains was reduced by 60%-70% during the first 180 min of P_i starvation compared to wild-type strains (Fig. 3-4). After 4 hr of P_i starvation, rAPase activity in *PHO5*^{mcm1} strains is only 40% lower than wild-type levels, and is essentially unchanged from wild-type levels by 7 hr of P_i starvation. *PHO5* activation in *PHO5*^{sff} strains was also reduced by about 70% during the first 60 min of starvation. After 90 min of starvation, *PHO5* activation in *PHO5*^{sff} strains was only 50% lower than wild-type strains and approximately 20% higher than activation in *PHO5*^{mcm1} strains (Fig. 3-4). Within 4 hr of P_i starvation, *PHO5* activation in *PHO5*^{sff} was similar to the wild-type strain. Together with the *mcm1*^{R19A} and *fkh1*Δ

*fkh2*Δ data above, these results suggest that Mcm1 and SFF are activators of *PHO5* transcription acting in both mitotic- and P_i starvation-induced expression.

Mcm1 is associated with acid phosphatase promoters. To establish further that Mcm1 acts as an activator of yeast acid phosphatases, we wanted to test if Mcm1 associates with the promoters of *PHO5*, *PHO3,* and *PHO11/12* by chromatin immunoprecipitation (ChIP) analysis. When a strain carrying an HA-tagged allele of *MCM1* was grown in YPD, Mcm1 association with the *PHO5* promoter is not detectable by ChIP (data not shown). This was surprising as Mcm1 is bound constitutively to the promoters of *SWI5*, *CDC6*, *CLN3,* and *SWI4* (3, 82). However, unlike *SWI5* and *CDC6*, Mcm1 is not the primary transcriptional activator at *PHO5*. It is therefore possible that the association of Mcm1 with the *PHO5* promoter is dependent on prior gene activation through P_i starvation. To assay for such a requirement, the *MCM1-3HA* strain was grown overnight in synthetic medium containing 13.4 mM P_i, washed, and resuspended in synthetic P_i-free medium. After 24 hr of P_i starvation, formaldehyde-treated cells were subjected to ChIP analysis. As in YPD medium, Mcm1 is not detected at any of the acid phosphatase promoters under high-P_i conditions (Fig. 3-5A, B). Upon P_i starvation, Mcm1 becomes associated with all four acid phosphatase promoters (Fig. 3-5A, B). Since the promoter regions of *PHO11* and *PHO12* are identical, the immuno-enriched signal is the sum of Mcm1 binding to both promoters. Mcm1 is not detected at the

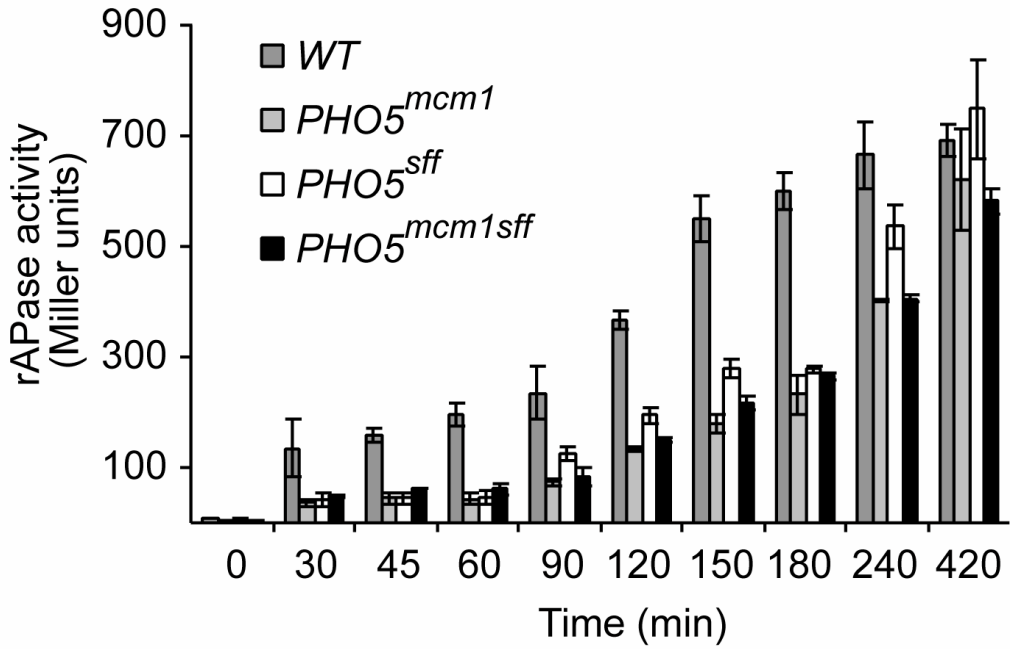

FIG. 3-4. Mcm1 and SFF contribute to the kinetics of P_i starvation-dependent activation of *PHO5*. Time course of *PHO5* activation in wild-type (*WT*), $PHO5^{mcm1}$, $PHO5^{sff}$, and $PHO5^{mcm1sff}$ strains. Asynchronous cultures were grown on defined 13.4 mM P_i medium, then starved for P_i and assayed for total rAPase activity at the indicated times (N = 3, mean ± 1SD).

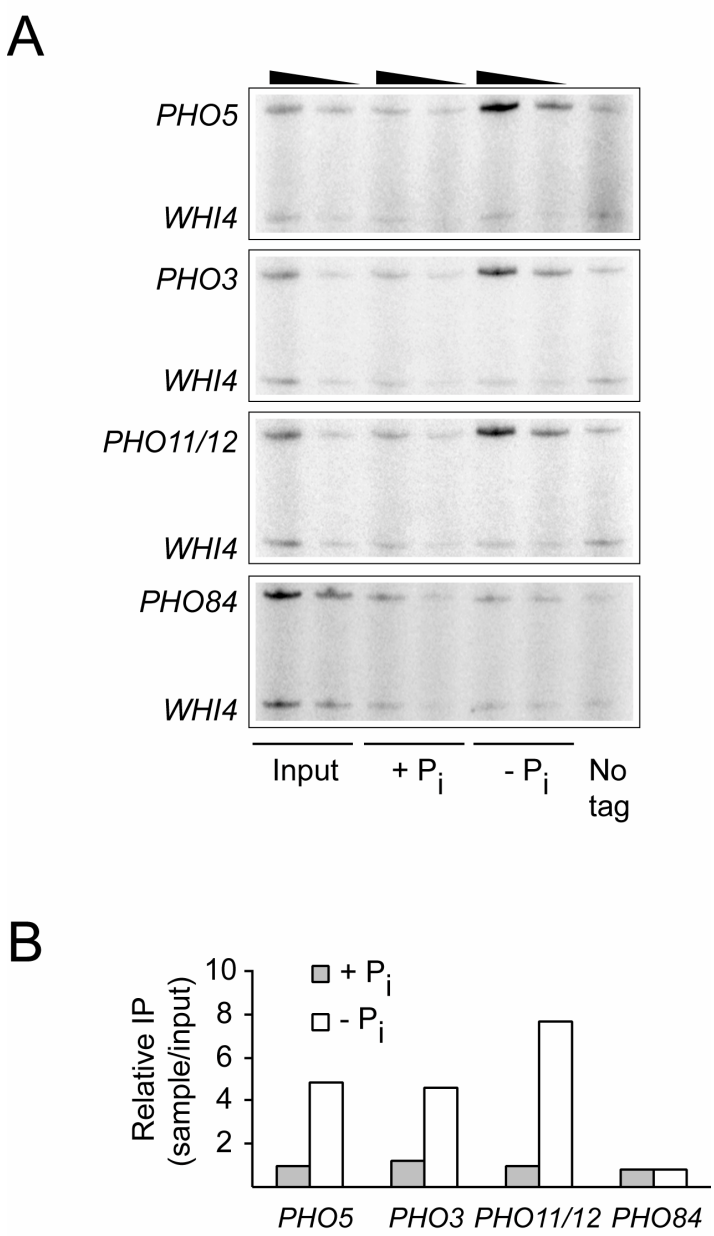

FIG. 3-5. Mcm1 associates with acid phosphatase promoters after P_i starvation. (A) An *MCM1-3HA* strain was grown overnight in synthetic medium containing 13.4 mM P_i, washed, and subsequently grown in synthetic P_i-free medium for 24 hr prior to ChIP analysis. Immunoselected DNA (4 μl) was PCR amplified for enrichment of either *PHO5*, *PHO3*, *PHO11/12*, *PHO84*, or *WHI4* promoter sequences in the presence of [α-^{32}P]dCTP, and was analyzed in a 5% polyacrylamide gel. A 2-fold dilution of each sample is indicated by the triangle. Non-diluted DNA from a wild-type strain with no HA tag (no tag) is analyzed on each gel. (B) Quantification of the association between Mcm1-HA and acid phosphatase promoters. Presented are ratios of each indicated promoter to the control promoter (*WHI4*), normalized to the ratio of the input sample, which was taken from the +P_i culture. Data shown are representative of four independent experiments.

PHO84 promoter in high- or low-P_i medium, consistent with it lacking a discernable Mcm1 binding site (Fig. 3-5A, B). Due to the functional importance of Mcm1 in *PHO5* activation in YPD medium (Fig. 3-2 and 3-3) and initially after P_i starvation (Fig. 3-4), conditions that are submaximal for induction we conclude that Mcm1 is likely to be associated with the *PHO5* promoter at levels below the detection limit of ChIP analysis.

Association of Mcm1 with the *PHO5* promoter is dependent on Pho4 and Pho2. The primary transcriptional activators Pho4 and Pho2 bind cooperatively to most PHO promoters (6). Therefore, we sought to determine if the association of Mcm1 with the *PHO5* promoter is similarly dependent on either Pho4 or Pho2. *MCM1-3HA* strains lacking either *PHO4* or *PHO2*, were starved for P_i for 24 hr at which time Mcm1 binding was assayed. Mcm1 associates with the *PHO5* promoter in wild-type cells as an approximately 7-fold enrichment of *PHO5* over the control sequence, *WHI4*, is detected (Fig. 3-6A, B). However, in *pho4*Δ and *pho2*Δ strains, the association of Mcm1 with the *PHO5* promoter is not detected. This suggests that, in addition to P_i starvation, the association of Mcm1 with the *PHO5* promoter depends on prior gene activation by Pho2 and Pho4.

***PHO5* gene activation in *pho80*Δ strains is not sufficient for Mcm1 binding.** Thus far, our data show that the association of Mcm1 with the *PHO5* promoter is dependent on P_i starvation (Fig. 3-5A, C), which leads to Pho4 and Pho2 binding and gene activation. To determine if Pho4 and Pho2 binding are sufficient for the interaction of Mcm1 and the *PHO5* promoter, we performed ChIP analysis in a strain lacking the Pho85-specific cyclin Pho80, which leads to constitutive activation in the presence of

high P_i. Wild-type and *pho80*Δ strains were grown overnight in high-P_i medium, washed in P_i-free medium, and then grown in 13.4 mM or P_i-free medium for 24 hr. As shown in Figure 3-7, Mcm1 is not detected at the *PHO5* promoter in the wild-type strain under high-P_i conditions. Similarly, despite the constitutive activation of *PHO5*, no significant association of Mcm1 with the *PHO5* promoter is observed in a *pho80*Δ strain

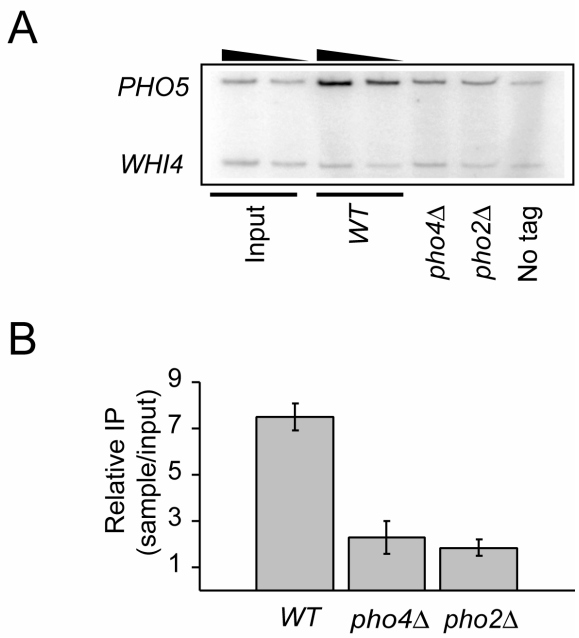

FIG. 3-6. Pho4 and Pho2 are required for Mcm1 to associate with the *PHO5* promoter. (A) Wild-type (*WT*), *pho4*Δ, and *pho2*Δ strains with *MCM1-3HA* alleles were grown overnight in synthetic medium containing 13.4 mM P_i, washed, and subsequently grown in synthetic P_i-free medium for 24 hr. Immunoselected DNA (4 μl) was amplified in all lanes except for the 2-fold dilutions as indicated by the triangles. (B) Quantification of the association between Mcm1-HA and the *PHO5* promoter. *WHI4* serves as a control for non-specific immunoprecipitation. Data shown are representative of two independent experiments.

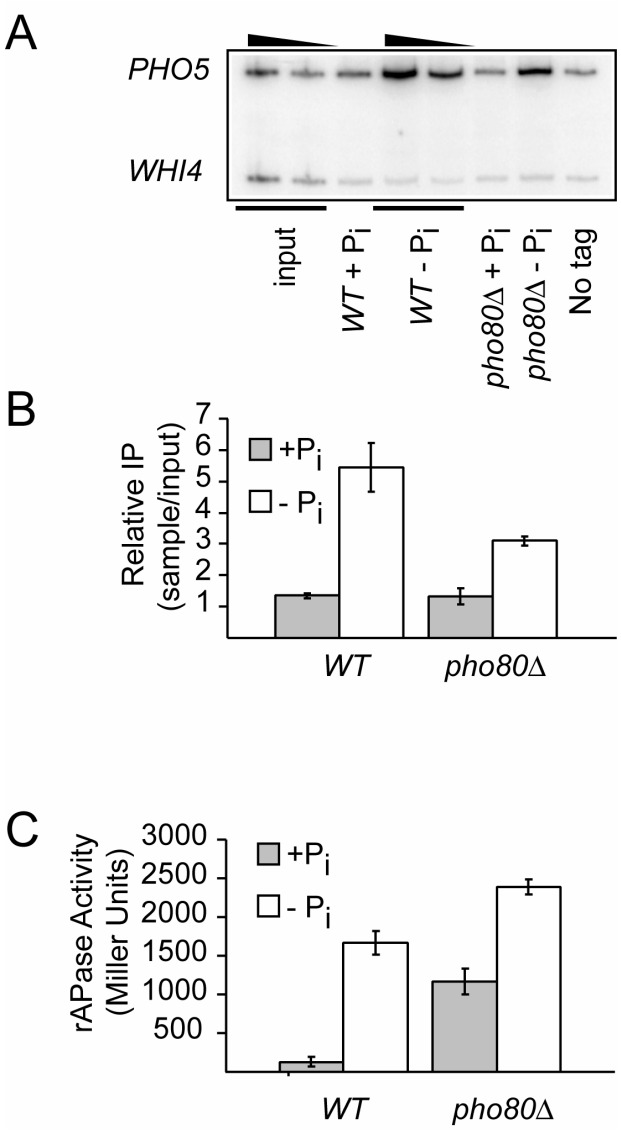

FIG. 3-7. *PHO5* derepression in *pho80*Δ strains is insufficient for Mcm1 binding. (A) Wild-type (*WT*) and *pho80*Δ strains with *MCM1-3HA* alleles were grown overnight in synthetic medium containing 13.4 mM P_i, washed, and subsequently grown in either 13.4 mM or synthetic P_i-free medium for 24 hr. ChIP samples were analyzed as in FIG. 3-5. (B) Quantification of the association between Mcm1-HA and the *PHO5* promoter. *WHI4* serves as a control for non-specific immunoprecipitation. (C) Total rAPase activities of internal aliquots of cells in A after 24 hr of P_i starvation. Data shown are representative of two independent experiments.

grown in high-P_i medium. Only when the *pho80*Δ strain was starved for P_i is Mcm1 detected at the *PHO5* promoter at levels similar to the wild-type strain. This suggests that while *PHO5* activation through Pho4 and Pho2 binding is essential, it is not sufficient for Mcm1 to associate with the *PHO5* promoter. As has been observed previously (43), deletion of *PHO80* leads to submaximal levels of *PHO5* induction, which approximately double upon P_i starvation (Fig. 3-7C). This suggests that an additional P_i-dependent starvation signal that is independent of the canonical PHO pathway may affect *PHO5* activation and Mcm1 binding.

Discussion

In this report, we have investigated the role of cell cycle-dependent transcriptional activators in the mitotic activation of *PHO5*. Sequence analysis of the *PHO5* promoter revealed consensus binding sites for both Mcm1 and SFF (Fig. 3-1), closely resembling those of *SWI5*, *KIN3*, and *SPO12*. Similar binding sites were also found in the promoters of *PHO3*, *PHO11*, and *PHO12*, coding for three highly related acid phosphatases, while neither binding site was found in the promoter of *PHO84* coding for the high-affinity P_i transporter, or *PHM4* coding for a subunit of the putative polyP synthase complex (110). We have shown that mitotic induction of *PHO5* is dependent, at least in part, on the transcriptional activators Mcm1 and Fkh1. Strains with the partial loss-of-function allele, $mcm1^{R19A}$ (Fig. 3-2A), as well as strains deleted for *FKH1* (Fig. 3-2C), exhibit a 40% loss of mitotic *PHO5* activation. Overexpression of *MCM1* further confirmed its role as a *PHO5* transactivator, resulting in a 5-fold

increase in *PHO5* expression (Fig. 3-2B). In order to establish Mcm1 as a direct activator of *PHO5* expression, point mutations (Fig. 3-3A) were introduced into either or both the Mcm1 and SFF binding sites and assayed for defects in mitotic *PHO5* activation. $PHO5^{mcm1}$, $PHO5^{sff}$, and $PHO5^{mcm1sff}$ strains showed approximately 2-fold lower induction of *PHO5* in mitosis (Fig. 3-3B), as observed for $mcm1^{R19A}$ (Fig. 3-2A) and *fkh1*Δ *fkh2*Δ (Fig. 3-2C) strains. Mutations in the Mcm1 and SFF binding sites also lead to significant defects in P_i starvation-dependent activation of *PHO5*, increasing at a slower rate and reaching only 30-40% of wild-type activity at early times of activation (Fig. 3-4). In contrast, $PHO5^{sff}$ strains had smaller defects in starvation-dependent activation, suggesting that Mcm1 is more important for *PHO5* activation (Fig. 3-4). The roles of Mcm1 and Fkh1 in activation are surprisingly similar to those previously reported for the chromatin remodeling enzymes Gcn5 and Snf2/Swi2, which also are important for mitotic *PHO5* activation (103) and the initial rate of *PHO5* activation following P_i starvation (7, 103).

To show that Mcm1 is a direct activator, we assayed its association with several P_i-responsive promoters by ChIP analysis. Surprisingly, Mcm1 is not detected at any of the acid phosphatase promoters in YPD, which is only partially limiting for P_i, or in high-P_i medium (Fig. 3-5A, B), though it does associate upon P_i starvation. Mcm1 does not interact with all P_i-responsive promoters though, as we were unable to detect it at the *PHO84* promoter under either high- or low-P_i conditions.

To distinguish between *PHO5* gene activation and P_i starvation as prerequisites for the association of Mcm1 with the *PHO5* promoter, we assayed promoter occupancy

by Mcm1 in strains lacking the cyclin Pho80, which results in *PHO5* activation under repressive conditions. Strains deleted for *PHO80* have no detectable Mcm1 at the *PHO5* promoter in YPD (data not shown) or high-P_i conditions (Fig. 3-6A, B), despite having high levels of *PHO5* expression (Fig. 3-6C). However, upon P_i starvation, Mcm1 associates with the *PHO5* promoter in both wild-type and *pho80*Δ strains, demonstrating that gene activation alone is insufficient for factor binding. Strains without the transactivators Pho4 and Pho2 also lacked detectable association of Mcm1 with the *PHO5* promoter even after 24 hr of P_i starvation, indicating that P_i starvation alone is not sufficient to allow for Mcm1 binding (Fig. 3-7A, B).

It is interesting that the association of Mcm1 with the promoters of *PHO5*, *PHO3,* and *PHO11/12* cannot be detected under repressing (high P_i) or partially activating conditions (YPD) (Fig. 3-5A, B), as the factor is constitutively bound to the *SWI5* and *CDC6* promoters (3). While the reasons for these differences are unclear, it is likely that the sensitivity of the ChIP assay precludes detection of low levels of Mcm1 binding. This is supported by the finding that mutations in the Mcm1 binding site, reduce *PHO5* activation at early points after P_i starvation is initiated (Fig. 3-4).

A novel finding of our work is that Mcm1 binding increases in response to P_i starvation. It is plausible that Mcm1 binds in response to a signal created by the PHO pathway. However, this is unlikely as Mcm1 binding is not detectable at the *PHO5* promoter during constitutive activation of the pathway in strains lacking the cyclin *PHO80*. It is possible, though, that a signal independent of the PHO pathway is generated by P_i starvation that contributes to Mcm1 binding. One such signal could be

created through nutrient starvation-dependent growth arrest that occurs when yeast cells are starved for essential nutrients like nitrogen, carbon, or phosphate. Cells will arrest in late G1 until the missing nutrient is acquired (78, 149). Nitrogen and carbon starvation cause rapid decreases in transcription of *CLN1*, *CLN2*, and *CLN3*. Similarly, arrest due to P_i starvation also leads to decreases in both *CLN1* and *CLN2,* but not *CLN3,* transcription (116). Though a direct connection is not yet apparent, it is interesting to speculate that the loss of *CLN1* or *CLN2* during P_i starvation may result in activation and increased binding of Mcm1. This hypothesis is supported by findings that suggest growth in poor carbon sources, such as glycerol or lactate, lowers both *CLN1* and *CLN2* transcription (116) and likewise results in increased binding of Mcm1 to the *CDC6* promoter (17, 82).

Our data show that a *PHO80*-independent signal is required for Mcm1 to become associated with the *PHO5* promoter. Yet, *PHO5* gene activation is similarly essential, as neither *pho4*Δ nor *pho2*Δ strains show any detectable Mcm1 at the promoter. Several possibilities exist for why Pho4 and Pho2 are required to detect Mcm1 at the *PHO5* promoter. First, Mcm1 may bind cooperatively with either Pho4 or Pho2. An interaction between Mcm1 and Pho2 is especially intriguing as Pho2 shares close homology to the homeodomain proteins Yhp1 and Yox1, both previously established as regulators of Mcm1 activity (125). Alternatively, it is possible that Pho4 and Pho2 are required to recruit chromatin remodeling machinery (44) to the *PHO5* promoter so as to make the promoter accessible for Mcm1 binding.

Together, our findings define two distinct requirements for the association of Mcm1 with the *PHO5* promoter, namely P_i starvation and transactivation of *PHO5* through Pho4 and Pho2. While these requirements are usually mutually exclusive, an important distinction needs to be made in this case, as both are essential but neither is sufficient for Mcm1 to bind the *PHO5* promoter.

We have shown that Mcm1 as well as Fkh1 are transcriptional activators of mitotic *PHO5* expression and contribute to the kinetics of *PHO5* induction upon P_i starvation (Fig. 3-3A). Furthermore, our data suggest that Mcm1 plays a more important role than SFF, as loss of SFF is consistently less severe to transactivation than a loss of Mcm1 function (Fig. 3-2, 3-3, 3-4). Our results support a model of mitotic *PHO5* induction in which cell cycle-dependent fluctuations in P_i (103) lead to binding of the canonical PHO activators, Pho4 and Pho2, which are aided by the mitotic regulators Mcm1 and SFF.

CHAPTER IV

CONSTITUTIVE ACTIVATION OF YEAST POLYPHOSPHATE SYNTHASES RESULTS IN OVERACIDIFICATION OF THE VACUOLE AND INCREASED SUSCEPTIBILITY TO TOXINS

Introduction

Single-cell microorganisms, like the budding yeast *Saccharomyces cerevisiae,* encounter a myriad of environmental stresses, including nutrient deprivation, rapid changes in temperature, pH and osmolarity, as well as the presence of toxic agents or metals. To counter these stresses, organisms utilize complex signal transduction cascades (148) to activate specific biological responses allowing for survival and propagation of the species. One such response is to sequester and detoxify the offending agent in the vacuole (147). Sequestration of potential toxins, such as high levels of Na^+ or Ca^{2+}, can occur directly through vacuolar membrane transporters, like Nhx1 and Vcx1, respectively (26, 102), or indirectly through endocytotic or autophagic mechanisms (89, 113). Like many vacuolar ion transporters, Nhx1 and Vcx1 are proton antiporters, requiring an acidified vacuole for proper function. Similarly, the endocytotic and autophagic machinery require acidified membrane vesicles (99).

The necessary vacuolar proton-motive force is generated by the vacuolar H^+-translocating ATPase (V-ATPase) that derives energy from ATP hydrolysis to pump protons into the vacuolar lumen. Deletion of components essential for V-ATPase stability leads to lethality on medium containing high levels of NaCl, $CaCl_2$, sorbitol, and certain metals (165). Recent work has shown that strains lacking either the cyclin-

dependent kinase (CDK) Pho85 or the corresponding cyclin Pho80 are, similar to V-ATPase mutants, sensitive to high salt concentrations and to low levels of certain toxins, including the protein synthesis inhibitor G418 and the DNA-damaging agent 4-nitroquinoline *N*-oxide (4-NQO) (52). These sensitivities are thought to be caused by vacuolar defects as vacuoles of both *pho85*Δ and *pho80*Δ strains are 4-fold larger than those of wild-type strains and are deficient in fluid-based endocytosis. Since loss of either *PHO85* or *PHO80* results in the constitutive activation of the PHO pathway and P_i-responsive genes, it is not surprising that both stress susceptibility as well as vacuolar morphology defects are suppressed by a secondary deletion of *PHO4* (52). Pho4, a transcriptional activator, controls expression of PHO genes during times of P_i starvation. During growth in high P_i, Pho4 is phosphorylated by Pho80/Pho85 at five different serine residues and exported to the cytoplasm. Upon P_i starvation, the CDK inhibitor Pho81 inhibits Pho85-dependent phosphorylation of Pho4, thereby allowing for its nuclear import and transcription of P_i-responsive genes (135).

Like a *PHO4* null allele, deletion of *PHM3*/*VTC4*, which is induced by Pho4 during P_i starvation, was found to suppress defects in both *pho80*Δ-dependent growth and vacuolar morphology (52). Phm3, together with Phm1/Vtc2, Phm2/Vtc3, and Phm4/Vtc1, are components of a biochemical complex that localizes to the vacuolar membrane and is thought to be responsible for a variety of cellular functions, including the synthesis of polyP (23, 110). PolyP is an extremely ubiquitous P_i polymer found in all organisms studied to date. It consists of tens to hundreds of P_i residues, linked by

high-energy phosphoanhydride bonds (66). In *S. cerevisiae*, the major form of cellular P_i is polyP, of which about 99% is stored in the vacuole.

The primary role of polyP seems to be that of a P_i reserve (66, 103). Due to its highly negative charge, other roles such as metal chelation have been proposed, but remain unproven (66). Phm3 and Phm4 are the only members of the PHM/VTC complex essential for its stability and loss of either protein results in the complete loss of cellular polyP. Surprisingly, *phm3*Δ and *phm4*Δ strains have no discernable growth phenotypes, suggesting that polyP is not an essential molecule under laboratory conditions. Phm1 and Phm2 most likely share redundant roles as strains singly deleted for *PHM1* and *PHM2* maintain integrity of the PHM complex and wild-type levels of polyP (23, 110). Similar to strains lacking *PHM3* or *PHM4*, *phm1*Δ *phm2*Δ double mutants have no detectable polyP or PHM complex (96, 110). Both Phm3 and Phm4 have been shown to co-immunoprecipitate with the V-ATPase component, Vph1 (97), which is also important for the synthesis of polyP (110). Originally isolated as vacuolar transport chaperones (VTC), *PHM1-4* were thought to stabilize or modulate the activity of the V-ATPase as the loss of either *PHM3* or *PHM4* result in reduced vacuolar acidification (23). It remains unclear what the exact relationships are between the V-ATPase and the PHM complex.

The finding that loss of *PHM3* suppresses *pho80*Δ-dependent growth defects suggests a relationship between stress susceptibility and polyP. Here we focus on better understanding the factors, especially those related to polyP synthesis, responsible for *pho80*Δ-dependent stress susceptibilities and the closely related vacuolar morphology

defects. We have found that constitutive activation of the PHM complex in a *pho80*Δ strain, results in hyperaccumulation of polyP, thereby dramatically increasing vacuolar size and acidification of the vacuolar lumen. Our results suggest that severe overacidification of the vacuole is a primary factor in stress susceptibility and emphasizes the importance of pH homeostasis.

Materials and methods

Yeast strains and media. All *S. cerevisiae* strains used were derived from the BY4743 background and share the following genotype, *MAT***a** *leu2*Δ*0 lys2*Δ*0 ura3*Δ*0 pho3*Δ::R, where R is a *Zygosaccharomyces rouxii* recombinase site that remains after intramolecular recombination. The strains and their relevant genotypes are DNY1061 (wild-type *MAT***a** *bar1*Δ::R), DNY974 (*MAT***a** *pho80*Δ::*kanMX4*), CCY1705 (*MAT***a** *PHO4*^{SA1234PA6}), DNY1660 (*MAT***a** *pho80*Δ::*kanMX4 pho2*Δ:: *kanMX4*), DNY2764 (*MAT***a** *pho80*Δ::*kanMX4 phm3*Δ::*kanMX4 bar1*Δ::R-*URA3*-R), DNY2766 (*MAT***a** *pho80*Δ::*kanMX4 phm4*Δ::*kanMX4 bar1*Δ::R-*URA3*-R), DNY2955 (*MAT***a** *vma5*Δ::*URA3*), DNY2958 (*MAT***a** *vma5*Δ::*URA3 pho8*0Δ::*kanMX4*). To test for polyP in the W303 strain background, we used DNY1048 (wild-type; *MAT***a** *ade2-1 his3-11,15 leu2-3,112 trp1-1 ura3-1 can1-100*) and DNY1062 (*MAT*α *ade2-1 his3-11,15 leu2-3,112 trp1-1 ura3-1 can1-100 pho80*Δ::*HIS3*). YPD plates containing 2% agar and liquid cultures consisted of 10 g/l yeast extract (Difco), 20 g/l peptone (Difco) and 2% glucose. Synthetic P_i-free medium contained 0.7 g yeast nitrogen base (YNB) without $(NH_4)_2SO_4$, phosphate, or amino acids (Bio101), 2 g glutamine, 20 g glucose, 3.9 g MES

(2-*N*-morpholino ethanesulfonic acid, pH 5.5) and 0.74 g complete synthetic medium lacking histidine, per liter. The P_i concentration was brought to either 10 μM or 13.4 mM by the addition of KH_2PO_4. As indicated, plates and liquid cultures were supplemented with 2 M sorbitol.

Growth assays. For growth assays on plates, all strains were grown overnight in YPD (10 ml cultures) at 30°C. Cultures were diluted with fresh YPD to an OD_{600} = 0.2, and then diluted with dH_20 to make a 10-fold serial dilution series (from undiluted to 1:1000). An aliquot (10 μl) of each dilution was spotted on plates and incubated at 30°C for 3 days (YPD and YPD + 2 M sorbitol) or 4-5 days (synthetic medium). For growth rate assays, cells were grown overnight at 30°C in synthetic medium (10 ml cultures) supplemented with 13.4 mM P_i. Cells were diluted to an OD_{600} = 0.2 in synthetic medium supplemented with either 10 μM or 13.4 mM P_i, with or without 2 M sorbitol. Cells were grown at 30°C and optical densities were recorded every 5-10 hr.

PolyP analysis, quinacrine staining, and FM4-64 staining. PolyP was isolated and analyzed as previously described (103). For quinacrine staining, strains were grown overnight in synthetic medium supplemented with either 13.4 mM or 10 μM P_i as indicated. Five hundred microliters of logarithmic phase cultures were resuspended in synthetic medium containing 100 mM HEPES, pH 7.5, 200 μM quinacrine and incubated for 10 min at 30°C. Cells were then washed twice in 1 ml viewing solution (100 mM HEPES, pH 7.5, 2% glucose) and resuspended in 500 μl. Ten microliters of cells were analyzed by fluorescence microscopy using a Zeiss Axiophot light microscope and filter set 16 with maximum excitation at 485 nm. Pictures were taken

with a Hamamatsu C5810-01 CCD camera. For FM4-64 staining, cells were grown overnight in synthetic medium supplemented with 13.4 mM KH_2PO_4. Mid-logarithmic phase cells (500 µl) were incubated with 12 µg FM4-64 and incubated at 30°C for 60 min. Cells were washed twice and resuspended in 1 ml synthetic medium supplemented with 13.4 mM P_i and grown for one additional hour at 30°C. Ten microliters of cells were analyzed by fluorescence microscopy as described for quinacrine-stained cells.

Results

Constitutive activation of PHO genes elevates polyP levels and reduces growth on sorbitol. *pho80*Δ strains exhibit severe vacuolar morphology defects, and in turn, are highly susceptible to a variety of stressors. Since stress susceptibility and vacuolar defects are suppressed by a secondary deletion of *PHM3* (40), we hypothesized a potential connection to polyP synthesis. As Pho80 negatively controls PHO gene expression, including that of *PHM1-4*, we anticipated that loss of *PHO80* would lead to constitutive PHM complex expression and increased polyP accumulation (110). To test this, we grew wild-type and *pho80*Δ strains overnight in rich medium (YPD) and then shifted the cells to fresh YPD, in which they were grown for 6 hr. PolyP was isolated and analyzed by the addition of the basic dye toluidine blue, which undergoes a metachromatic shift from 630 nm to 530 nm upon interacting with polyP (21). The metachromatic shift is directly proportional to the amount of polyP and thus provides an excellent measure of polyP in a given culture (21). As anticipated, strains lacking

PHO80 had polyP levels approximately 5-fold higher than those of wild-type strains (Table 4-1). These results are highly reproducible but are in contrast to a previous report that a *pho80*Δ strain has undetectable levels of polyP (110). To rule out a potential difference due to strain background, we determined that, like our S288C-derived

TABLE 4-1. PolyP levels of various strains in rich medium

Strains	PolyP
WT (BY4743)	0.09 ± 0.003
*pho80*Δ (BY4743)	0.4 ± 0.05
WT (W303)	0.3 ± 0.05
*pho80*Δ (W303)	2 ± 0.5
PHO4^{c} (BY4743)	0.4 ± 0.02
*pho80*Δ *pho2*Δ (BY4743)	0.05 ± 0.01
*pho80*Δ *phm3*Δ (BY4743)	ND
*pho80*Δ *phm4*Δ (BY4743)	ND

ND, not detectable
(N = 3, mean ± 1SD)

*pho80*Δ strains, a *pho80*Δ strain in the W303 background also accumulates more polyP (Table 4-1). We also verified that these strains had the classic *pho80*Δ phenotype, overexpression of repressible acid phosphatases (data not shown). In addition, previous evidence shows that strains lacking *PHO85* have approximately 4-fold more polyP than wild-type strains (87). We conclude that deletion of *PHO80* leads to elevated polyP accumulation.

Similar to *pho85*Δ or *pho80*Δ strains, a strain carrying a constitutive *PHO4* allele (*PHO4*^{c}), lacking all *PHO85*-specific kinase sites (64), exhibits activated transcription of *PHM1-4* and other P_i-responsive genes (110). We hypothesized that like *pho80*Δ strains, *PHO4*^{c} strains should have elevated levels of polyP. This is the case as polyP levels of *PHO4*^{c} strains are elevated by approximately 5-fold (Table 4-1).

If a relationship exists between elevated polyP and osmotic stress susceptibility, then *PHO4*^{c} strains should, like *pho80*Δ strains, show reduced growth on high-sorbitol medium. To test this, we grew wild-type, *pho80*Δ, and *PHO4*^{c} strains in YPD to mid-log phase and spotted them on YPD or YPD + 2 M sorbitol plates. As previously observed (52), wild-type cells are affected minimally by the osmotic stress, whereas a *pho80*Δ strain has a severe growth defect (Fig. 4-1). *PHO4*^{c} strains were likewise sensitive to high-sorbitol medium, albeit slightly less than a *pho80*Δ strain.

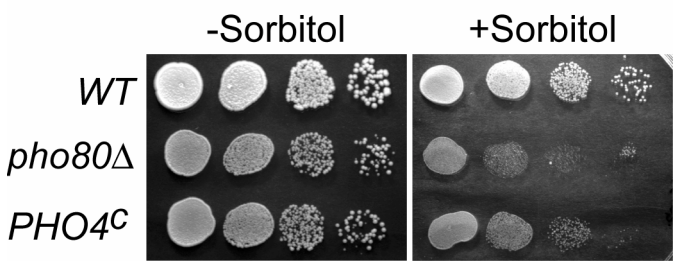

FIG. 4-1. Constitutive activation of the PHO pathway causes susceptibility to osmotic stress. Wild-type (*WT*), *pho80*Δ, and *PHO4*^{c} strains were grown to an OD_{600} = 0.2 and plated as a 10-fold serial dilution series on either YPD (left panel) or YPD + 2 M sorbitol (right panel). Plates were incubated for 4 days at 30^{o}C. Data shown are representative of three independent experiments.

Osmotic hypersensitivity of *pho80*Δ strains is suppressed by loss of *PHO2, PHM3,* and *PHM4*. Deletion of *PHO4* was shown to suppress *pho80*Δ-dependent growth defects in response to toxins, suggesting that constitutive expression of a downstream target is responsible for stress sensitivity (52). While all downstream targets of the PHO pathway are dependent on Pho4 for transcription, not all targets require the homeodomain protein Pho2 (98). We therefore determined if deletion of *PHO2* similarly suppresses *pho80*Δ phenotypes, thereby further elucidating effectors of *pho80*Δ stress susceptibility. Wild-type, *pho80*Δ, and p*ho80*Δ *pho2*Δ strains were grown overnight in YPD and spotted on YPD and YPD + 2M sorbitol plates. The additional deletion of *PHO2* almost entirely suppressed the susceptibility to sorbitol of *pho80*Δ strains (Fig. 4-2A). When assayed, polyP levels of *pho80*Δ *pho2*Δ strains were similar to those of wild-type strains (Table 4-1), further correlating increased polyP levels with reduced growth under osmotic stress conditions.

Like deletions of *PHO4* and *PHO2,* secondary deletions of *PHM3* suppressed the growth phenotypes of *pho80*Δ strains (52). *PHM3* is thought to code for a putative polyP synthase component. We therefore wanted to test the ability of a deletion in *PHM4*, the only gene other than *PHM3* essential for polyP synthesis (103, 110), to suppress *pho80*Δ toxicity phenotypes. This would confirm the correlation between polyP synthesis and stress susceptibility. As above, wild-type, *pho80*Δ, *pho80*Δ *phm3*Δ, and *pho80*Δ *phm4*Δ strains were spotted on YPD and YPD + 2M sorbitol medium and

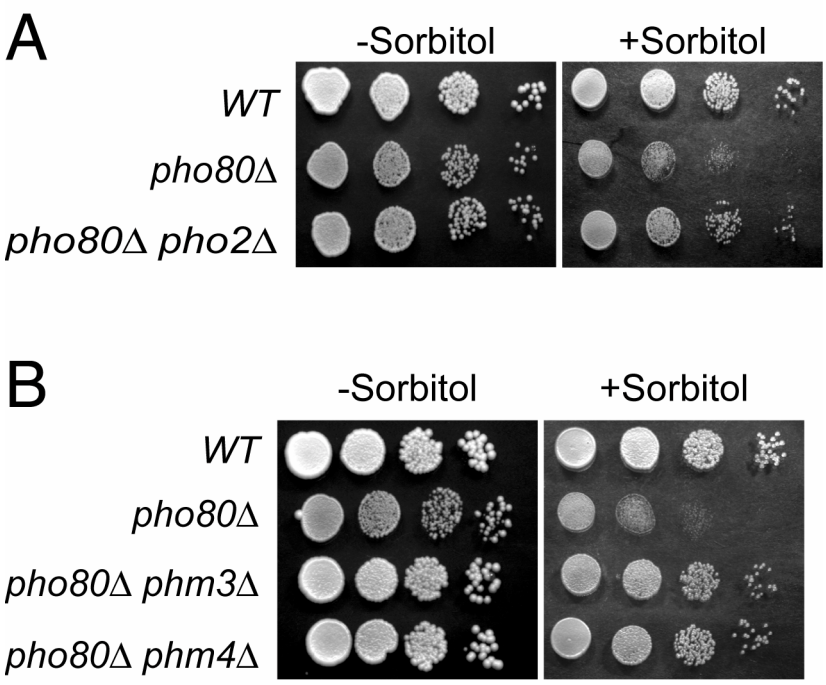

FIG. 4-2. Suppression of *pho80*Δ growth defects by deletion of *PHO2*, *PHM3,* and *PHM4*. (A) Wild-type (*WT*), *pho80*Δ, and *pho80*Δ *pho2*Δ strains were grown to an OD_{600} of 0.2 and plated as a 10-fold serial dilution series on either YPD (left) or YPD + 2 M sorbitol (right). Plates were grown for 4 days at 30°C. (B) Wild-type, *pho80*Δ, *pho80*Δ *phm3*Δ, and *pho80*Δ *phm4*Δ strains were grown and plated as in A. Data shown are representative of three independent experiments.

grown for 3 days at 30°C. As previously shown (52), growth of wild-type and *pho80*Δ *phm3*Δ strains was indistinguishable under both stress and non-stress conditions (Fig. 4-2B). Deletion of *PHM4,* the other gene required for PHM complex integrity, similarly suppressed the stress sensitivity of a *pho80*Δ strain (Fig. 4-2B). In accordance with these results, polyP levels were undetectable in either *pho80*Δ *phm3*Δ or *pho80*Δ *phm4*Δ strains, further establishing a relationship between polyP hyperaccumulation, stress susceptibility, and Pho4/Pho2-dependent expression of the PHM complex.

Furthermore, since the exact functions of Phm1-4 have been disputed (96), these results support a genuine role for the PHM complex in polyP synthesis.

Low inorganic phosphate restores growth on sorbitol. Thus far, our efforts have shown that the susceptibility of *pho80*Δ strains to osmotic stress can be efficiently suppressed by deletion of genes important for polyP synthesis. Unfortunately, this approach risks possible pleiotropic and unintended side effects as genes can impact a variety of cellular functions (72). If polyP hyperaccumulation is responsible for the growth defect of *pho80*Δ strains on sorbitol, reducing the amount of cellular polyP by P_i starvation (103, 110) should restore growth. As in YPD (Fig. 4-1), wild-type and *pho80*Δ strains grew similarly in high and low P_i medium in the absence of osmotic stress (Fig. 4-3A). When 2 M sorbitol was added to high-P_i plates, *pho80*Δ strains are severely defective for growth (Fig. 4-3A). However, when sorbitol was added to low-P_i plates, no significant difference in growth was observed (Fig. 4-3A), thereby establishing cellular P_i as a contributor to *pho80*Δ-dependent stress susceptibility.

We also determined the effects of P_i concentration and osmotic stress on growth rate. Wild-type and *pho80*Δ strains were grown overnight in high-P_i liquid medium to mid-log phase, and subsequently both cultures were shifted to either high- or low-P_i defined medium, with or without 2 M sorbitol, and optical densities were monitored over time. No significant differences in growth rate were observed between *pho80*Δ and wild-type strains in either high- or low-P_i medium, despite the ~1000-fold difference in

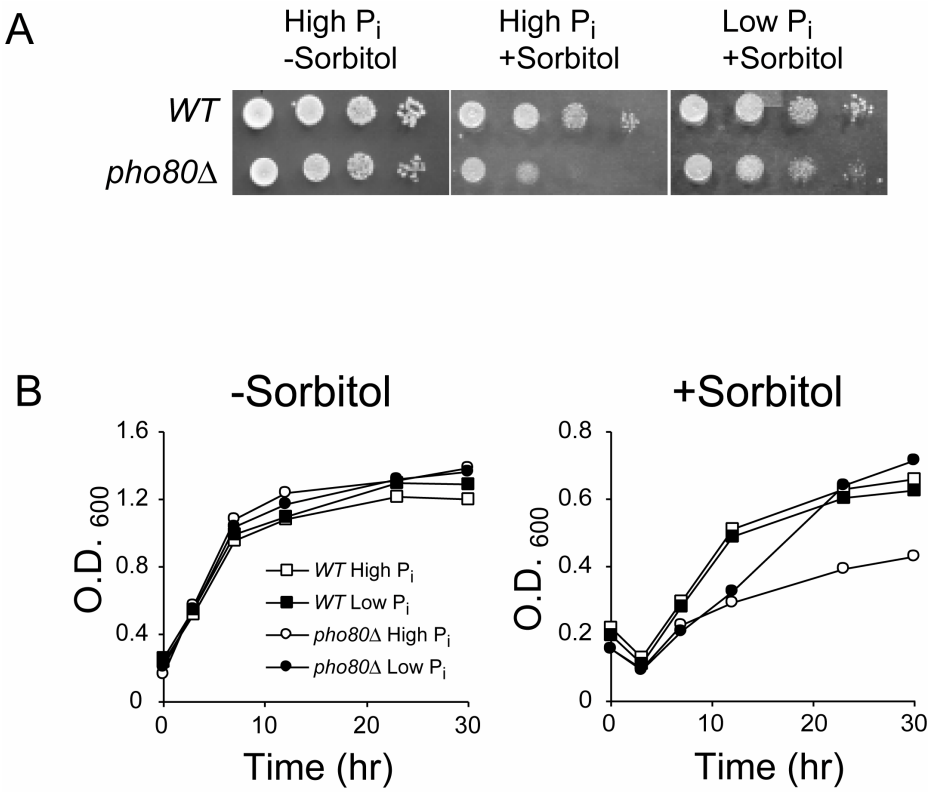

FIG. 4-3. Suppression of *pho80*Δ growth defects by growth on low-P_i medium. (A) Wild-type (*WT*) and *pho80*Δ strains were grown to an $O.D._{600}$ of 0.2 and plated as a 10-fold serial dilution series on synthetic media plates containing either 13.4 mM (high) or 10 μM (low) P_i with or without 2 M sorbitol. Plates were incubated for 4 days at 30°C. Data shown are representative of two independent experiments. (B) Growth of wild-type (*WT*) and *pho80*Δ strains in synthetic medium containing either 13.4 mM (high) or 10 μM (low) P_i with or without 2 M sorbitol. Data shown are representative of two independent experiments.

P_i concentration (Fig. 4-3B). In contrast, the addition of sorbitol significantly reduced the ability of the *pho80*Δ but not the wild-type strain to grow in high-P_i medium (Fig. 4-3B). When *pho80*Δ strains were shifted to sorbitol medium containing low levels of P_i, initial growth was extremely slow (Fig. 4-3B, 0-10 hr). Surprisingly, after approximately 10 hr growth in low-P_i sorbitol medium, the growth rate of *pho80*Δ strains increased and within 20 hr achieved optical densities similar to the wild-type strain. For approximately

4-5 hr after being shifted to sorbitol containing medium, wild-type and *pho80*Δ strains appear to be decreasing in optical density irrespective of P_i concentration. We attribute this to a cell shrinkage phenomenon previously observed in cells exposed to osmotic shock, in which their vacuole shrinks by as much as 45% (157).

TABLE 4-2. PolyP levels of wild-type and *pho80*Δ strains grown under various P_i concentrations

Strain	$[P_i]$	PolyP
WT	13 mM	0.2 ± 0.0006
WT	10 μM	ND
*pho80*Δ	13 mM	0.5 ± 0.07
*pho80*Δ	10 μM	ND

ND, not detectable
(N = 3, mean ± 1SD)

PolyP was isolated from wild-type and *pho80*Δ strains grown in both high- and low-P_i medium and quantitatively analyzed using the toluidine blue metachromatic shift assay. As we showed previously (103), wild-type strains grown in high-P_i medium had approximately 2-fold higher polyP levels than those grown in YPD (compare Table 4-2 to Table 4-1). Similarly, *pho80*Δ strains had 20% higher polyP levels when grown in excess P_i than in YPD and were still elevated from wild-type levels (compare Table 4-2 to Table 4-1). When both wild-type and *pho80*Δ strains were grown in 10 μM P_i, no polyP was detected (Table 4-2). Since cellular P_i needs are met prior to synthesizing

polyP reserves (103), it is likely that under extremely limiting P_i conditions, P_i demand exceeds P_i supply, thereby leaving little or no P_i to be assimilated into polyP. We propose that preexisting polyP levels must be depleted before P_i limitation can suppress the osmotic sensitivity of *pho80*Δ strains (29, 86).

PolyP hyperaccumulation results in overacidified vacuoles. Past work has shown that polyP synthesis is tightly linked to the vacuole, the V-ATPase, and the vacuolar proton-motive force (96, 110), though it is unclear what exact role proton transport plays in polyP synthesis. Since loss of *PHM3* or *PHM4* is thought to decrease vacuolar acidity (104), it is possible that components important for polyP synthesis, potentially those interacting with the V-ATPase, stimulate proton transport. If polyP synthesis is coupled to the resulting proton gradient (110), stimulation of the V-ATPase would generate a more favorable environment for polyP synthesis. Furthermore, it is possible that misregulation of these components, as in a *pho80*Δ strain, could alter vacuolar pH and render the cell susceptible to stress.

To determine if vacuolar acidification is altered in *pho80*Δ strains, we stained cells from logarithmically growing yeast cultures with either quinacrine or FM4-64. Quinacrine passively diffuses into the vacuolar lumen and fluoresces under acidic conditions, allowing for an estimate of vacuolar pH. FM4-64, on the other hand, fluoresces after intercalating into the vacuolar membrane irrespective of vacuolar pH and enables one to monitor vacuolar size and shape. Wild-type cells revealed multiple, relatively small globular vacuoles (Fig. 4-4A) when stained with FM4-64, which exhibited only moderate fluorescence after quinacrine staining (Fig. 4-4B). As

previously demonstrated (52, 107), *pho80*Δ strains stained with FM4-64 possess one extremely large vacuole that occupies most of the cell volume (Fig. 4-4A). Intriguingly, quinacrine staining of *pho80*Δ cells revealed a highly fluorescent vacuole, suggesting that *pho80*Δ vacuoles are not only much larger than wild-type vacuoles but are also much more acidic. A deletion in *PHO2*, which suppresses both elevated polyP levels and the osmotic stress susceptibility of *pho80*Δ strains (Fig. 4-2A and Table 4-1), also reestablishes wild-type vacuolar acidification and size (Fig. 4-4A). This provides strong evidence that polyP synthesis or an overaccumulation of polyanions results in vacuolar defects. This is supported further as a *pho80*Δ strain with a deletion of *PHM3*, which suppresses polyP-dependent growth defects on sorbitol (Fig. 4-2B and Table 4-1), also has a wild-type vacuolar morphology (Fig. 4-4A, B). Interestingly, *pho80*Δ *phm3*Δ strains seem to lack detectable vacuolar acidification (Fig. 4-4B), supporting previous data suggesting that wild-type acidification is at least partly dependent on the PHM complex (104).

We also determined if limiting external P_i would suppress the overacidification of *pho80*Δ vacuoles. Wild-type and *pho80*Δ strains were grown overnight in medium containing either 13.4 mM or 10 μM P_i to mid-log phase and stained with quinacrine. As in Figure 4-4B, wild-type cells had mildly acidified vacuoles under both high- and low-P_i conditions (Fig. 4-5), while *pho80*Δ strains had highly acidic vacuoles in high-P_i medium (Fig. 4-5). Moreover, *pho80*Δ strains grown in low-P_i medium had small, mildly acidified vacuoles almost indistinguishable from wild-type strains (Fig. 4-5), confirming that the vacuolar acidification defect is linked to polyP synthesis.

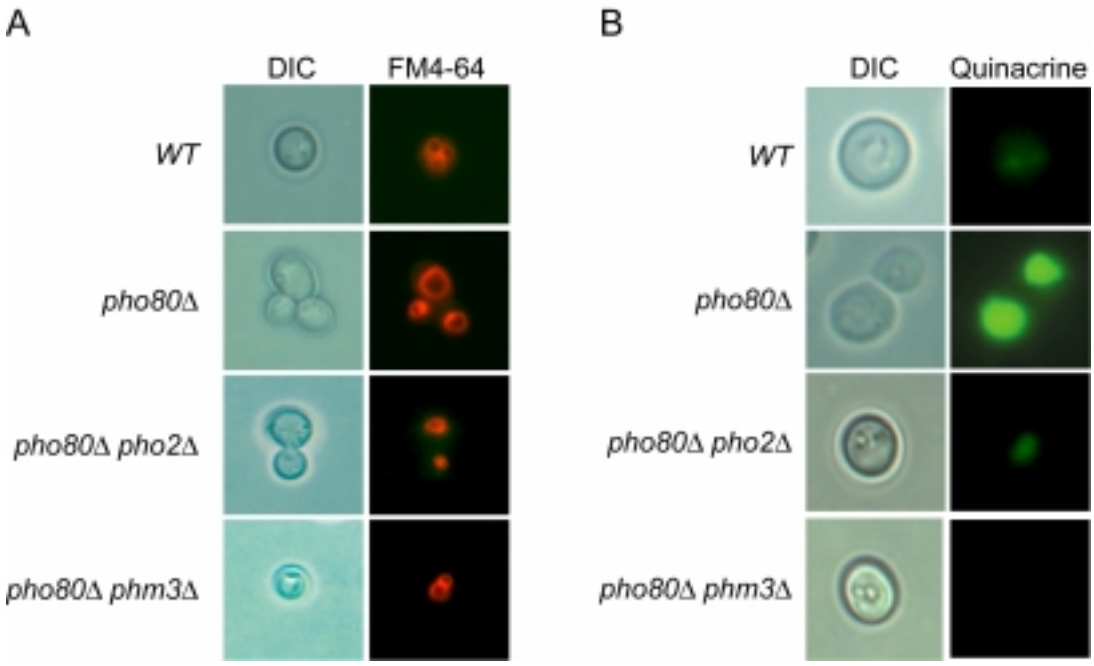

FIG. 4-4. Vacuolar defects of *pho80*Δ strains are suppressed by deletion of *PHO2* and *PHM3*. (A) Vacuolar morphology. Wild-type (*WT*), *pho80*Δ, *pho80*Δ *pho2*Δ, and *pho80*Δ *phm3*Δ strains were grown to mid-log phase in synthetic medium. Cells (250 μl) were stained with FM4-64 for 1 hr at 25°C, washed, resuspended in fresh medium, and grown for an additional 2 hr at 25°C. Data shown are representative of two independent experiments. (B) Vacuolar acidification. Cells (500 μl) were stained with 200 μM quinacrine for 10 min at 30°C, washed, and resuspended in 100 mM HEPES + 2% glucose solution. In both A and B, cells were viewed with differential interference contrast (DIC) optics (panels on left) for observation of normal cell morphology and by fluorescence microscopy (panels on right) for observation of vacuolar staining with FM4-64 or quinacrine. Data shown are representative of four independent experiments.

Hyperacidification of *pho80*Δ vacuoles occurs through the V-ATPase. The PHM complex has been suggested to be involved in regulating the localization of Pma1, the plasma membrane H^+-translocating ATPase (P-ATPase), as *phm4*Δ cells nominally mislocalize Pma1 from the plasma membrane to the vacuole (23). However, it remains

unclear if vacuolar targeting of Pma1 in *phm4*Δ strains serves the purpose of degradation or if Pma1 forms a functional ATPase in the vacuolar membrane and aids in vacuolar acidification. Nonetheless, if the PHM complex is a true regulator of Pma1 targeting, it is plausible that overexpression of the complex could misdirect Pma1 to the vacuole and result in hyperacidification. Therefore, to determine if overacidification of the vacuole is dependent on mislocalization of Pma1 or is occurring via the V-ATPase, we assayed vacuolar acidity by quinacrine fluorescence in strains lacking Vma5, an essential component of the V-ATPase. Strains deleted for *VMA5* are almost entirely deficient in vacuolar acidification and thus have no quinacrine-based fluorescence (Fig. 4-6) (27). *pho80*Δ *vma5*Δ strains also show no detectable vacuolar acidification (Fig. 4-6), demonstrating that *pho80*Δ-dependent vacuolar hyperacidification is primarily dependent on the V-ATPase and does not result from Pma1 mislocalization.

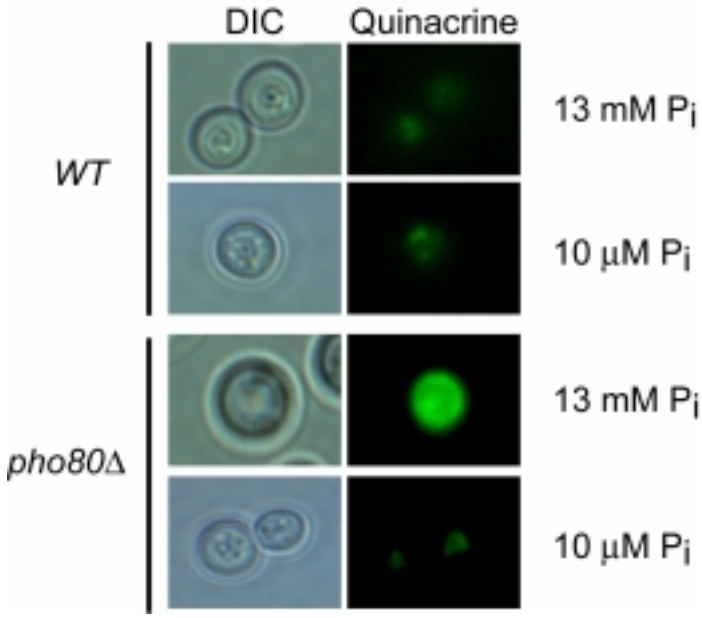

FIG. 4-5. Vacuolar defects of *pho80*Δ strains are suppressed by growth on low-P_i medium. (A) Wild-type (*WT*) and *pho80*Δ strains were grown to mid-log phase in either 13 mM or 10 μM P_i medium. Cells were stained with quinacrine as in Fig. 4-4. Data shown are representative of two independent experiments.

Discussion

Here we have shown that yeast strains lacking the Pho85-specific cyclin *PHO80*, have increased levels of polyP and are highly susceptible to osmotic stress (Fig. 4-1 and Table 4-1). We find that a constitutively active *PHO4* allele, which similarly derepresses the PHO pathway, also results in both increased levels of polyP and susceptibility to 2 M sorbitol (Table 4-1 and Fig. 4-1). Furthermore, our data show that both the increased levels of polyP as well as the stress susceptibility of *pho80*Δ strains are suppressed by secondary mutations in the transcriptional activator *PHO2* (Table 4-1and Fig. 4-2A), as well as the putative polyP synthase components *PHM3* and *PHM4* (Table 4-1 and Fig. 4-2B). These results link stress susceptibility in *pho80*Δ strains to increased polyP synthesis. This correlation is further supported as growth of *pho80*Δ strains under conditions of high osmolarity is fully restored when extracellular P_i is limited (Fig. 4-3), resulting in non-detectable levels of polyP (Table 4-2).

To understand better the mechanism of how polyP hyperaccumulation contributes to stress susceptibility, we explored the effect of *PHO80* deletions on vacuolar homeostasis. FM4-64 and quinacrine staining of *pho80*Δ strains reveals extremely large and highly acidic vacuoles (Fig 4-4). Both the increased size and overacidification of *pho80*Δ vacuoles is suppressed by secondary deletions in *PMH3* (Fig. 4-4) (40), *PHO2* (Fig. 4-4), and *VMA5* (Fig. 4-6) as well as growth on low-P_i medium (Fig. 4-5), supporting our hypothesis that increased polyP synthesis results in vacuolar overacidification through the V-ATPase.

Our results begin to shed light on how polyP is synthesized in *S. cerevisiae* and show that maintaining proper regulation of its synthesis is critical to avoid susceptibility to stress. Primary regulation of polyP, at least in budding yeast, seems to occur through the transcriptional control of *PHM1-4* (110) as loss of *PHO80* results in the constitutive activation of these genes and elevates polyP levels (Table 4-1).

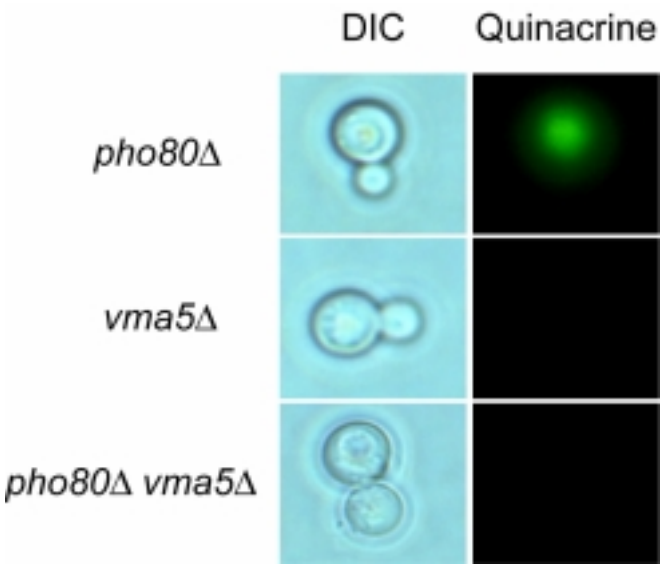

FIG. 4-6. Hyperacidification of *pho80*Δ vacuoles is dependent on the V-ATPase. *pho80*Δ, *vma5*Δ, and *pho80*Δ *vma5*Δ strains were grown to mid-log phase on synthetic medium and stained with quinacrine as in Fig. 4-4. Data shown are representative of two independent experiments.

Our finding of polyP hyperaccumulation in *pho80*Δ cells differs from that of published literature (110). However, our finding is supported by the similarly high polyP levels that are present in two different strain backgrounds as well as when a

PHO4^{c} allele is expressed. A likely explanation for the different results is that the vulnerability of *pho80*Δ cells to various stresses may lead to a high rate of secondary mutations, especially in PHM genes, which would suppress growth defects and eliminate polyP accumulation.

Our studies confirm the finding that *pho80*Δ cells have reduced ability to grow on high levels of sorbitol (Fig. 4-1) and $CaCl_2$ (data not shown) (52) and have extended this further to strains carrying a constitutive *PHO4* allele (Fig. 4-1). Our data thus add further support to the hypothesis that the growth phenotypes of *pho80*Δ strains are caused by the overexpression of Pho4-dependent genes and not through pleiotropic effects of *PHO80* deletion. We have also confirmed that the reduced growth of *pho80*Δ stains under various stress conditions is suppressed by the deletion of *PHM3* (52), and now include *PHM4* and the homeodomain protein *PHO2*. These results show that *pho80*Δ-dependent stress sensitivities do not result from overexpression of *PHM3* alone as previously suggested (52), but rather from the overexpression of the entire PHM complex. In support of this, overexpression of *PHM3* alone from a galactose-inducible promoter does not cause reduced growth on sorbitol- or $CaCl_2$-containing medium (data not shown).

Secondary deletions in *PHO2* suppress the growth phenotype of *pho80*Δ strains on sorbitol (Fig. 4-2A) and reduce polyP levels to that of wild-type strains (Table 4-1), suggesting that Pho2 is an important transcriptional activator of *PHM1-4*. It is important to note that, despite the loss of a primary transcriptional activator, polyP levels in *pho80*Δ *pho2*Δ strains were not reduced to undetectable levels as is the case for

*pho80*Δ *phm3*Δ or *pho80*Δ *phm4*Δ strains (Table 4-1), but were similar to those of wild-type strains. Several possibilities exist to explain this finding. First, a PHM-independent mechanism could exist to synthesize polyP, relegating *PHM1-4* to generate polyP only upon P_i starvation. This explanation seems unlikely, as deletions of *PHM3* or *PHM4* result in the complete loss of polyP. A more plausible explanation is that *PHM1-4* are expressed at high basal levels and are induced further upon P_i starvation through Pho4 and Pho2.

Early work showed that *vac5-1* strains, carrying a partially truncated version of *PHO80*, had severe vacuolar inheritance defects. These phenotypes were found to result from the overproduction of a small molecule, detectable in *pho80*Δ but not in wild-type cells (106). This molecule, between 0.7-3.0 kDa in size, while never identified, was shown not to be a nucleic acid or a polypeptide. We speculate that this unidentified molecule is polyP. Utilizing 0.7 and 3.0 kDa as limits, we propose that the inhibitory molecule could be a polyP chain between 17-75 residues in length. This is not surprising as the average length of a polyP molecule in yeast is ~60 residues in length (92). Our hypothesis is supported by findings that suggest high polyP concentrations inhibit HIV infection of Molt-3 cells, possibly by preventing the docking of the virus, and the subsequent membrane fusion event (79). Similarly, polyP chains also efficiently inhibit the interaction of the bovine assembly protein AP-2 with pre-formed clathrin cages (58), that are essential for endocytosis, which is also defective in *pho80*Δ cells. Nicolson *et al.* (106) predict that the inhibitory molecule is an important contributor to membrane fusion under wild-type levels and only its overproduction inhibits the fusion

process. This prediction is provocative as recent data has shown that deletions of *PHM3* and *PHM4*, eliminating polyP, result in ~90% reduction of *in vitro* vacuolar fusion (96). While the exact functions of Phm1-4 and polyP in vacuolar fusion are unclear, it is thought that they mediate an interaction between Sec18 and the V-ATPase (9) or the v-SNARE Nyv1 (96). Whatever their functions, current data support a role for polyP and the PHM complex as integral components of the fusion machinery.

Constitutive expression of the PHM complex in *pho80*Δ strains results in significant vacuolar defects (Fig. 4-4). Our results indicate that these defects result from the increased synthesis of polyP, possibly in response to the heightened activation of the V-ATPase through Phm3 and Phm4, as no detectable acidification is seen in *phm3*Δ cells (Fig. 4-7). Increased activation of the V-ATPase is likely the primary cause for hyperacidification of the vacuole (Fig. 4-4). Since it has been well documented that the loss of vacuolar acidification has significant effects on stress survival, we suggest that vacuolar hyperacidification is equally likely to cause stress susceptibilities (Fig. 4-7). It is possible that the vacuolar fusion and inheritance defects seen in *pho80*Δ strains also result from vacuolar hyperacidification. We propose that maintaining pH homeostasis in the vacuole is critically important to a myriad of cellular functions required for detoxification., including autophagy, endocytosis, and vacuolar-ion transport.

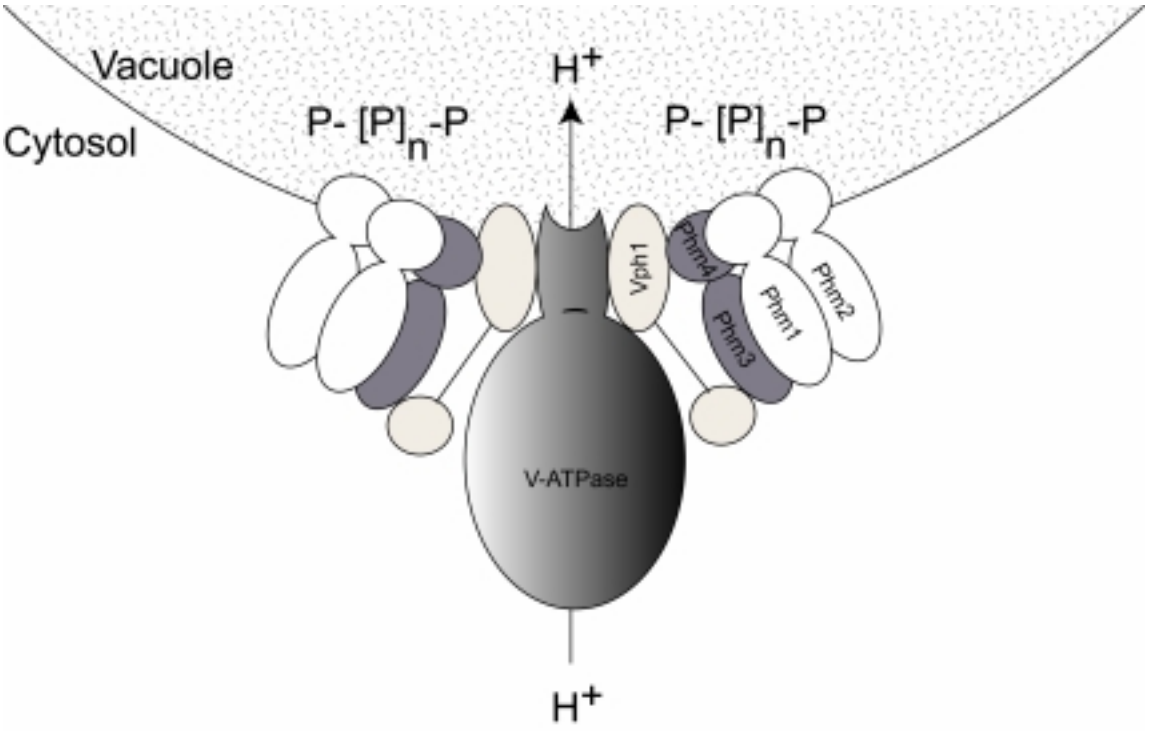

FIG. 4-7. Association of the V-ATPase with the PHM complex. Schematic representation of the interactions between the V-ATPase and the PHM complex. Phm3 and Phm4 interact with Vph1 and potentially modulate V-ATPase activate thereby creating a favorable environment for polyP synthesis as an acidified vacuole is essential for polyP synthesis.

CHAPTER V

SUMMARY AND CONCLUSIONS

Our work has shown that mitotic induction of *PHO5* is dependent on the transcriptional activators Pho4 and Pho2 as well as the cyclin-dependent kinase inhibitor Pho81 (Fig. 2-1). The activation is also dependent on the chromatin remodeling enzymes Gcn5 and Snf2 (Fig. 2-2) and responds to the cell cycle-dependent fluctuations of ortho- and polyphosphate. The addition of P_i to YPD completely represses the mitotic induction (Fig. 2-3), suggesting that YPD is limiting for orthophosphate. Deletions of *PHM3* or *PHM4*, required for polyP synthesis, led to increases in mitotic *PHO5* induction, suggesting the mitotic induction was responding to polyP levels (Fig. 2-5, 2-8). In synchronized cultures, we found that polyP cycles in a cell cycle-dependent manner. Yeast cells are rich in polyP in early G1, but levels decrease quickly as cells enter S phase to provide needed P_i for DNA replication (Fig. 2-7, 5-1). When polyP levels reach a low point during mitosis, induction of *PHO5* and other P_i-responsive genes occurs, allowing for polyP to be replenished (Fig. 5-1). These results have defined polyP fluctuation as an effector of for mitotic *PHO5* induction.

The replenishment of polyP is so important to the cell that it has devised a support system, that assures maximum *PHO5* induction during each cell cycle. Binding sites for the transcriptional activators Mcm1 and SFF are found in the promoters of *PHO5* as well as three other mitotically-induced acid phosphatases, *PHO3*, *PHO11*, and *PHO12* (Fig. 3-1). Partial loss-of-function alleles of *MCM1* revealed that the factor contributes as much as 50% to the mitotic activation of *PHO5* (Fig. 3-2A). Since SFF is

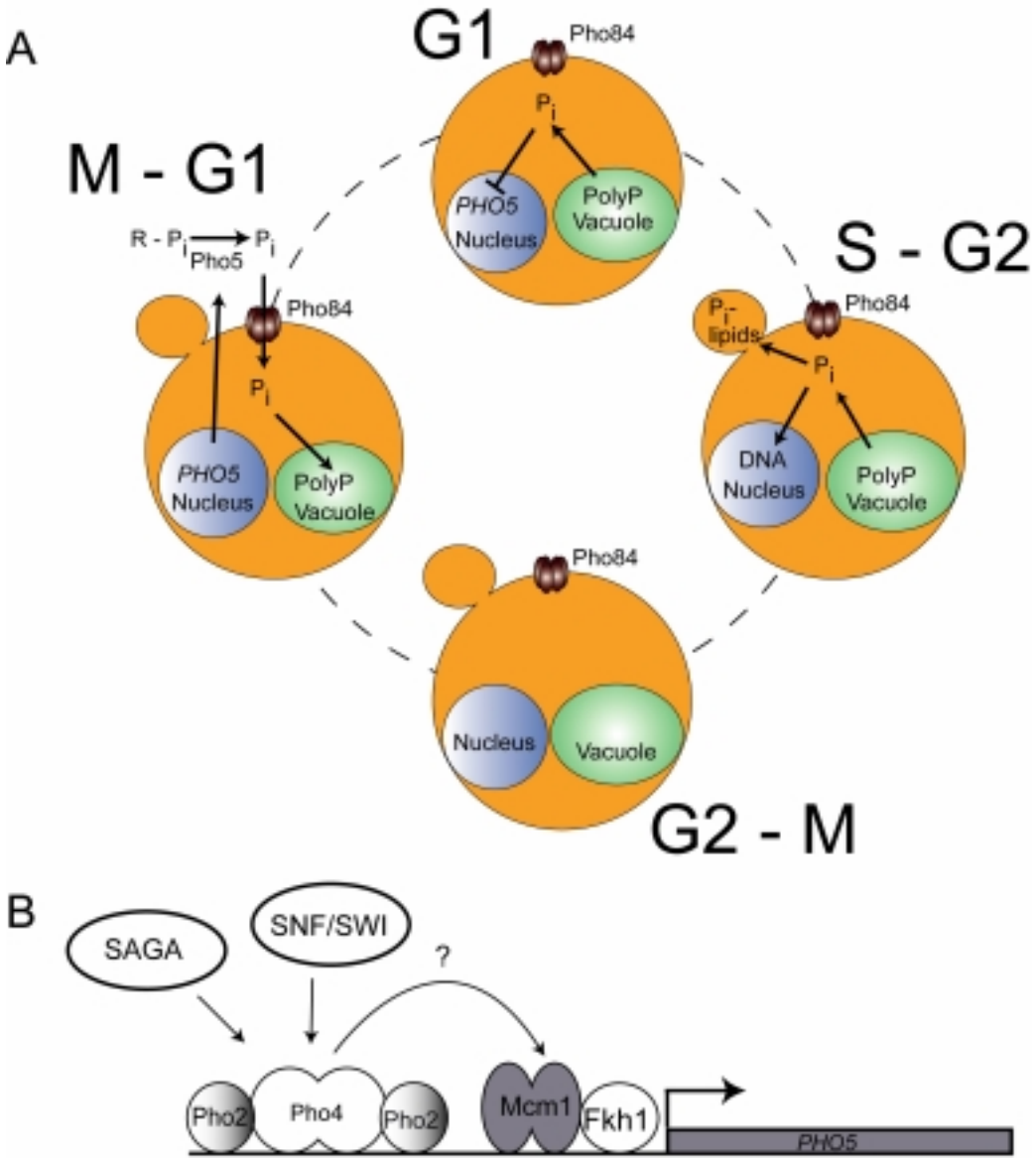

FIG. 5-1. Cell cycle-dependent regulation of polyphosphate. (A) PolyP levels fluctuate in a cell cycle-dependent manner. In G1, high polyP levels cause repression of *PHO5*. During S phase, polyP is depleted for DNA replication and bud synthesis. During G2, low levels of polyP induce expression of *PHO5*. In mitosis, Pho5 scavenges P_i from P_i esters in the media, thereby allowing for replenishment of polyP. (B) Mitotic expression of *PHO5*. Pho4 and Pho2 bind to the *PHO5* promoter and recruit SAGA and SNF/SWI. Mcm1 and Fkh1 associate with the *PHO5* promoter and aid in transcription. A potential interaction between Pho4/Pho2 and Mcm1/Fkh1 is shown.

defined by either Fkh1 or Fkh2, we assayed the ability of *fkh1*Δ, *fkh2*Δ, and *fkh1*Δ *fkh2*Δ strains to activate *PHO5* during mitosis. Surprisingly, loss of Fkh2, the dominant binding partner of Mcm1, has no effect on *PHO5* activation, while Fkh1 loss reduces *PHO5* activation by 30% (Fig. 3-2C). A double deletion of both FKH genes results in a 40% loss of activation. Mutations in the Mcm1 and SFF binding sites revealed that the contribution of Mcm1 to the mitotic induction is slightly higher than that of SFF. Furthermore, mutations in both binding sites results in 60% reduced *PHO5* activation, similar to mutations in the Mcm1 binding site alone (Fig. 3-3B). Chromatin immunoprecipitation experiments revealed that while Mcm1 binding can not be detected in YPD or high-P_i medium, Mcm1 binds readily to the *PHO5* promoter during P_i starvation in a Pho4- and Pho2-dependent manner (Fig. 3-5, 3-6).

Finally, we have elucidated the importance of regulating polyP synthesis. Loss of the Pho85-specific cyclin Pho80, or expression of a constitutively active *PHO4* allele results in the constitutive expression of P_i-responsive genes, including *PHM1-4*. The uncontrolled expression of these polyP synthases elevates polyP levels by 5-fold (Table 4-1) and results in severe growth defects under stress conditions (Fig. 4-1). Growth defects on osmotically-stressing medium is suppressed by secondary deletions in *PHO2*, *PHM3*, and *PHM4*, which all restore polyP levels to or below wild-type levels (Fig. 4-2). Furthermore, growing *pho80*Δ strains on medium containing only 10 μM P_i completely restores wild-type growth even in the presence of osmotic stress (Fig. 4-3). When assayed, no polyP was detected in *pho80*Δ strains grown under P_i-limiting conditions (Table 4-2). To understand better the cause of *pho80*Δ-dependent growth defects, we

assayed vacuolar morphology by staining with FM4-64 and quinacrine. FM4-64 staining revealed that *pho80*Δ strains have extremely large vacuoles that occupy most of the cell, while quinacrine staining revealed that these vacuoles are highly overacidified (Fig. 4-4). Both increased size and acidity are suppressed by secondary deletions in *PHO2* and *PHM3* as well as growth on low-P_i medium (Fig. 4-5), supporting the interpretation that polyP synthesis is directly responsible for causing both defects.

Since little is known about polyP in eukaryotes it is difficult to compare our findings in *S. cerevisiae* to other systems. However, our results suggest significantly different functions for polyP in *S. cerevisiae* versus bacteria. As discussed earlier (Chapter 1), in prokaryotes, polyP is important for stress survival. Ppk1 and polyP are important for the expression of *rpoS* and the induction of stress-responsive genes (66). Our experiments suggest that polyP serves no such function in *S. cerevisiae*. For example, in *E. coli*, polyP is required for surviving osmotic shock, as *ppk1*– strains are almost 100-fold more sensitive than wild-type strains (66). In our system, strains deleted for *PHM3* or *PHM4*, which lack polyP, show no significant susceptibility to osmotic shock (Fig. 4-2). In prokaryotes, long-chain polyphosphates accumulate in response to osmotic stress (66), presumably serving as a signaling molecule. In budding yeast, large amounts of polyP increase susceptibility to osmotic stress (Fig. 4-1). Furthermore, polyP is especially important in *E. coli* stationary phase (66). Inhibition of the *E. coli* exopolyphosphatase during stationary phase leads to large increases in polyP (66). These large increases are important as only 7% of strains lacking polyP survive in stationary phase. Contrary to this, *S. cerevisiae* strains lacking the exo- and

endopolyphosphatase accumulate high levels of polyphosphates and lose viability rapidly upon entering stationary phase (137).

Lactobacillus plantarum lacks a superoxide dismutase, a ubiquitous enzyme required for detoxification of oxidative metals. Instead, it utilizes high concentrations of polyP to bind and sequester oxidative metals. Our findings suggest that polyP is also not required for this function in yeast, as *phm3*Δ and *phm4*Δ strains are not susceptible to high levels of Cu^{2+} (data not shown). Our results suggest that in yeast, polyP does not have the same signaling functions as it has in prokaryotes. Its likely that novel mechanism exist in eukaryotes to perform the functions that polyP performs in prokaryotes, relegating polyP in yeast to the role of a phosphate reserve.

Our work on polyP and the mechanisms involved in its regulation will likely have impacts beyond the system of *Saccharomyces cerevisiae*. The regulation of genes like *PHO5* by cell cycle-dependent fluctuations in nutrients, seemingly independent of the cell cycle machinery, will likely extend to higher eukaryotes. Understanding cell cycle regulation in higher eukaryotes is especially important due to its innate relationship with cancer and apoptosis (2, 29, 49). If genes implicated in cancer were found to be regulated through nutrient fluctuation, it might be possible to influence their expression by varying dietary intake. It has for example been shown that glucose transporters, as well as methionine-regulated genes are up-regulated during certain cancers (5, 36, 151). Efforts have been undertaken to potentially regulate such genes through dietary changes (108).

Furthermore, our findings of polyP-dependent vacuolar defects will likely contribute to a variety of fields. For example, *btn1*Δ strains, deficient in a vacuolar protein of unknown function, like *pho80*Δ strains, have highly overacidified vacuoles (119). Btn1 is a functional homologue of the human CLN3 protein, which when defective results in Battens disease, a fatal disorder of the nervous system (120). Loss of CLN3 results in overacidification of the human lysosome (41) and hyperaccumulation of an unknown lysosomal substance (28). Thus, understanding how hyperacidification causes vacuolar and/or lysosomal defects could lead to possible therapies or cures of Battens disease. It is possible that a human polyP synthase will, like the PHM complex in yeast, utilize and affect a proton-motive force, and could therefore also result in acidification defects. Therefore, it is possible that several human diseases will be found to result from the missregulation of polyP metabolism.

Lastly, a basic understanding of polyP and its functions is essential due to its ubiquitous nature in humans. High levels of polyP are found especially in the bone and brain tissues of humans (68). Although it is not known why polyP is more prevalent in these tissues as opposed to others, its abundance suggests important functions. As we have shown, the hyperaccumulation of polyP can cause severe defects in yeast. It will be important to understand how high-abundance polyP tissues properly maintain their polyP levels to avoid hyperaccumulation defects. In addition, the hyperaccumulation of polyP also results in increased susceptibilities to DNA damaging agents (52), thereby increasing the accumulation of cancer-causing mutations.

Additional work studying polyP synthesis needs to be undertaken. Understanding if and how the PHM complex synthesizes polyP will constitute an important advance. An *in vitro* polyP synthesis experiment would be utilized to determine if the PHM complex is in fact a polyP synthase. The individual PHM proteins could be expressed and purified from *E. coli* and then reconstituted into synthetic membrane vesicles. Since a proton-motive force is required for polyP synthesis, it may be difficult to achieve this gradient *in vitro*. Furthermore, since the exact substrate for polyP synthesis is unknown, several possibilities would have to be explored.

While polyP resides in the vacuole, nothing is known about where the polymer is synthesized. Critical experiments will define whether it is synthesized in the cytoplasm and transported to the vacuole, similar to glycogen, or if it is synthesized directly in the vacuole. We envision a microscopic technique to assay polyP localization, utilizing the preferential staining of polyP with toluidine blue. We have engineered *phm3*Δ, strains lacking endogenous polyP, to express *ppk1*, the *E. coli* polyP kinase. Since *ppk1* is localized to the cytoplasm we predict that the resulting polyP would initially be localized to the cytoplasm. To determine if polyP remains in the cytoplasm or if it is transported to the vacuole, polyP localization could potentially be monitored utilizing toluidine blue. The yeast deletion panel could then be screened for genes required for polyP transport. Alternatively, subcellular fractionation could be used to assay the localization of polyP.

REFERENCES

1. **Acton, T. B., J. Mead, A. M. Steiner, and A. K. Vershon**. 2000. Scanning mutagenesis of Mcm1: residues required for DNA binding, DNA bending, and transcriptional activation by a MADS-box protein. Mol. Cell. Biol. **20**:1-11.

2. **Adams, P. D.** 2001. Regulation of the retinoblastoma tumor suppressor protein by cyclin/cdks. Biochim. Biophys. Acta **1471**:M123-M133.

3. **Althoefer, H., A. Schleiffer, K. Wassmann, A. Nordheim, and G. Ammerer**. 1995. Mcm1 is required to coordinate G(2)-specific transcription in *Saccharomyces cerevisiae*. Mol. Cell. Biol. **15**:5917-5928.

4. **Amar, N., F. Messenguy, M. El Bakkoury, and E. Dubois**. 2000. ArgRII, a component of the ArgR-Mcm1 complex involved in the control of arginine metabolism in *Saccharomyces cerevisiae*, is the sensor of arginine. Mol. Cell. Biol. **20**:2087-2097.

5. **Ashendel, C. L.** 1995. Diet, signal transduction and carcinogenesis. J. Nutr. **125**:686S-691S.

6. **Barbaric, S., M. Munsterkotter, J. Svaren, and W. Hörz**. 1996. The homeodomain protein Pho2 and the basic-helix-loop-helix protein Pho4 bind DNA cooperatively at the yeast *PHO5* promoter. Nucleic Acids Res. **24**:4479-4486.

7. **Barbaric, S., J. Walker, A. Schmid, J. Q. Svejstrup, and W. Hörz**. 2001. Increasing the rate of chromatin remodeling and gene activation -- a novel role for the histone acetyltransferase Gcn5. EMBO J. **20**:4944-4951.

8. **Battini, J. L., J. E. Rasko, and A. D. Miller**. 1999. A human cell-surface receptor for xenotropic and polytropic murine leukemia viruses: possible role in G protein-coupled signal transduction. Proc. Natl. Acad. Sci. USA **96**:1385-1390.

9. **Bayer, M. J., C. Reese, S. Buhler, C. Peters, and A. Mayer**. 2003. Vacuole membrane fusion: V_0 functions after trans-SNARE pairing and is coupled to the Ca^{2+}-releasing channel. J. Cell Biol. **162**:211-222.

10. **Berner, Y. N. and M. Shike**. 1988. Consequences of phosphate imbalance. Annu. Rev. Nutr. **8**:121-148.

11. **Brachmann, C. B., A. Davies, G. J. Cost, E. Caputo, J. Li, P. Hieter, and J. D. Boeke**. 1998. Designer deletion strains derived from *Saccharomyces*

cerevisiae S288C: a useful set of strains and plasmids for PCR-mediated gene disruption and other applications. Yeast **14**:115-132.

12. **Brinch-Pedersen, H., L. D. Sorensen, and P. B. Holm**. 2002. Engineering crop plants: getting a handle on phosphate. Trends Plant Sci. **7**:118-125.

13. **Brownell, J. E., J. X. Zhou, T. Ranalli, R. Kobayashi, D. G. Edmondson, S. Y. Roth, and C. D. Allis**. 1996. *Tetrahymena* histone acetyltransferase A: a homolog to yeast Gcn5p linking histone acetylation to gene activation. Cell **84**:843-851.

14. **Bun-ya, M., M. Nishimura, S. Harashima, and Y. Oshima**. 1991. The *PHO84* gene of *Saccharomyces cerevisiae* encodes an inorganic phosphate transporter. Mol. Cell. Biol. **11**:3229-3238.

15. **Bun-ya, M., K. Shikata, S. Nakade, C. Yompakdee, S. Harashima, and Y. Oshima**. 1996. Two new genes, *PHO86* and *PHO87*, involved in inorganic phosphate uptake in *Saccharomyces cerevisiae*. Curr. Genet. **29**:344-351.

16. **Chang, V. K., M. J. Fitch, J. J. Donato, T. W. Christensen, A. M. Merchant, and B. K. Tye**. 2003. Mcm1 binds replication origins. J. Biol. Chem. **278**:6093-6100.

17. **Chen, Y. and B. K. Tye**. 1995. The yeast Mcm1 protein is regulated posttranscriptionally by the flux of glycolysis. Mol. Cell. Biol. **15**:4631-4639.

18. **Chien, M. L., J. L. Foster, J. L. Douglas, and J. V. Garcia**. 1997. The amphotropic murine leukemia virus receptor gene encodes a 71-kilodalton protein that is induced by phosphate depletion. J. Virol. **71**:4564-4570.

19. **Cho, R. J., M. J. Campbell, E. A. Winzeler, L. Steinmetz, A. Conway, L. Wodicka, T. G. Wolfsberg, A. E. Gabrielian, D. Landsman, D. J. Lockhart, and R. W. Davis**. 1998. A genome-wide transcriptional analysis of the mitotic cell cycle. Mol. Cell **2** :65-73.

20. **Chrispeels, M. J., N. M. Crawford, and J. I. Schroeder**. 1999. Proteins for transport of water and mineral nutrients across the membranes of plant cells. Plant Cell **11**:661-676.

21. **Clark, J. E., H. Beegen, and H. G. Wood**. 1986. Isolation of intact chains of polyphosphate from *Propionibacterium shermanii* grown on glucose or lactate. J. Bacteriol. **168**:1212-1219.

22. **Clarke, D. J.** 2002. Proteolysis and the cell cycle. Cell Cycle **1**:233-234.

23. **Cohen, A., N. Perzov, H. Nelson, and N. Nelson**. 1999. A novel family of yeast chaperons involved in the distribution of V-ATPase and other membrane proteins. J. Biol. Chem. **274**:26885-26893.

24. **Creasy, C. L., D. Shao, and L. W. Begman**. 1996. Negative transcriptional regulation of *PH081* expression in *Saccharomyces cerevisiae*. Gene **168**:23-29.

25. **Cross, F. R. and A. H. Tinkelenberg**. 1991. A potential positive feedback loop controlling *CLN1* and *CLN2* gene expression at the start of the yeast cell cycle. Cell **65**:875-883.

26. **Cunningham, K. W. and G. R. Fink**. 1996. Calcineurin inhibits *VCX1*-dependent H^+/Ca^{2+} exchange and induces Ca^{2+} ATPases in *Saccharomyces cerevisiae*. Mol. Cell. Biol. **16**:2226-2237.

27. **Curtis, K. K., S. A. Francis, Y. Oluwatosin, and P. M. Kane**. 2002. Mutational analysis of the subunit C (Vma5p) of the yeast vacuolar H^+-ATPase. J. Biol. Chem. **277**:8979-8988.

28. **Dawson, G. and S. Cho**. 2000. Batten's disease: clues to neuronal protein catabolism in lysosomes. J. Neurosci. Res. **60**:133-140.

29. **Delavaine, L. and N. B. La Thangue**. 1999. Control of E2F activity by p21Waf1/Cip1. Oncogene **18**:5381-5392.

30. **Dunn, T., K. Gable, and T. Beeler**. 1994. Regulation of cellular Ca^{2+} by yeast vacuoles. J. Biol. Chem. **269**:7273-7278.

31. **Edwards, R. M.** 2002. Disorders of phosphate metabolism in chronic renal disease. Curr. Opin. Pharmacol. **2**:171-176.

32. **Eisen, A., R. T. Utley, A. Nourani, S. Allard, P. Schmidt, W. S. Lane, J. C. Lucchesi, and J. Cote**. 2001. The yeast NuA4 and *Drosophila* MSL complexes contain homologous subunits important for transcription regulation. J. Biol. Chem. **276**:3484-3491.

33. **Elble, R. and B. K. Tye**. 1991. Both activation and repression of **a**-mating-type-specific genes in yeast require transcription factor Mcm1. Proc. Natl. Acad. Sci. USA **88**:10966-10970.

34. **Elble, R. and B. K. Tye**. 1992. Chromosome loss, hyperrecombination, and cell cycle arrest in a yeast mcm1-mutant. Mol. Biol. Cell. **3**:971-980.

35. **Elledge, S. J. and R. W. Davis** . 1989. DNA damage induction of ribonucleotide reductase. Mol. Cell. Biol. **9**:4932-4940.

36. **Flier, J. S., M. M. Mueckler, P. Usher, and H. F. Lodish**. 1987. Elevated levels of glucose transport and transporter messenger RNA are induced by *ras* or *src* oncogenes. Science **235**:1492-1495.

37. **Gaudreau, L., A. Schmid, D. Blaschke, M. Ptashne, and W. Hörz**. 1997. RNA polymerase II holoenzyme recruitment is sufficient to remodel chromatin at the yeast *PHO5* promoter. Cell **89**:55-62.

38. **Gavin, I. M., M. P. Kladde, and R. T. Simpson**. 2000. Tup1p represses Mcm1p transcriptional activation and chromatin remodeling of an **a**-cell-specific gene. EMBO J. **19**:5875-5883.

39. **Gillies, R. J., K. Ugurbil, J. A. den Hollander, and R. G. Shulman**. 1981. ^{31}P NMR studies of intracellular pH and phosphate metabolism during cell division cycle of *Saccharomyces cerevisiae*. Proc. Natl. Acad. Sci. USA **78**:2125-2129.

40. **Goebl, M. G., J. Yochem, S. Jentsch, J. P. McGrath, A. Varshavsky, and B. Byers**. 1988. The yeast cell cycle gene *CDC34* encodes a ubiquitin-conjugating enzyme. Science **241**:1331-1335.

41. **Golabek, A. A., E. Kida, M. Walus, W. Kaczmarski, M. Michalewski, and K. E. Wisniewski**. 2000. Cln3 protein regulates lysosomal pH and alters intracellular processing of Alzheimer's amyloid-beta protein precursor and cathepsin D in human cells. Mol. Genet. Metab. **70**:203-213.

42. **Grant, P. A., L. Duggan, J. Cote, S. M. Roberts, J. E. Brownell, R. Candau, R. Ohba, T. Owen Hughes, C. D. Allis, F. Winston, S. L. Berger, and J. L. Workman**. 1997. Yeast Gcn5 functions in two multisubunit complexes to acetylate nucleosomal histones: characterization of an Ada complex and the SAGA (Spt/Ada) complex. Genes Dev. **11**:1640-1650.

43. **Gregory, P. D., A. Schmid, M. Zavari, L. Lui, S. L. Berger, and W. Hörz**. 1998. Absence of Gcn5 HAT activity defines a novel state in the opening of chromatin at the *PHO5* promoter in yeast. Mol. Cell **1**:495-505.

44. **Gregory, P. D., A. Schmid, M. Zavari, M. Munsterkotter, and W. Hörz**. 1999. Chromatin remodeling at the *PHO8* promoter requires SWI-SNF and SAGA at a step subsequent to activator binding. EMBO J. **18**:6407-6414.

45. **Guschin, D. and A. P. Wolffe**. 1999. SWItched-on mobility. Curr. Biol. **9**:R742-R746.

46. **Han, M., U. J. Kim, P. Kayne, and M. Grunstein**. 1988. Depletion of histone H4 and nucleosomes activates the *PHO5* gene in *Saccharomyces cerevisiae*. EMBO J. **7**:2221-2228.

47. **Hereford, L. M., M. A. Osley, T. R. Ludwig, and C. S. McLaughlin**. 1981. Cell-cycle regulation of yeast histone mRNA. Cell **24**:367-375.

48. **Hess, K. R., W. Zhang, K. A. Baggerly, D. N. Stivers, and K. R. Coombes**. 2001. Microarrays: handling the deluge of data and extracting reliable information. Trends Biotechnol. **19**:463-468.

49. **Hiyama, H., A. Iavarone, and S. A. Reeves**. 1998. Regulation of the cdk inhibitor p21 gene during cell cycle progression is under the control of the transcription factor E2F. Oncogene **16**:1513-1523.

50. **Hollenhorst, P. C., M. E. Bose, M. R. Mielke, U. Muller, and C. A. Fox**. 2000. Forkhead genes in transcriptional silencing, cell morphology and the cell cycle. Overlapping and distinct functions for *FKH1* and *FKH2* in *Saccharomyces cerevisiae.* Genetics **154**:1533-1548.

51. **Holstege, F. C. P., E. G. Jennings, J. J. Wyrick, T. I. Lee, C. J. Hengartner, M. R. Green, T. Golub, E. S. Lander, and R. A. Young**. 1998. Dissecting the regulatory circuitry of a eukaryotic genome. Cell **95**:717-728.

52. **Huang, D., J. Moffat, and B. Andrews**. 2002. Dissection of a complex phenotype by functional genomics reveals roles for the yeast cyclin-dependent protein kinase Pho85 in stress adaptation and cell integrity. Mol. Cell. Biol. **22**:5076-5088.

53. **Hwang-Shum, J. J., D. C. Hagen, E. E. Jarvis, C. A. Westby, and G. F. Sprague, Jr.** 1991. Relative contributions of Mcm1 and Ste12 to transcriptional activation of **a**- and alpha-specific genes from *Saccharomyces cerevisiae*. Mol. Gen. Genet. **227**:197-204.

54. **Iyer, V. R., C. E. Horak, C. S. Scafe, D. Botstein, M. Snyder, and P. O. Brown**. 2001. Genomic binding sites of the yeast cell-cycle transcription factors SBF and MBF. Nature **409**:533-538.

55. **Jarvis, E. E., K. L. Clark, and G. F. Sprague, Jr.** 1989. The yeast transcription activator PRTF, a homolog of the mammalian serum response factor, is encoded by the *MCM1* gene. Genes Dev. **3**:936-945.

56. **Johann, S. V., J. J. Gibbons, and B. O'Hara**. 1992. GLVR1, a receptor for gibbon ape leukemia virus, is homologous to a phosphate permease of *Neurospora crassa* and is expressed at high levels in the brain and thymus. J. Virol. **66**:1635-1640.

57. **Kaffman, A., I. Herskowitz, R. Tjian, and E. K. O'Shea**. 1994. Phosphorylation of the transcription factor Pho4 by a cyclin-CDK complex, Pho80-Pho85. Science **263**:1153-1156.

58. **Keen, J. H., K. A. Beck, T. Kirchhausen, and T. Jarrett**. 1991. Clathrin domains involved in recognition by assembly protein AP-2. J. Biol. Chem. **266**:7950-7956.

59. **Kim, K. S., N. N. Rao, C. D. Fraley, and A. Kornberg**. 2002. Inorganic polyphosphate is essential for long-term survival and virulence factors in *Shigella* and *Salmonella spp*. Proc. Natl. Acad. Sci. USA **99**:7675-7680.

60. **Kladde, M. P., M. Xu, and R. T. Simpson**. 1996. Direct study of DNA-protein interactions in repressed and active chromatin in living cells. EMBO J. **15**:6290-6300.

61. **Klionsky, D. J. and S. D. Emr**. 1989. Membrane protein sorting: biosynthesis, transport and processing of yeast vacuolar alkaline phosphatase. EMBO J. **8**:2241-2250.

62. **Koch, C., T. Moll, M. Neuberg, H. Ahorn, and K. Nasmyth**. 1993. A role for the transcription factors Mbp1 and Swi4 in progression from G1 to S phase. Science **261**:1551-1557.

63. **Koch, C., A. Schleiffer, G. Ammerer, and K. Nasmyth**. 1996. Switching transcription on and off during the yeast cell cycle: Cln/Cdc28 kinases activate bound transcription factor SBF (Swi4/Swi6) at start, whereas Clb/Cdc28 kinases displace it from the promoter in G2. Genes Dev. **10**:129-141.

64. **Komeili, A. and E. K. O'Shea**. 1999. Roles of phosphorylation sites in regulating activity of the transcription factor Pho4. Science **284**:977-980.

65. **Koranda, M., A. Schleiffer, L. Endler, and G. Ammerer**. 2000. Forkhead-like transcription factors recruit Ndd1 to the chromatin of G2/M-specific promoters. Nature **406**:94-98.

66. **Kornberg, A., N. N. Rao, and D. Ault-Riché**. 1999. Inorganic polyphosphate: a molecule of many functions. Annu. Rev. Biochem. **68**:89-125.

67. **Krebs, J. E., C. J. Fry, M. L. Samuels, and C. L. Peterson**. 2000. Global role for chromatin remodeling enzymes in mitotic gene expression. Cell **102**:587-598.

68. **Kumble, K. D. and A. Kornberg**. 1995. Inorganic polyphosphate in mammalian cells and tissues. J. Biol. Chem. **270**:5818-5822.

69. **Kumble, K. D. and A. Kornberg**. 1996. Endopolyphosphatases for long chain inorganic polyphosphate in yeast and mammals. J. Biol. Chem. **271**:27146-27151.

70. **Kuo, M. H., E. T. Nadeau, and E. J. Grayhack**. 1997. Multiple phosphorylated forms of the *Saccharomyces cerevisiae* Mcm1 protein include an isoform induced in response to high salt concentrations. Mol. Cell. Biol. **17**:819-832.

71. **Kuroda, A., K. Nomura, R. Ohtomo, J. Kato, T. Ikeda, N. Takiguchi, H. Ohtake, and A. Kornberg**. 2001. Role of inorganic polyphosphate in promoting ribosomal protein degradation by the Lon protease in *E. coli*. Science **293**:705-708.

72. **Lambertson, D., L. Chen, and K. Madura**. 1999. Pleiotropic defects caused by loss of the proteasome-interacting factors Rad23 and Rpn10 of *Saccharomyces cerevisiae*. Genetics **153**:69-79.

73. **Lau, W. W., K. R. Schneider, and E. K. O'Shea**. 1998. A genetic study of signaling processes for repression of *PHO5* transcription in *Saccharomyces cerevisiae*. Genetics **150**:1349-1359.

74. **Laurent, B. C., I. Treich, and M. Carlson**. 1993. The yeast *SNF2*/*SWI2*-protein has DNA-stimulated ATPase activity required for transcriptional activation. Genes Dev. **7**:583-591.

75. **Leggewie, G., L. Willmitzer, and J. W. Riesmeier**. 1997. Two cDNAs from potato are able to complement a phosphate uptake-deficient yeast mutant: identification of phosphate transporters from higher plants. Plant Cell **9**:381-392.

76. **Lenburg, M. E. and E. K. O'Shea**. 1996. Signaling phosphate starvation. Trends Biochem. Sci. **21**:383-387.

77. **Lew, D. J., T. Weinert, and J. R. Pringle**. 1997. Cell cycle control in *Saccharomyces cerevisiae*, p. 607-695. *In* J. R. Pringle, J. R. Broach, and E. W. Jones (ed.), The molecular and cellular biology of the yeast *Saccharomyces*. Cold Spring Harbor Laboratory Press, Plainview, NY.

78. **Lillie, S. H. and J. R. Pringle**. 1980. Reserve carbohydrate metabolism in *Saccharomyces cerevisiae*: responses to nutrient limitation. J. Bacteriol. **143**:1384-1394.

79. **Lorenz, B., J. Leuck, D. Kohl, W. E. Muller, and H. C. Schroder**. 1997. Anti-HIV-1 activity of inorganic polyphosphates. J. Acquir. Immune. Defic. Syndr. Hum. Retrovirol. **14**:110-118.

80. **Lydall, D., G. Ammerer, and K. Nasmyth**. 1991. A new role for Mcm1 in yeast: cell cycle regulation of *SWI5* transcription. Genes Dev. **5**:2405-2419.

81. **Maher, M., F. Cong, D. Kindelberger, K. Nasmyth, and S. Dalton**. 1995. Cell cycle-regulated transcription of the *CLB2* gene is dependent on Mcm1 and a ternary complex factor. Mol. Cell. Biol. **15**:3129-3137.

82. **Mai, B., S. Miles, and L. L. Breeden**. 2002. Characterization of the ECB binding complex responsible for the M/G(1)-specific transcription of *CLN3* and *SWI4*. Mol. Cell. Biol. **22**:430-441.

83. **Maine, G. T., P. Sinha, and B. K. Tye**. 1984. Mutants of *S. cerevisiae* defective in the maintenance of minichromosomes. Genetics **106**:365-385.

84. **Mann, B. J., R. A. Akins, A. M. Lambowitz, and R. L. Metzenberg**. 1988. The structural gene for a phosphorus-repressible phosphate permease in *Neurospora crassa* can complement a mutation in positive regulatory gene *nuc-1*. Mol. Cell. Biol. **8**:1376-1379.

85. **Mann, B. J., B. J. Bowman, J. Grotelueschen, and R. L. Metzenberg**. 1989. Nucleotide sequence of *pho-4*+, encoding a phosphate-repressible phosphate permease of *Neurospora crassa*. Gene **83**:281-289.

86. **Martinez, P. and B. L. Persson** . 1998. Identification, cloning and characterization of a derepressible Na^+-coupled phosphate transporter in *Saccharomyces cerevisiae*. Mol. Gen. Genet. **258**:628-638.

87. **McDonald, A. E., J. O. Niere, and W. C. Plaxton**. 2001. Phosphite disrupts the acclimation of *Saccharomyces cerevisiae* to phosphate starvation. Can. J. Microbiol. **47**:969-978.

88. **McInerny, C. J., J. F. Partridge, G. E. Mikesell, D. P. Creemer, and L. L. Breeden**. 1997. A novel Mcm1-dependent element in the *SWI4*, *CLN3*, *CDC6*, and *CDC47* promoters activates M/G1-specific transcription. Genes Dev. **11**:1277-1288.

89. **Meaden, P. G., N. Arneborg, L. U. Guldfeldt, H. Siegumfeldt, and M. Jakobsen**. 1999. Endocytosis and vacuolar morphology in *Saccharomyces cerevisiae* are altered in response to ethanol stress or heat shock. Yeast **15**:1211-1222.

90. **Mendenhall, M. D.** 1998. Cyclin-dependent kinase inhibitors of *Saccharomyces cerevisiae* and *Schizosaccharomyces pombe*. Curr. Top. Microbiol. Immunol. **227**:1-24.

91. **Messenguy, F. and E. Dubois**. 1993. Genetic evidence for a role for *MCM1* in the regulation of arginine metabolism in *Saccharomyces cerevisiae*. Mol. Cell. Biol. **13**:2586-2592.

92. **Meyhack, B., W. Bajwa, H. Rudolph, and A. Hinnen**. 1982. Two yeast acid phosphatase structural genes are the result of a tandem duplication and show different degrees of homology in their promoter and coding sequences. EMBO J. **1**:675-680.

93. **Mitsukawa, N., S. Okumura, Y. Shirano, S. Sato, T. Kato, S. Harashima, and D. Shibata**. 1997. Overexpression of an *Arabidopsis thaliana* high-affinity phosphate transporter gene in tobacco cultured cells enhances cell growth under phosphate-limited conditions. Proc. Natl. Acad. Sci. USA **94**:7098-7102.

94. **Miyamoto, K. I. and M. Itho**. 2001. Transcriptional regulation of the *NPT2* gene by dietary phosphate. Kidney Int. **60**:412-415.

95. **Moll, T., L. Dirick, H. Auer, J. Bonkovsky, and K. Nasmyth**. 1992. Swi6 is a regulatory subunit of two different cell cycle START-dependent transcription factors in *Saccharomyces cerevisiae*. J. Cell Sci. Suppl. **16**:87-96.

96. **Muller, O., M. J. Bayer, C. Peters, J. S. Andersen, M. Mann, and A. Mayer**. 2002. The Vtc proteins in vacuole fusion: coupling NSF activity to V_0 *trans*-complex formation. EMBO J. **21**:259-269.

97. **Muller, O., H. Neumann, M. J. Bayer, and A. Mayer**. 2003. Role of the Vtc proteins in V-ATPase stability and membrane trafficking. J. Cell Sci. **116**:1107-1115.

98. **Munsterkotter, M., S. Barbaric, and W. Hörz**. 2000. Transcriptional regulation of the yeast *PHO8* promoter in comparison to the coregulated *PHO5* promoter. J. Biol. Chem. **275**:22678-22685.

99. **Nakamura, N., A. Matsuura, Y. Wada, and Y. Ohsumi**. 1997. Acidification of vacuoles is required for autophagic degradation in the yeast, *Saccharomyces cerevisiae*. J. Biochem.(Tokyo) **121**:338-344.

100. **Nakao, J., A. Miyanohara, Toh-e A, and K. Matsubara**. 1986. *Saccharomyces cerevisiae PHO5* promoter region: location and function of the upstream activation site. Mol. Cell. Biol. **6**:2613-2623.

101. **Nasmyth, K.** 1993. Control of the yeast cell cycle by the Cdc28 protein kinase. Curr. Opin. Cell Biol. **5**:166-179.

102. **Nass, R. and R. Rao**. 1999. The yeast endosomal Na^+/H^+ exchanger, Nhx1, confers osmotolerance following acute hypertonic shock. Microbiology **145**:3221-3228.

103. **Neef, D. W. and M. P. Kladde**. 2003. Polyphosphate loss promotes SNF/SWI- and Gcn5-dependent mitotic induction of *PHO5*. Mol. Cell. Biol. **23**:3788-3797.

104. **Nelson, N., N. Perzov, A. Cohen, K. Hagai, V. Padler, and H. Nelson**. 2000. The cellular biology of proton-motive force generation by V-ATPases. J. Exp. Biol. **203**:89-95.

105. **Nicolay, K., W. A. Scheffers, P. M. Bruinenberg, and R. Kaptein**. 1983. *In vivo* ^{31}P NMR studies on the role of the vacuole in phosphate metabolism in yeasts. Arch. Microbiol. **134**:270-275.

106. **Nicolson, T., B. Conradt, and W. Wickner**. 1996. A truncated form of the Pho80 cyclin of *Saccharomyces cerevisiae* induces expression of a small cytosolic factor which inhibits vacuole inheritance. J. Bacteriol. **178**:4047-4051.

107. **Nicolson, T. A., L. S. Weisman, G. S. Payne, and W. T. Wickner**. 1995. A truncated form of the Pho80 cyclin redirects the Pho85 kinase to disrupt vacuole inheritance in *S. cerevisiae*. J. Cell Biol. **130**:835-845.

108. **Niculescu, M. D. and S. H. Zeisel**. 2002. Diet, methyl donors and DNA methylation: interactions between dietary folate, methionine, and choline. J. Nutr. **132**:2333S-2335S.

109. **O'Neill, E. M., A. Kaffman, E. R. Jolly, and E. K. O'Shea**. 1996. Regulation of *PHO4* nuclear localization by the *PHO80-PHO85* cyclin-CDK complex. Science **271**:209-212.

110. **Ogawa, N., J. DeRisi, and P. O. Brown**. 2000. New components of a system for phosphate accumulation and polyphosphate metabolism in *Saccharomyces cerevisiae* revealed by genomic expression analysis. Mol. Biol. Cell **11**:4309-4321.

111. **Ogawa, N., K. Noguchi, Y. Yamashita, T. Yasuhara, N. Hayashi, K. Yoshida, and Y. Oshima**. 1993. Promoter analysis of the *PHO81* gene encoding a 134 kDa protein bearing ankyrin repeats in the phosphatase regulon of *Saccharomyces cerevisiae*. Mol. Gen. Genet. **238**:444-454.

112. **Ogawa, N., C. M. Tzeng, C. D. Fraley, and A. Kornberg**. 2000. Inorganic polyphosphate in *Vibrio cholerae*: genetic, biochemical, and physiologic features. J. Bacteriol. **182**:6687-6693.

113. **Ogier-Denis, E. and P. Codogno**. 2003. Autophagy: a barrier or an adaptive response to cancer. Biochim. Biophys. Acta **1603**:113-128.

114. **Okumura, S., N. Mitsukawa, Y. Shirano, and D. Shibata**. 1998. Phosphate transporter gene family of *Arabidopsis thaliana*. DNA Res. **5**:261-269.

115. **Oshima, Y., N. Ogawa, and S. Harashima**. 1996. Regulation of phosphatase synthesis in *Saccharomyces cerevisiae* - a review. Gene **179**:171-177.

116. **Parviz, F. and W. Heideman**. 1998. Growth-independent regulation of *CLN3* mRNA levels by nutrients in *Saccharomyces cerevisiae*. J. Bacteriol. **180**:225-230.

117. **Passmore, S., R. Elble, and B. K. Tye**. 1989. A protein involved in minichromosome maintenance in yeast binds a transcriptional enhancer conserved in eukaryotes. Genes Dev. **3**:921-935.

118. **Passmore, S., G. T. Maine, R. Elble, C. Christ, and B. K. Tye**. 1988. *Saccharomyces cerevisiae* protein involved in plasmid maintenance is necessary for mating of MAT alpha cells. J. Mol. Biol. **204**:593-606.

119. **Pearce, D. A., T. Ferea, S. A. Nosel, B. Das, and F. Sherman**. 1999. Action of Btn1, the yeast orthologue of the gene mutated in Batten disease. Nat. Genet. **22**:55-58.

120. **Pearce, D. A. and F. Sherman**. 1997. *BTN1*, a yeast gene corresponding to the human gene responsible for Batten's disease, is not essential for viability, mitochondrial function, or degradation of mitochondrial ATP synthase. Yeast **13**:691-697.

121. **Persson, B. L., J. Petersson, U. Fristedt, R. Weinander, A. Berhe, and J. Pattison**. 1999. Phosphate permeases of *Saccharomyces cerevisiae*: structure, function and regulation. Biochim. Biophys. Acta **1422**:255-272.

122. **Peters, J. M.** 2002. The anaphase-promoting complex: proteolysis in mitosis and beyond. Mol. Cell **9**:931-943.

123. **Peterson, C. L. and J. W. Tamkun**. 1995. The SWI-SNF complex: a chromatin remodeling machine? Trends Biochem. Sci. **20**:143-146.

124. **Pic, A., F. L. Lim, S. J. Ross, E. A. Veal, A. L. Johnson, M. R. Sultan, A. G. West, L. H. Johnston, A. D. Sharrocks, and B. A. Morgan**. 2000. The forkhead protein Fkh2 is a component of the yeast cell cycle transcription factor SFF. EMBO J. **19** :3750-3761.

125. **Pramila, T., S. Miles, D. GuhaThakurta, D. Jemiolo, and L. L. Breeden**. 2002. Conserved homeodomain proteins interact with MADS box protein Mcm1 to restrict ECB-dependent transcription to the M/G1 phase of the cell cycle. Genes Dev. **16**:3034-3045.

126. **Pringle, J. R. and L. H. Hartwell**. 1981. The *Saccharomyces cerevisiae* cell cycle, p. 97-142. *In* J. N. Strathern, E. W. Jones, and J. R. Broach (ed.), The molecular biology of the yeast Saccharomyces: life cycle and inheritance. Cold Spring Harbor Laboratory Press, Plainview, NY.

127. **Raghothama, K. G.** 2000. Phosphorus acquisition; plant in the driver's seat! Trends Plant Sci. **5**:412-413.

128. **Rashid, M. H. and A. Kornberg** . 2000. Inorganic polyphosphate is needed for swimming, swarming, and twitching motilities of *Pseudomonas aeruginosa*. Proc. Natl. Acad. Sci. USA **97**:4885-4890.

129. **Rashid, M. H., K. Rumbaugh, L. Passador, D. G. Davies, A. N. Hamood, B. H. Iglewski, and A. Kornberg**. 2000. Polyphosphate kinase is essential for biofilm development, quorum sensing, and virulence of *Pseudomonas aeruginosa*. Proc. Natl. Acad. Sci. USA **97**:9636-9641.

130. **Rausch, C., P. Daram, S. Brunner, J. Jansa, M. Laloi, G. Leggewie, N. Amrhein, and M. Bucher**. 2001. A phosphate transporter expressed in arbuscule-containing cells in potato. Nature **414**:462-470.

131. **Reggiori, F. and H. R. Pelham** . 2001. Sorting of proteins into multivesicular bodies: ubiquitin-dependent and -independent targeting. EMBO J. **20**:5176-5186.

132. **Reynolds, D., B. J. Shi, C. McLean, F. Katsis, B. Kemp, and S. Dalton**. 2003. Recruitment of Thr 319-phosphorylated Ndd1p to the FHA domain of Fkh2p requires Clb kinase activity: a mechanism for CLB cluster gene activation. Genes Dev. **17**:1789-1802.

133. **Rose, M. D., F. Winston, and P. Hieter**. 1990. Methods in yeast genetics: A laboratory course manual. Cold Spring Harbor Laboratory Press, Plainview, NY.

134. **Schmid, A., K. D. Fascher, and W. Hörz**. 1992. Nucleosome disruption at the yeast *PHO5* promoter upon *PHO5* induction occurs in the absence of DNA replication. Cell. **71**:853-864.

135. **Schneider, K. R., R. L. Smith, and E. K. O'Shea**. 1994. Phosphate-regulated inactivation of the kinase Pho80-Pho85 by the CDK inhibitor Pho81. Science **266**:122-126.

136. **Schwob, E., T. Bohm, M. D. Mendenhall, and K. Nasmyth**. 1994. The B-type cyclin kinase inhibitor p40^{SIC1} controls the G1 to S transition in *S. cerevisiae*. Cell **79**:233-244.

137. **Sethuraman, A., N. N. Rao, and A. Kornberg**. 2001. The endopolyphosphatase gene: essential in *Saccharomyces cerevisiae*. Proc. Natl. Acad. Sci. USA **98**:8542-8547.

138. **Shao, D., C. L. Creasy, and L. W. Bergman**. 1996. Interaction of *Saccharomyces cerevisiae* Pho2 with Pho4 increases the accessibility of the activation domain of Pho4. Mol. Gen. Genet. **251**:358-364.

139. **Shimizu, T., A. Toumoto, K. Ihara, M. Shimizu, Y. Kyogoku, N. Ogawa, Y. Oshima, and T. Hakoshima**. 1997. Crystal structure of *PHO4* bHLH domain-DNA complex: flanking base recognition. EMBO J. **16**:4689-4697.

140. **Shirahama, K., Y. Yazaki, K. Sakano, Y. Wada, and Y. Ohsumi**. 1996. Vacuolar function in the phosphate homeostasis of the yeast *Saccharomyces cerevisiae*. Plant Cell Physiol. **37**:1090-1093.

141. **Shnyreva, M. G., E. V. Petrova, S. N. Egorov, and A. Hinnen**. 1996. Biochemical properties and excretion behavior of repressible acid phosphatases with altered subunit composition. Microbiol. Res. **151**:291-300.

142. **Smith, D. L. and A. D. Johnson**. 1994. Operator-constitutive mutations in a DNA sequence recognized by a yeast homeodomain. EMBO J. **13**:2378-2387.

143. **Spellman, P. T., G. Sherlock, M. Q. Zhang, V. R. Iyer, K. Anders, M. B. Eisen, P. O. Brown, D. Botstein, and B. Futcher**. 1998. Comprehensive identification of cell cycle-regulated genes of the yeast *Saccharomyces cerevisiae* by microarray hybridization. Mol. Biol. Cell **9**:3273-3297.

144. **Strahl, B. D. and C. D. Allis** . 2000. The language of covalent histone modifications. Nature **403**:41-45.

145. **Sudarsanam, P., V. R. Iyer, P. O. Brown, and F. Winston**. 2000. Whole-genome expression analysis of *snf/swi* mutants of *Saccharomyces cerevisiae*. Proc. Natl. Acad. Sci. USA **97**:3364-3369.

146. **Svaren, J., J. Schmitz, and W. Hörz**. 1994. The transactivation domain of Pho4 is required for nucleosome disruption at the *PHO5* promoter. EMBO J. **13**:4856-4862.

147. **Szczypka, M. S., Z. Zhu, P. Silar, and D. J. Thiele**. 1997. *Saccharomyces cerevisiae* mutants altered in vacuole function are defective in copper detoxification and iron-responsive gene transcription. Yeast **13**:1423-1435.

148. **Toone, W. M. and N. Jones**. 1998. Stress-activated signaling pathways in yeast. Genes Cells **3**:485-498.

149. **Unger, M. W. and L. H. Hartwell**. 1976. Control of cell division in *Saccharomyces cerevisiae* by methionyl-tRNA. Proc. Natl. Acad. Sci. USA **73**:1664-1668.

150. **Urech, K., M. Durr, T. Boller, A. Wiemken, and J. Schwencke**. 1978. Localization of polyphosphate in vacuoles of *Saccharomyces cerevisiae*. Arch. Microbiol. **116**:275-278.

151. **van der, W. J.** 1985. Methionine metabolism and cancer. Nutr. Cancer **7**:179-183.

152. **van Voorthuysen, T., B. Regierer, F. Springer, C. Dijkema, D. Vreugdenhil, and J. Kossmann**. 2000. Introduction of polyphosphate as a novel phosphate pool in the chloroplast of transgenic potato plants modifies carbohydrate partitioning. J. Biotechnol. **77**:65-80.

153. **Veinot-Drebot, L. M., G. C. Johnston, and R. A. Singer**. 1991. A cyclin protein modulates mitosis in the budding yeast *Saccharomyces cerevisiae*. Curr. Genetics **19**:15-19.

154. **Venter, U. and W. Hörz**. 1989. The acid phosphatase genes *PHO10* and *PHO11* in *S. cerevisiae* are located at the telomeres of chromosomes VIII and I. Nucleic Acids Res. **17**:1353-1369.

155. **Venter, U., J. Svaren, J. Schmitz, A. Schmid, and W. Hörz**. 1994. A nucleosome precludes binding of the transcription factor Pho4 *in vivo* to a critical target site in the *PHO5* promoter. EMBO J. **13**:4848-4855.

156. **Versaw, W. K.** 1995. A phosphate-repressible, high-affinity phosphate permease is encoded by the *pho-5+* gene of *Neurospora crassa*. Gene **153**:135-139.

157. **Vindelov, J. and N. Arneborg**. 2002. *Saccharomyces cerevisiae* and *Zygosaccharomyces mellis* exhibit different hyperosmotic shock responses. Yeast **19**:429-439.

158. **Visintin, R., S. Prinz, and A. Amon**. 1997. *CDC20* and *CDH1*: a family of substrate-specific activators of APC-dependent proteolysis. Science **278**:460-463.

159. **Vogel, K., W. Hörz, and A. Hinnen**. 1989. The two positively acting regulatory proteins Pho2 and Pho4 physically interact with *PHO5* upstream activation regions. Mol. Cell. Biol. **9**:2050-2057.

160. **Wang, L., C. D. Fraley, J. Faridi, A. Kornberg, and R. A. Roth**. 2003. Inorganic polyphosphate stimulates mammalian TOR, a kinase involved in the proliferation of mammary cancer cells. Proc. Natl. Acad. Sci. USA **100**:11249-11254.

161. **Wang, Y., C. L. Liu, J. D. Storey, R. J. Tibshirani, D. Herschlag, and P. O. Brown**. 2002. Precision and functional specificity in mRNA decay. Proc. Natl. Acad. Sci USA **99**:5860-5865.

162. **Wijnen, H., A. Landman, and B. Futcher**. 2002. The G(1) cyclin Cln3 promotes cell cycle entry via the transcription factor Swi6. Mol. Cell. Biol. **22**:4402-4418.

163. **Wurst, H., T. Shiba, and A. Kornberg**. 1995. The gene for a major exopolyphosphatase of *Saccharomyces cerevisiae*. J. Bacteriol. **177**:898-906.

164. **Wykoff, D. D. and E. K. O'Shea**. 2001. Phosphate transport and sensing in *Saccharomyces cerevisiae*. Genetics **159**:1491-1499.

165. **Zhang, J. W., K. J. Parra, J. Liu, and P. M. Kane**. 1998. Characterization of a temperature-sensitive yeast vacuolar ATPase mutant with defects in actin distribution and bud morphology. J. Biol. Chem. **273**:18470-18480.

166. **Zhu, G., P. T. Spellman, T. Volpe, P. O. Brown, D. Botstein, T. N. Davis, and B. Futcher**. 2000. Two yeast forkhead genes regulate the cell cycle and pseudohyphal growth. Nature **406**:90-94.

VITA

Daniel Wilhelm Neef

1140 Dresden Dr.
Hoffman Estates, Il 60195
(847) 359-2836

EDUCATION

2004 Ph.D. Biochemistry, Texas A&M University, TX
1999 B.S. Biology, Valparaiso University, IN

HONORS and AWARDS

1999 First Place winner at Celebration of Undergraduate Scholarship
1999 Phi Lambda Upsilon Honor Society
1998 Valparaiso University Dean's List
1998 National Science Foundation REU Award

PUBLICATION

Neef, D. W. and M. P. Kladde. 2003. Polyphosphate loss promotes SNF/SWI- and Gcn5-dependent mitotic induction of *PHO5*. Mol. Cell. Biol. **23**:3788-3797.